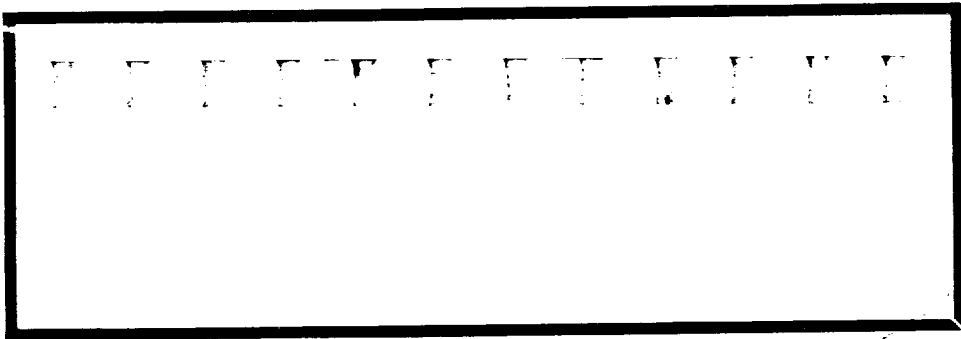
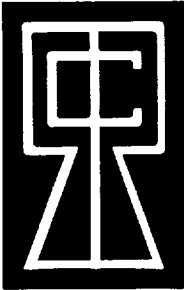


RD

C5



ROCKET RESEARCH CORPORATION

FACILITY FORM 602	N 67 19122	(THRU)
	<i>[scribble]</i>	<i>None</i>
	CR-82457	28
	(PAGES)	(CODE)
	(NASA CR OR TMX OR AD NUMBER)	(CATEGORY)

Seattle, Washington

Reproduced by
NATIONAL TECHNICAL
INFORMATION SERVICE
U.S. Department of Commerce
Springfield VA 22151

162ps

N67-19122

DEVELOPMENT OF DESIGN AND SCALING CRITERIA
FOR MONOPROPELLANT HYDRAZINE REACTORS
EMPLOYING SHELL 405 SPONTANEOUS CATALYST
RRC-66-R-76 - Volume I

Final Report

Prepared under NASA Contract NAS 7-372


Submitted To:

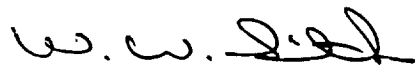
NASA Western Operations Office
Santa Monica, California

By

Rocket Research Corporation
Seattle, Washington

Approved by:


B. W. Schmitz, Project Manager


W. W. Smith, Manager
Hydrazine Programs

REPRODUCED BY
NATIONAL TECHNICAL
INFORMATION SERVICE
U.S. DEPARTMENT OF COMMERCE
SPRINGFIELD, VA. 22161

January 19, 1967

762

TABLE OF CONTENTS

	<u>Page</u>
SUMMARY	
1.0 INTRODUCTION	1
2.0 CONTRACT SCOPE OF WORK	3
2.1 General	3
2.2 Phase I	3
2.3 Phase II	5
3.0 TEST PLAN	7
3.1 General	7
3.2 Phase I Test Plan	7
4.0 REACTOR DESIGN	11
4.1 Injector Optimization Tests	11
4.2 Catalyst Bed Parameter Studies	18
5.0 TEST APPARATUS AND TEST PROCEDURES	33
5.1 Propellant Supply System	33
5.2 Thrust Stand	33
5.3 Instrumentation	33
5.4 Test Procedures	45
6.0 INJECTOR OPTIMIZATION TEST RESULTS	49
6.1 Data Reduction Techniques	49
6.2 Test Results	51
6.3 Summary of Injector Optimization Testing	106
7.0 CATALYST BED DESIGN PARAMETER STUDIES	111
7.1 Test Conditions Studied	111
7.2 Test Results	111
7.3 Summary of Test Data	123
8.0 CATALYST DEGRADATION MEASUREMENTS	139
9.0 100 lbf ENGINE	143
9.1 Design	143
9.2 Test Results	143
10.0 FLIGHTWEIGHT 5 lbf ENGINE	151
10.1 Design	151
10.2 Low Freezing Point Propellant Mixture Tests	158

LIST OF FIGURES

<u>Figure Number</u>		<u>Page</u>
1	5 lbf Thrust Engine Showerhead Injector Test Matrix	8
2	Typical Test Matrix for Bed Loading, Chamber Pressure, and Bed Length Tests	10
3	Cross-Sectional View 0.5 lbf Engine	12
4	Cross-Sectional View 5 lbf Engine	13
5	Cross-Sectional View 50 lbf Engine	14
6	50 lbf Engine Rigimesh and Showerhead Injector Plates	20
7	Test Set - 50 lbf Hydrazine Reactor - RRC Drawing 24199, (2 Sheets)	21
8	Test Bed - Rocket Motor - RRC Drawing 24671	27
9	0.5 lbf Engine Assembly	31
10	Test Cell Schematic	34
11	Thrust Stand Assembly - .5 lbf Hydrazine Reactor, RRC Drawing 24233, (3 Sheets)	35
12	Test Installation & Flexure Assembly - 50 lbf Rocket Engine RRC Drawing 24255, (2 Sheets)	41
13	Data Recording System	46
14	0.5 lbf Engine Showerhead Injector Scatter Diagram	54
15	0.5 lbf Engine Showerhead Injector Average Cold Bed Response Time vs. Injector Pressure Drop	55
16	0.5 lbf Engine Showerhead Injector Average Ignition Delay vs. Injector Pressure Drop	56
17	0.5 lbf Engine Showerhead Injector Average Chamber Pressure Roughness vs. Injector Pressure Drop	57
18	0.5 lbf Engine Rigimesh Injector Scatter Diagram	58
19	0.5 lbf Engine Rigimesh Injector Average Cold Bed Response Time vs. Injector Pressure Drop	59
20	5 lbf Engine Showerhead Injector Scatter Diagram Cold Bed Response Time	65
21	5 lbf Engine Showerhead Injector Scatter Diagram Decay Time	66
22	5 lbf Engine Showerhead Injector Scatter Diagram Ignition Delay	67
23	5 lbf Engine Showerhead Injector Scatter Diagram Chamber Pressure Roughness	68

LIST OF FIGURES (Cont'd)

<u>Figure Number</u>		<u>Page</u>
24	5 lbf Engine Showerhead Injector Average Cold Bed Response Time vs. Injector Pressure Drop	72
25	5 lbf Engine Showerhead Injector Average Cold Bed Response vs. Distance from Catalyst Bed	73
26	5 lbf Engine Showerhead Injector Average Cold Bed Response Time vs. Number of Orifices	74
27	5 lbf Engine Showerhead Injector Average Ignition Delay vs. Number of Orifices	76
28	5 lbf Engine Showerhead Injector Average Ignition Delay vs. Distance from Catalyst Bed	77
29	5 lbf Engine Showerhead Injector Average Chamber Pressure Decay Time vs. Number of Orifices	78
30	5 lbf Engine Rigimesh Injector Scatter Diagram Cold Bed Response Time	81
31	5 lbf Engine Rigimesh Injector Scatter Diagram Ignition Delay	82
32	5 lbf Engine Rigimesh Injector Scatter Diagram Decay Time	83
33	5 lbf Engine Rigimesh Injector Scatter Diagram Chamber Pressure Roughness	84
34	5 lbf Engine Rigimesh Injector Cold Bed Response Time vs. Injector Pressure Drop	85
35	50 lbf Engine Showerhead Injector Scatter Diagram Cold Bed Response Time	90
36	50 lbf Engine Showerhead Injector Scatter Diagram Chamber Pressure Roughness	91
37	50 lbf Engine Showerhead Injector Scatter Diagram Ignition Delay	92
38	50 lbf Engine Showerhead Injector Scatter Diagram	93
39	50 lbf Engine Showerhead Injector Cold Bed Response Data vs. Injector Pressure Drop	94
40	50 lbf Engine Showerhead Injector Cold Bed Response Time vs. Injector Pressure Drop	95
41	50 lbf Engine Showerhead Injector Chamber Pressure Roughness vs. Injector Pressure Drop	96
42	50 lbf Engine 60 Hole Showerhead Injector Chamber Pressure Roughness vs. Injector Pressure Drop	97

LIST OF FIGURES (Cont'd)

<u>Figure Number</u>		<u>Page</u>
43	50 lbf Engine Rigimesh Injector Scatter Diagram Cold Bed Response Time	100
44	50 lbf Engine Rigimesh Injector Scatter Diagram Ignition Delay	101
45	50 lbf Engine Rigimesh Injector Scatter Diagram Decay Time	102
46	50 lbf Engine Rigimesh Injector Scatter Diagram Chamber Pressure Roughness	103
47	50 lbf Engine Rigimesh Injector Average Cold Bed Response Time vs. Injector Pressure Drop	104
48	0.5 lbf Engine Test Matrix for Bed Loading, Chamber Pressure, and Bed Length Studies	112
49	5 lbf Engine Test Matrix for Bed Loading, Chamber Pressure, and Bed Length Studies	113
50	50 lbf Engine Test Matrix for Bed Loading, Chamber Pressure, and Bed Length Studies	114
51	Corrected Characteristic Velocity vs. Ammonia Dissociation for 5 lbf Engine	117
52	Sea Level Thrust Coefficient vs. Chamber Pressure for 5 lbf Engine	118
53	Corrected Characteristic Velocity vs. Ammonia Dissociation for 50 lbf Engine	124
54	Sea Level Thrust Coefficient vs. Chamber Pressure for = 2.0:1 50 lbf Engine	125
55	Corrected Characteristic Velocity vs. Ammonia Dissociation for 0.5 lbf Engine	126
56	Sea Level Thrust Coefficient vs. Chamber Pressure for = 20:1 0.5 lbf Engine	127
57	Correlation of Ammonia Dissociation Data for a Diffusion Controlled Reaction	132
58	General Correlation of Ammonia Dissociation Data	134
59	Correlation of Catalyst Bed Length Requirements	135
60	Correlation of Catalyst Bed Pressure Drop Data with Grant's Equation	137
61	Rocket Engine - 100 lbf Hydrazine, Showerhead Injector	145
62	100 lbf Monopropellant Hydrazine Engine	147

LIST OF FIGURES (Cont'd)

<u>Figure Number</u>		<u>Page</u>
63	Reactor Assembly - 5 lbf Flightweight - RRC Drawing 24600 (2 Sheets)	153
64	5.0 lbf Flightweight Engine Assembly	159
65	Performance of Ternary Propellant Mixtures	160
66	Hydrazine-Hydrazine Nitrate-Water Ternary Diagram Showing Freezing Point and Vacuum Specific Impulse	161
67	Ignition Delay Time vs. Propellant Freezing Point for 5 lbf Flightweight Engine	164
68	Chamber Pressure Roughness vs. Propellant Freezing Point for 5 lbf Flightweight Engine	165

LIST OF TABLES

<u>Table Number</u>		<u>Page</u>
I	Task I - Engine Design Summary	15
II	Showerhead Injector Design Summary	17
III	Rigimesh Injector Design Summary	19
IV	0.5 lbf Engine - Test Data Summary - Showerhead Injector	52
V	0.5 lbf Engine - Test Data Summary - Rigimesh Injector	60
VI	5 lbf Engine - Test Data Summary - Showerhead Injector	69
VII	5 lbf Engine - Test Data Summary - Rigimesh Injector	86
VIII	Summary of 50 lbf Engine Catalyst Particle Size Studies	88
IX	50 lbf Engine - Test Data Summary - Showerhead Injector	98
X	50 lbf Engine - Test Data Summary - Rigimesh Injector	105
XI	Instrumentation List for Reactor Design Parameter Studies	115
XII	Summary of 5 lbf Engine Catalyst Particle Size Studies	119
XIII	Summary of 1.205 Diameter Reactor Bed Loading, Chamber Pressure, and Bed Length Tests	120
XIV	Summary of 3.010 Diameter Reactor Bed Loading, Chamber Pressure, and Bed Length Tests	128
XV	Summary of 0.5 lbf Engine Bed Loading, Chamber Pressure, and Bed Length Studies	129
XVI	Catalyst Surface Area Changes	141
XVII	100 lbf Engine Design Parameters	148
XVIII	Summary of 100 lbf Engine Test Data	149
XIX	5 lbf Flightweight Engine Design	157
XX	Low Freezing Point Propellant Mixtures	162
XXI	Summary of 5 lbf Flightweight Engine Propellant Mixture Tests	166

SUMMARY

Under NASA Contract NAS 7-372, issued by NASA OART and technically directed by the Jet Propulsion Laboratory, Rocket Research Corporation, Seattle, Washington, undertook a program for development of design and scaling criteria for monopropellant hydrazine reactors employing Shell 405 spontaneous catalyst. The contract effort was initiated April 17, 1965. This document represents the final report on Contract NAS 7-372 and is contained in two volumes; Volume I presents the contract scope of work, test plan, engine design employed and summarizes the test data obtained; Volume II presents the correlation of the test data into design and scaling formulae and represents a design manual for monopropellant hydrazine reactors employing the Shell 405 catalyst.

Initial tests on the program were conducted to determine the effects of injector parameters on engine operation. A showerhead injector and a rigimesh injector were evaluated. Injector pressure drop, propellant mass distribution onto the catalyst bed, and injector height from the catalyst bed were varied in a systematic manner. Tests were carried out at thrust levels of 0.5, 5, and 50 lbf. The results indicate that the showerhead injector is superior to the rigimesh injector on the basis of smoother operation.

With the showerhead injector it was found that smooth start transients and steady state operation could be obtained with low pressure drop injectors. As a design guideline the injector pressure drop can be held at 10 to 20% of chamber pressure. Reactor operation was rather insensitive to the number of injector orifices (propellant mass distribution onto the catalyst bed) but it does appear that approximately 6 orifices per square inch of catalyst bed cross-sectional area results in optimum performance. Under certain conditions smooth operation could be obtained with the injector away from the catalyst bed, but better overall performance was obtained with the injector flush with the top of the catalyst bed.

During initial engine testing, large chamber pressure oscillations were encountered. It was found that these oscillations could be reduced and/or eliminated through the use of a layer of fine mesh catalyst on the top of the catalyst bed. This provides higher catalyst surface area per unit volume of catalyst and apparently stabilizes the flame front near the top of the catalyst bed on ignition.

Subsequent testing on the program investigated the effects of reactor design parameters on engine operation and performance. Chamber pressure was varied from 50 to 1,000 psia,

bed loading from 0.01 to 0.045 lbm/in²-sec, and catalyst bed length from that required for satisfactory (smooth) engine performance to a value which resulted in approximately 85% ammonia dissociation. Tests were carried out at thrust levels of 0.5, 5, and 50 lbf. This data, correlated with theoretical models of reactor operation, served as a basis for development of design and scaling formulae for monopropellant hydrazine reactors. Equations and design criteria were developed to define catalyst bed configuration, ammonia dissociation, catalyst bed pressure drop, and chamber pressure rise time as a function of the reactor design parameters.

The design and scaling criteria developed at the 0.5 to 50 lbf thrust level were used to design a 100 lbf engine. This engine was fabricated and tested to demonstrate the applicability of the scaling formula to higher thrust levels. Performance of this engine was as predicted by the scaling criteria and demonstrated the validity of the design and scaling criteria over a 200:1 thrust range.

A 5 lbf flightweight engine was designed and fabricated as a final task of the program. This engine was subjected to testing with propellant mixtures of hydrazine, hydrazinium nitrate, and water with the mixtures so selected that they had the same theoretical flame temperature but reduced freezing points as neat hydrazine. Three mixtures, which had freezing points of +20°F, 0°F, and -20°F, were successfully tested with very little difference noted in reactor operation between the three propellant mixtures.

Changes in catalyst carrier surface area and active metal surface area with accrued test time were measured during the program. It was found that the surface areas drop to approximately 70% of their original value after a short period of time and stabilize at that point. No change in reactor operation was noted as a result of this surface area change.

1.0 INTRODUCTION

This document constitutes Volume I of the Final Report of the Rocket Research Corporation "Development of Design and Scaling Criteria for Monopropellant Hydrazine Reactors Employing Shell 405 Spontaneous Catalyst" program conducted under Contract to the NASA Western Operations Office, Santa Monica, California, Contract NAS 7-372. This volume covers the contract scope of work, program test plan, engine design used in the study, and summarizes test data obtained during the program.

2.0 CONTRACT SCOPE OF WORK

2.1 General

The objective of NASA Contract NAS 7-372 was to determine and demonstrate the design techniques and to develop the empirical scaling formulae necessary for the design of monopropellant hydrazine reactors over a thrust range of 0.5 to 100 lbf. All of the reactor designs and tests employed the Shell 405 spontaneous catalyst developed under NASA Contract NAS 7-97. The design techniques and scaling formulae developed are applicable to the design of either rocket engines or gas generators. An additional part of the contract was the demonstration of a lightweight 5 lbf engine operating under pulsed and throttled modes of operation and also operating with hydrazine mixtures (hydrazine, hydrazinium nitrate, and water) which have low freezing points.

To develop the necessary scaling and design criteria, an experimental and analytical program was performed which includes the design, test, and evaluation of several engine configurations. Based on these evaluations, the design and scaling formulae were developed. The program was divided into two main phases which are summarized in the following sections.

2.2 Phase I

The work performed in Phase I provided the necessary data for development of design and scaling formulae. This work was divided into the three following tasks:

2.2.1 Task I

The Task I effort involved the evaluation of several catalyst bed and injector configurations at thrust levels of 0.5, 5, and 50 pounds. The engines were designed for a nominal chamber pressure of 150 psia. At each thrust level at least the following parameters were varied in a systematic manner to determine their influence on reactor operation:

- a. Chamber pressure
- b. Catalyst bed loading
- c. Catalyst bed length

- d. Catalyst particle size, shape, and roughness
- e. Injector design parameters such as pressure drop, orifice types, uniformity of flow distribution in catalyst bed, and injector location from catalyst bed
- f. Catalyst bed porosity.

The influence of each of the variables were judged by determination of the following:

- a. Injector and chamber configuration(s) which minimize ignition delay time, chamber pressure rise and decay times, and prevent excursions of chamber pressure from the design level
- b. Minimum residence time required for reliable ignition
- c. Ammonia dissociation as a function of bed loading, chamber pressure, characteristic length, catalyst bed porosity, and catalyst particle size, shape, and roughness
- d. Determination of catalyst bed pressure loss as a function of bed loading, chamber pressure, catalyst bed porosity, catalyst particle size, shape and roughness, and catalyst bed length
- e. Reactor operation as a function of catalyst bed pressure loss
- f. Factors which significantly degrade catalyst life. In particular the change in surface area and activity as a function of engine run time
- g. Characteristic velocity and specific impulse as a function of chamber pressure, characteristic length, bed loading, injector configuration, and catalyst bed configuration.

2.2.2 Task II

Based on the design and scaling criteria developed in Task I, a 100 lbf engine was designed, fabricated, and evaluated to validate the scaling formulae developed at the thrust levels of 0.5, 5, and 50 pounds.

The evaluation was based on determination of the following minimum reactor performance factors:

- a. Characteristic velocity
- b. Ignition delay time and repeatability
- c. Chamber pressure rise and decay time and repeatability
- d. Catalyst degradation
- e. Combustion stability.

2.2.3 Task III

Based on the data obtained in Tasks I and II, the appropriate design and scaling formulae were developed to define the design of rocket engines and gas generators with the following items being developed:

- a. Formulae defining catalyst bed configuration as a function of the reactor design parameters including chamber pressure, bed loading, and catalyst size.
- b. Formulae or guidelines which define the pertinent injector design parameters necessary for reactor design
- c. Equations which predict catalyst bed pressure loss as a function of the physical properties of the catalyst, chamber pressure, bed loading, and catalyst bed length
- d. Physical properties of the catalyst bed such as porosity and specific surface area as a function of reactor configuration and catalyst particle size, shape, and roughness
- e. Formulae or curves defining ammonia dissociation as a function of the catalyst physical and chemical properties, residence time, and chamber pressure.

2.3 Phase II

The results of the Phase I effort provided design criteria for the optimum design of rocket engines and gas generators within the limits of the variables tested. Based on these design techniques, a flightweight 5 lbf engine was designed, fabricated,

and tested. The engine was to be subjected to three types of testing described below.

Pulse mode testing in a vacuum environment for two conditions as specified below:

- a. A duty cycle of 100 ± 10 milliseconds on a 500 ± 10 milliseconds off for a total elapsed time of one and one-half hours (approximately 13,500 pulses).
- b. A duty cycle of 100 ± 10 milliseconds on and 15 to 30 minutes off for 3 days of continuous operation (144 to 288 pulses).

Using the same engine design, throttling tests were to be conducted at a variety of throttled conditions. The tests were to utilize a variable area valve, located immediately upstream of the propellant valve, which would create pressure loss upstream of the injector. Tests were to be conducted over at least a 10:1 ratio of thrust.

Additional steady state tests were conducted with propellant mixtures of hydrazine, hydrazinium nitrate, and water. The mixtures were selected such that the flame temperature was equal to or less than that of anhydrous hydrazine. Testing was conducted with mixtures having freezing points of -20°F , 0°F , and $+20^{\circ}\text{F}$.

The aforementioned pulse mode and throttling tests were not conducted on the program due to funding limitations.

3.0 TEST PLAN

3.1 General

To accomplish the objectives of the scope of work contained in Section 2.0, a series of experiments were developed at varied thrust levels to explore the effects of operating conditions, catalyst characteristics, and geometry of injector and reactor on the performance of monopropellant hydrazine rocket engines and gas generators employing the Shell 405 spontaneous catalyst.

During the experimental test program, theoretical reactor models were developed which attempted to define both the transient and steady state phases of reactor operation. These models served as a basis for correlating the experimental test data and development of the design and scaling criteria.

Details of the test plan for the program are presented in Rocket Research Corporation document 65-R-36 "Contract NAS 7-372 Program Plan" dated May 24, 1965. The highlights of this test plan are covered in the ensuing sections for each of the phases of the contract.

3.2 Phase I Test Plan

3.2.1 Task I Test Plan

In order to minimize the number of test variables occurring at any one time, the test plan for Task I was divided into three separate subtasks. Each of the subtasks is described in the following paragraphs.

3.2.1.1 Subtask I

The first part of the program was an investigation of two injector designs and the effect of the injector design variables on reactor performance and operation. For these tests, bed loading, chamber pressure, bed length, and catalyst particle size and shape were held constant at each thrust level. The injector designs are described in Section 4.1. A typical test matrix used for the injector testing is shown in Figure 1. Testing in such a manner allowed independent determination of the effects of injector pressure drop, mass distribution, and injector distance from the catalyst bed. It

5 LBF THRUST ENGINE
SHOWERHEAD INJECTOR TEST MATRIX

Number of Orifices									
3			6			9			
Injector Pressure Drop									
15 psid	45 psid	75 psid	15 psid	45 psid	75 psid	15 psid	45 psid	75 psid	
B1-1	B1-2	B1-3	B1-4	B1-5	B1-6	B1-7	B1-8	B1-9	
B1-10	B1-11	B1-12	B1-13	B1-14	B1-15	B1-16	B1-17	B1-18	
B1-19	B1-20	B1-21	B1-22	B1-23	B1-24	B1-25	B1-26	B1-27	
Height from Catalyst Bed									
0 inches									
0.2 inches									
0.4 inches									

FIGURE 1

is emphasized that this portion of the study was not necessarily aimed at determination of the optimum injector for use with the Shell 405 catalyst. Rather it was aimed at defining rational injector design criteria that could be effectively employed in the latter phases of the program.

3.2.1.2 Subtask II

Subtask II of the test program is concerned with optimizing the catalyst size and shape. The injector type and configuration, bed loading, bed length, and chamber pressure were held constant at each thrust level for these tests. Tests were conducted with a variety of catalyst sizes to determine that required for smooth and stable engine operation.

3.2.1.3 Subtask III

Having determined injector and catalyst particle size and shape effects, the third Subtask was concerned with determining the effects of chamber pressure, bed loading, and catalyst bed length on reactor operation. Chamber pressure was investigated over a range of 50 to 1,000 psia, bed loading over a 4.5:1 range (approximately 0.010 to 0.045 lbm/in²-sec), and bed length from the minimum required for ignition to that required for approximately 90% ammonia dissociation. A typical test matrix used for this phase of the testing is shown in Figure 2.

3.2.2 Task II Test Plan

Upon completion of the Phase I testing, the design data was extended to the design, fabrication, and evaluation of a 100 lbf engine. The evaluation criteria for this engine are as described in Paragraph 2.2.2.

3.2.3 Task III Test Plan

Throughout the first two phases of the program, theoretical reactor models were generated and the test data fit to the models. Upon completion of the Phase I and II test program, the final design and scaling criteria were developed based on correlation of the test data to fit the theoretical models.

TYPICAL TEST MATRIX FOR BED LOADING,
CHAMBER PRESSURE, AND BED LENGTH TESTS

BED LOADING (lbm/in ² -sec)															
0.01						0.02115						0.0447			
CHAMBER PRESSURE (psia)															
	50	105	225	475	1000	50	105	225	475	1000	50	105	225	475	1000
L ₁	A-1	A-2	A-3	A-4	A-5	A-6	A-7	A-8	A-9	A-10	A-11	A-12	A-13	A-14	A-15
L ₂	A-16	A-17	A-18	A-19	A-20	A-21	A-22	A-23	A-24	A-25	A-26	A-27	A-28	A-29	A-30
L ₃	A-31	A-32	A-33	A-34	A-35	A-36	A-37	A-38	A-39	A-40	A-41	A-42	A-43	A-44	A-45
L ₄	A-46	A-47	A-48	A-49	A-50	A-51	A-52	A-53	A-54	A-55	A-56	A-57	A-58	A-59	A-60

4.0 REACTOR DESIGN

4.1 Injector Optimization Tests

4.1.1 Thrust Chamber Assembly

The engine designs used for the injector optimization testing are summarized in Table I with the pertinent design parameters being listed for each engine. A cross sectional view of the 0.5, 5, and 50 lbf engines is shown in Figures 3, 4, and 5 respectively.

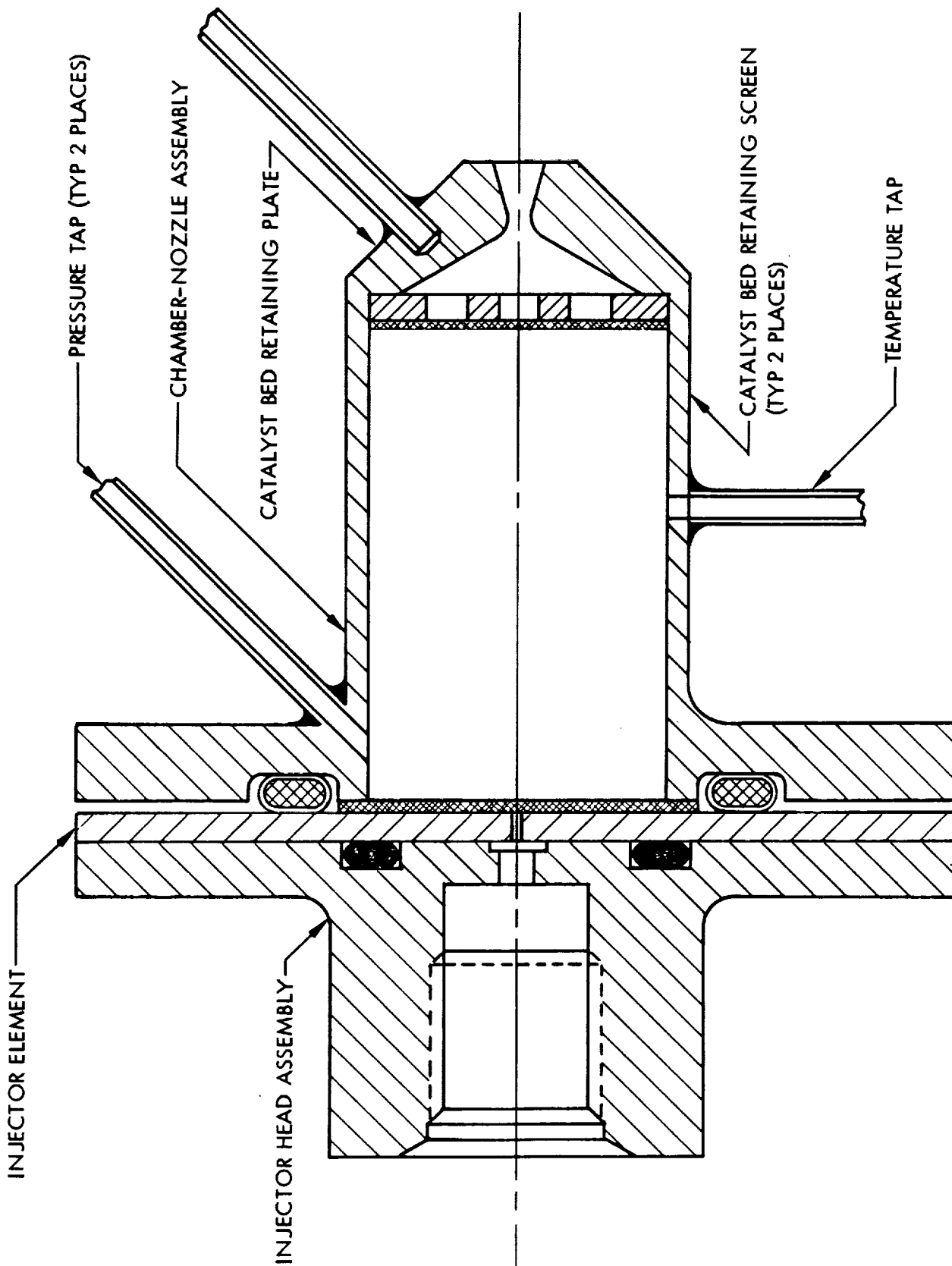
The chamber and nozzle assembly of the 0.5 and 5 lbf engines are machined from 347 stainless steel bar stock. On the 50 lbf engine, the chamber is made of Haynes Alloy No. 25 sheet stock. The nozzle and chamber flange are made of 347 stainless steel and are welded to the Haynes Alloy No. 25 chamber. The chamber walls of all three engines are coated with a 0.020 inch thickness of Rokide Z (zirconium oxide) to minimize heat losses.

The injector is flanged to the chamber to facilitate changes of injector configurations and catalyst particles sizes and shapes. A retaining plate-screen assembly is used to retain the catalyst at the downstream end of the chamber. The retaining plate is made of 347 stainless steel. The lower screen for the 0.5 and 5 lbf engines is 60 x 60 mesh molybdenum screen of 0.005 inches wire diameter. The lower screen for the 50 lbf engine is 10 x 10 mesh molybdenum screen of 0.025 inches wire diameter. At the upstream end of the chamber, a screen, held in place by the chamber and injector flanges, retains the catalyst bed. The size of the upper screen for all three thrust levels is 60 x 60 mesh molybdenum screen of 0.005 inches wire diameter.

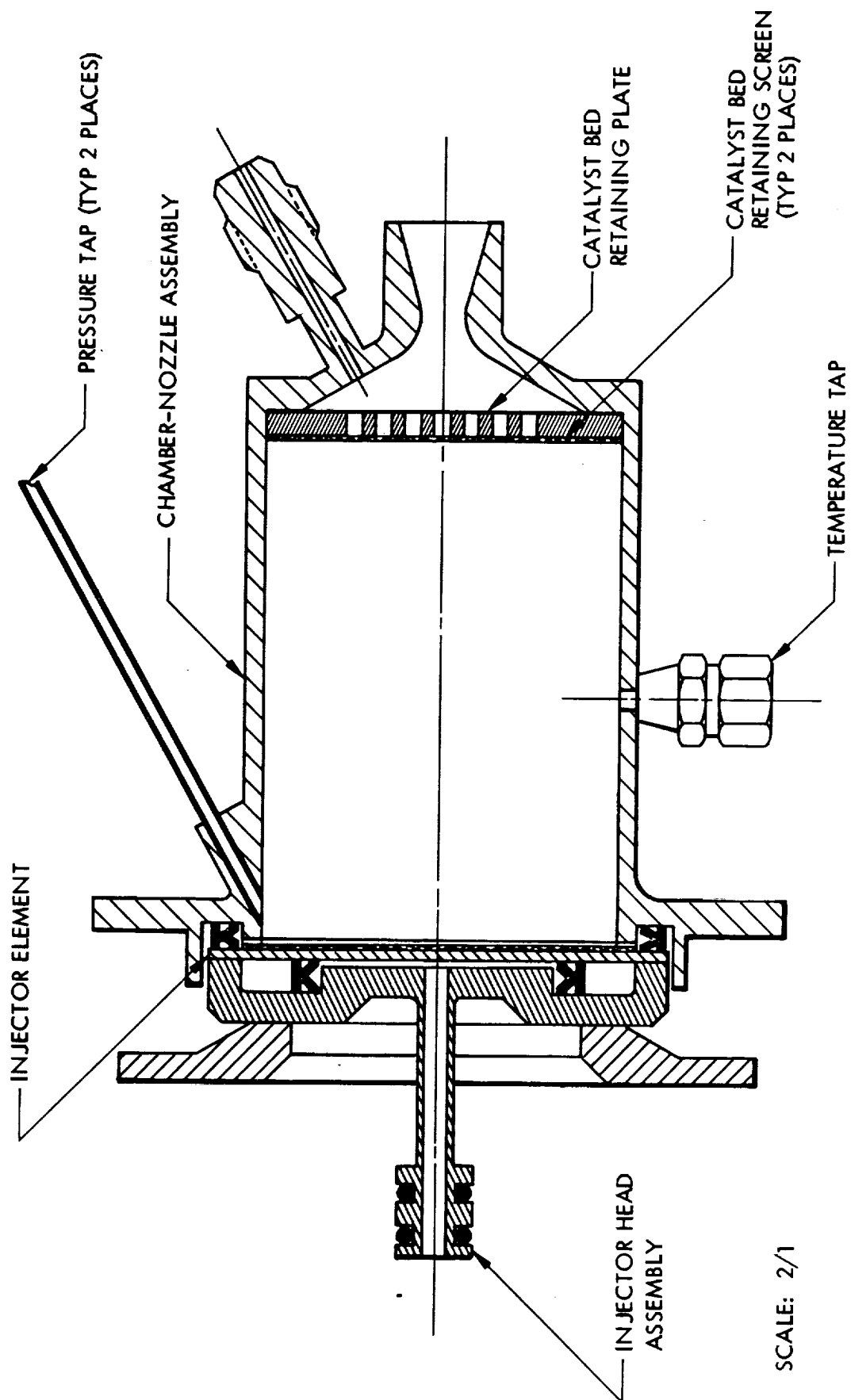
The injector consists of a flat plate in which various orifice sizes (to vary hydraulic pressure drop) and various numbers of orifices (to vary mass distribution) are machined.

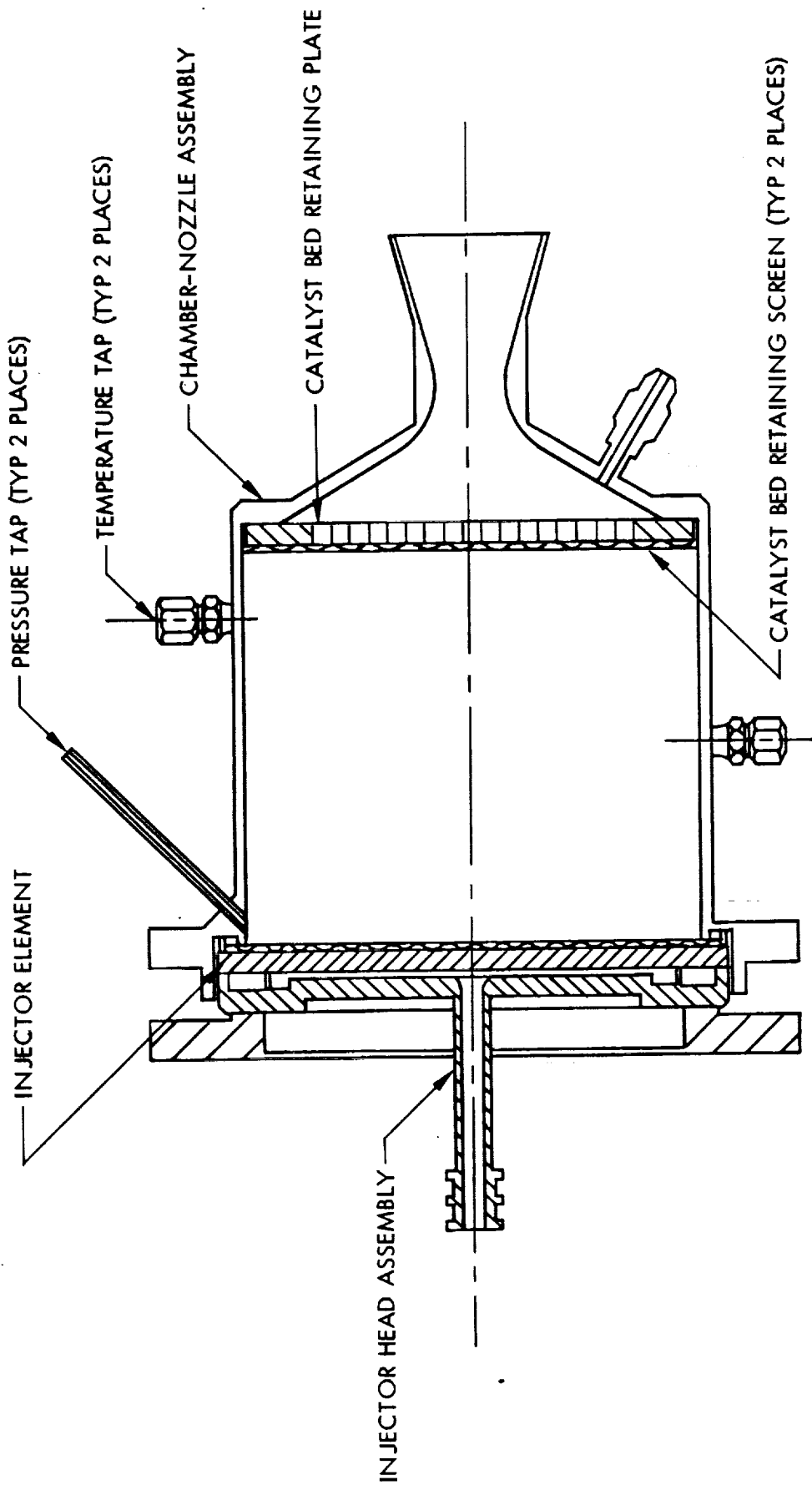
Propellant is fed to a distribution manifold through a single tube for all three thrust levels.

Either K-seals or copper-asbestos gaskets are used for the injector to chamber gas seal.



CROSS-SECTIONAL VIEW 5 Ibf ENGINE





CROSS-SECTIONAL VIEW 50 lb ENGINE
 SCALE: FULL SIZE

TABLE I
TASK I - ENGINE DESIGN SUMMARY

<u>Design Parameters</u>	<u>0.5 lbf Thrust Engine</u>	<u>5.0 lbf Thrust Engine</u>	<u>50 lbf Thrust Engine</u>
Vacuum Thrust, lbf at $\epsilon = 50:1$	0.5	5.0	50.0
Predicted Sea Level Thrust, lbf at $\epsilon = 4:1$	0.34	3.4	34.0
Chamber Pressure, psia	150	150	150
Engine Flow Rate, lbm/sec	0.0022	0.0213	0.213
Chamber Diameter, in	0.544	1.205	3.010
Catalyst Bed Length, in	0.880	1.785	2.680
Characteristic Length ⁽¹⁾ , in	100	100	100
Throat Diameter, in	0.050	0.156	0.492
Exit Diameter, in	0.100	0.312	0.984
Chamber Wall Thickness, in	0.022	0.050	0.035

(1) Based on empty catalyst bed volume.

4.1.2 Showerhead Injector

The showerhead injector consists of a flat plate in which orifices of various size (to vary pressure drop) and of various numbers (to vary mass distribution) are drilled. The following criteria was used in the analysis and design of the showerhead injector elements:

- a. The orifices shall be located in circular rows
- b. The minimum orifice diameter shall be approximately 0.010 inches
- c. The distance between the chamber wall and the outer orifice row shall be equal to the spacing between orifices
- d. The orifices shall cover equal areas of the catalyst bed.

Analysis of criteria (a), (c), and (d) above results in the following equation for determination of the spacing between orifices:

$$S = \frac{\pi n D_c}{N_T + \pi n^2 + \pi n}$$

Where:

- S = Spacing between orifices
D_c = Catalyst bed diameter
n = Number of rows of orifices
N_T = Total number of orifices
 π = 3.1416

A summary of the showerhead injector design details used in the testing is presented in Table II.

4.1.3 Rigimesh Injector

The rigimesh injector is basically a modified showerhead type injector in which the local bed loading (bed loading under each orifice) is

TABLE II
SHOWERHEAD INJECTOR DESIGN SUMMARY

0.5 lbf THRUST ENGINE

<u>Pressure Drop</u> psid	<u>Number</u> <u>Orifices</u>	<u>Orifice</u> <u>Dia., in.</u>	<u>Orifice Spacing</u>
15	1	0.0145	Single Orifice in Center
45	1	0.0112	Single Orifice in Center
75	1	0.0097	Single Orifice in Center

5.0 lbf THRUST ENGINE

15	3	0.0275	Equally Spaced on 0.377 Diameter B.C.
45	3	0.021	Equally Spaced on 0.377 Diameter B.C.
75	3	0.0185	Equally Spaced on 0.377 Diameter B.C.
15	6	0.0182	Equally Spaced on 0.569 Diameter B.C.
45	6	0.0140	Equally Spaced on 0.569 Diameter B.C.
75	6	0.0123	Equally Spaced on 0.569 Diameter B.C.
15	9	0.015	Equally Spaced on 0.685 Diameter B.C.
45	9	0.0114	Equally Spaced on 0.685 Diameter B.C.
75	9	0.0100	Equally Spaced on 0.685 Diameter B.C.

50 lbf THRUST ENGINE

15	20	0.0320	13 on 2.036 Diameter B.C. 7 on 1.062 Diameter B.C.
45	20	0.0243	
75	20	0.0213	
15	40	0.0225	20 on 2.276 Diameter B.C. 13 on 1.542 Diameter B.C. 7 on 0.808 Diameter B.C.
45	40	0.0172	
75	40	0.0151	
15	60	0.0183	24 on 2.394 Diameter B.C. 18 on 1.778 Diameter B.C. 12 on 1.162 Diameter B.C. 6 on 0.546 Diameter B.C.
45	60	0.0140	
75	60	0.0123	

appreciably less than the injector described in Paragraph 4.1.2. The rigimesh injector consists of a number of circular rigimesh discs which were press fit into a retaining plate. Each disc is approximately 0.25 inches in diameter.

The spacing criteria utilized for the showerhead injector described in Paragraph 4.1.2 was also used for the rigimesh injector.

Table III summarizes the design of the rigimesh injectors for each engine thrust level. Figure 6 shows a photograph of typical rigimesh and showerhead injectors tested on the 50 lbf engine.

4.2 Catalyst Bed Parameter Studies

The reactor designs for the catalyst bed parameter studies were designed to be capable of independent variations in bed loading, chamber pressure, and catalyst bed length. Various length chambers were manufactured for variations of catalyst bed length. Each chamber had removable nozzles so that bed loading and/or chamber pressure could be varied. The nozzles were sized to permit bed loading studies at 0.01, 0.021, and 0.045 lb/in²-sec and chamber pressure studies at 50, 105, 225, 475, and 1,000 psia.

A showerhead injector was utilized for all of the tests with the design criteria for the injector based on the results of the injector optimization tests. At all conditions the injector pressure drop was maintained at 10 to 20% of steady state chamber pressure.

The following sections describe the details of the engine designs at the 0.5, 5, and 50 lbf thrust levels.

4.2.1 50 lbf Engine

The 50 lbf engine design is shown in Figure 7. The injector design criteria is based on the results of the injector optimization testing and is as follows:

- a. 40 orifices with 7 holes on a 0.808 inch diameter, 13 holes on a 1.542 inch diameter, and 20 holes on a 2.276 inch diameter.

TABLE III
RIGIMESH INJECTOR DESIGN SUMMARY

0.5 lbf THRUST ENGINE

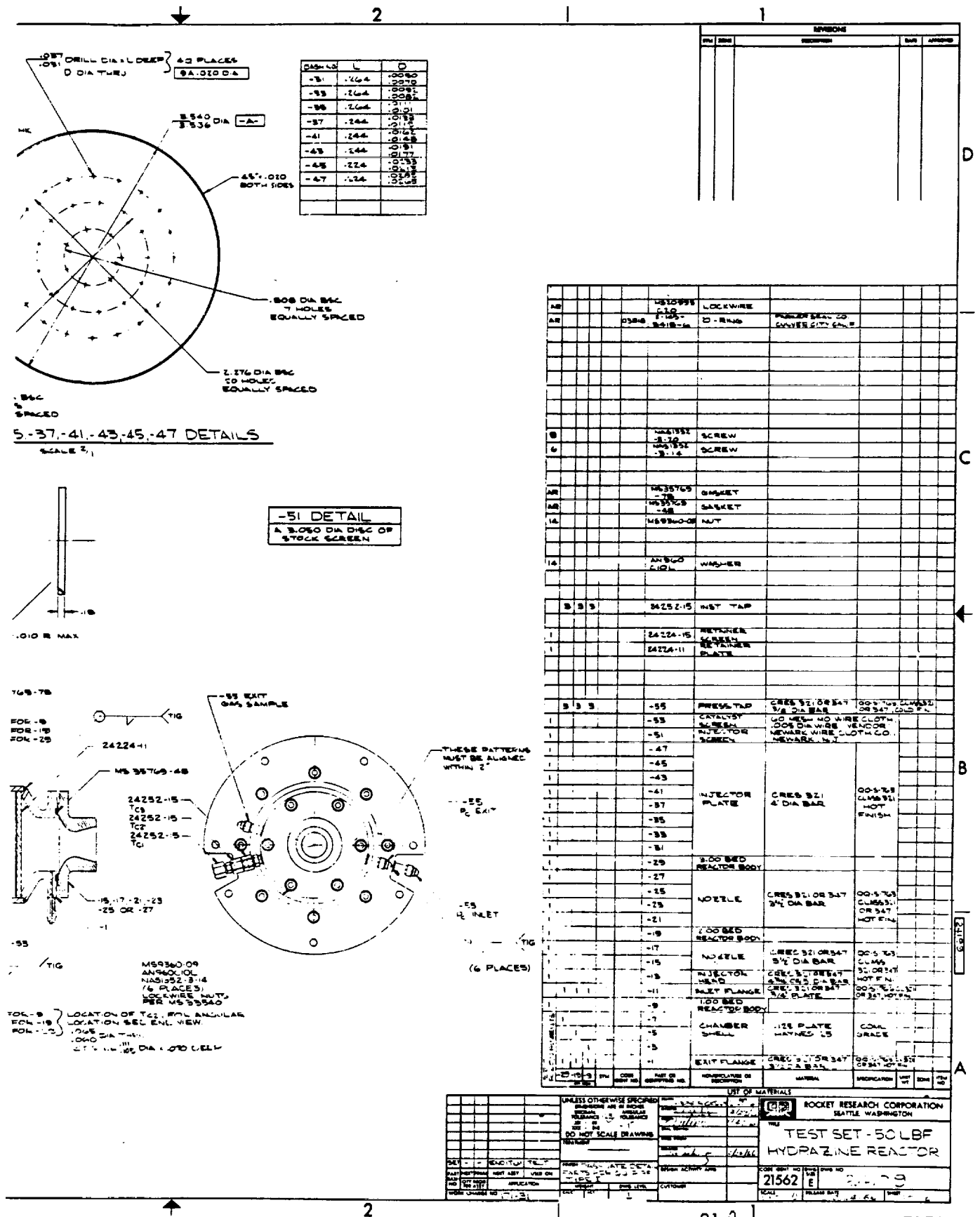
Pressure Drop psid	Number Discs	Rigimesh Disc Spacing
15	1	Single Disc in Center
45	1	Single Disc in Center
75	1	Single Disc in Center

5.0 lbf THRUST ENGINE

15	1	Single Disc in Center
45	1	Single Disc in Center
75	1	Single Disc in Center
15	4	Equally Spaced on 0.469 Diameter B.C.
45	4	Equally Spaced on 0.469 Diameter B.C.
75	4	Equally Spaced on 0.469 Diameter B.C.
15	7	Equally Spaced on 0.635 Diameter B.C.
45	7	Equally Spaced on 0.635 Diameter B.C.
75	7	Equally Spaced on 0.635 Diameter B.C.

50 lbf THRUST ENGINE

15	7	Equally Spaced on 1.586 Diameter B.C.
45	7	Equally Spaced on 1.586 Diameter B.C.
75	7	Equally Spaced on 1.586 Diameter B.C.
15	13	Four Equally Spaced on 0.638 Diameter B.C.
45	13	Nine Equally Spaced on 1.824 Diameter B.C.
75	13	
15	19	Six Equally Spaced on 1.014 Diameter B.C.
45	19	Thirteen Equally Spaced on 2.012 Diameter B.C.
75	19	



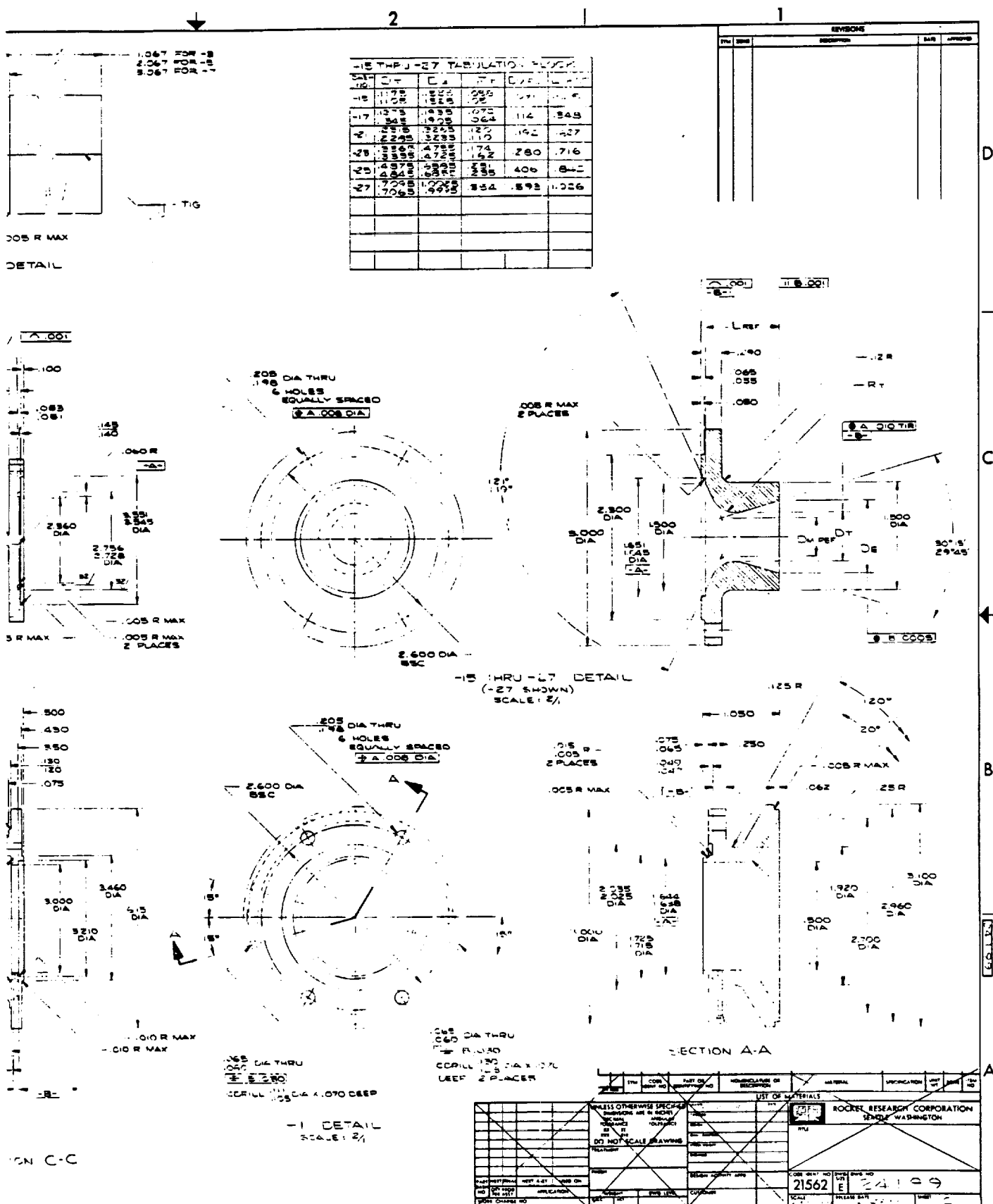


FIGURE 7

- b. Injector pressure drop to be approximately 10 to 20% of steady state chamber pressure.
- c. The injector is to be mounted flush with the top of the catalyst bed.

The chamber of 3.01 inches diameter is flanged on both ends to permit removal and replacement of various injectors and nozzles as required for the test program. The chamber is made of Haynes Alloy Number 25 Sheet Stock. All remaining parts are made of 321 or 347 stainless steel.

Three thermocouple taps are utilized on the engine. Two measure catalyst bed temperatures and the third measures exit gas temperature. Pressure taps are utilized to measure upstream and downstream chamber pressure. An additional tap is utilized for taking gas samples.

A Marotta solenoid valve MV-100 is used as the propellant valve.

4.2.2 5 lbf Engine

An assembly drawing of the 5 lbf engine is shown in Figure 8. A showerhead injector design is used with the following design parameters:

- a. Six orifices machined on a 0.569 diameter
- b. Injector pressure drop is maintained at 10 to 20% of chamber pressure
- c. The injector is mounted flush with the top of the catalyst bed.

The chamber of 1.205 inches diameter is flanged at the upper end to permit removal and replacement of injector plates. The outlet of the reactor consists of an AN fitting to which various sized nozzles, machined in AN 929 fittings, are attached. All parts are made of 321 or 347 stainless steel. Thermocouple taps are located along the chamber to measure catalyst bed and gas outlet temperatures. Three pressure taps are utilized to measure upstream and downstream chamber pressure and to take gas samples downstream of the catalyst bed.

An Eckel solenoid valve Model No. AF 56C-A51 is used as the propellant valve.

-29 ASSEMBLY

 TC_1, TC_2, TC_3

- 27. A

FIGURE 8

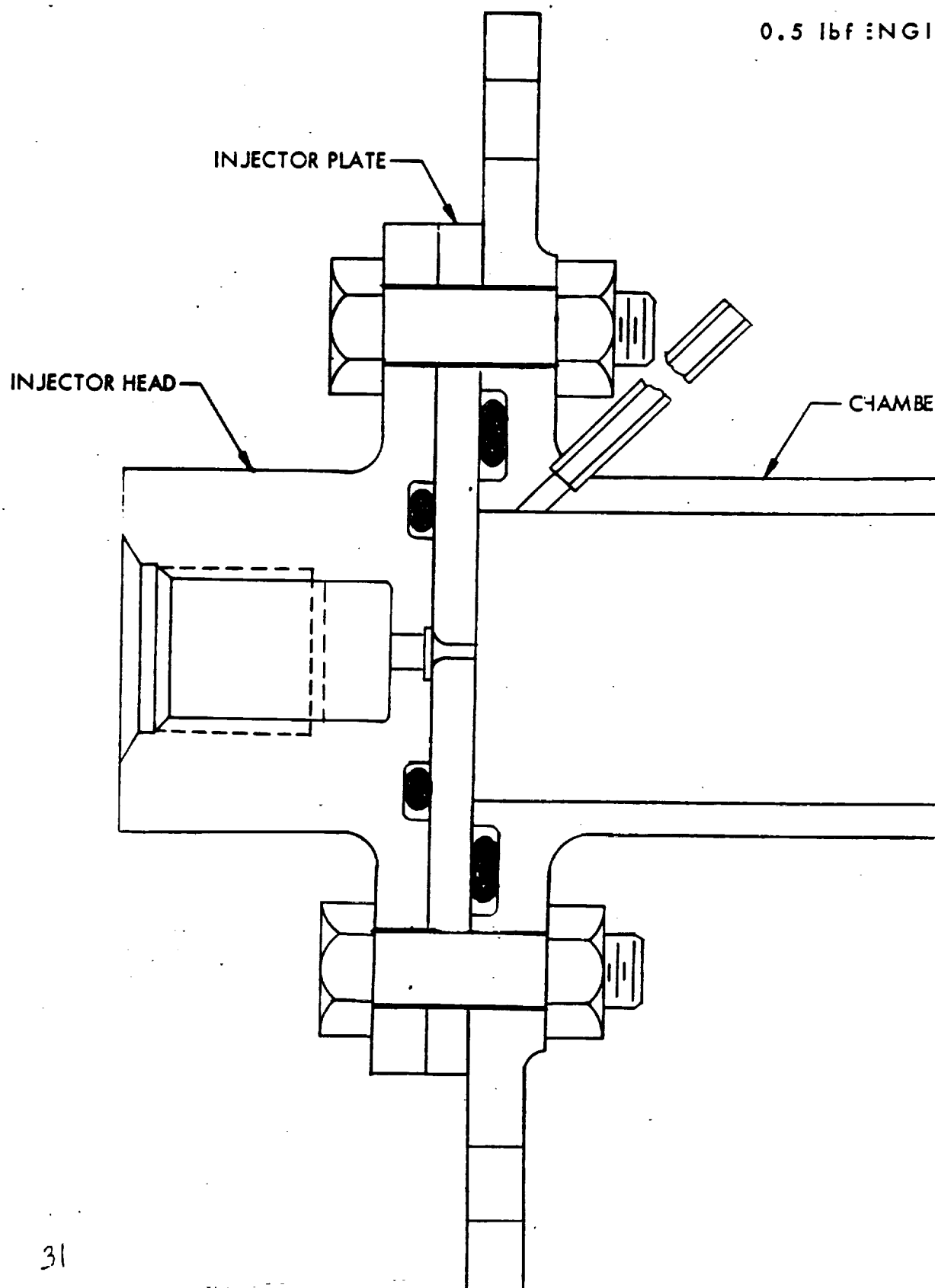
4.2.3 0.5 lbf Engine

An assembly drawing of the 0.5 lbf engine is shown in Figure 9. A single element showerhead injector is utilized which is mounted flush with the top of the catalyst bed.

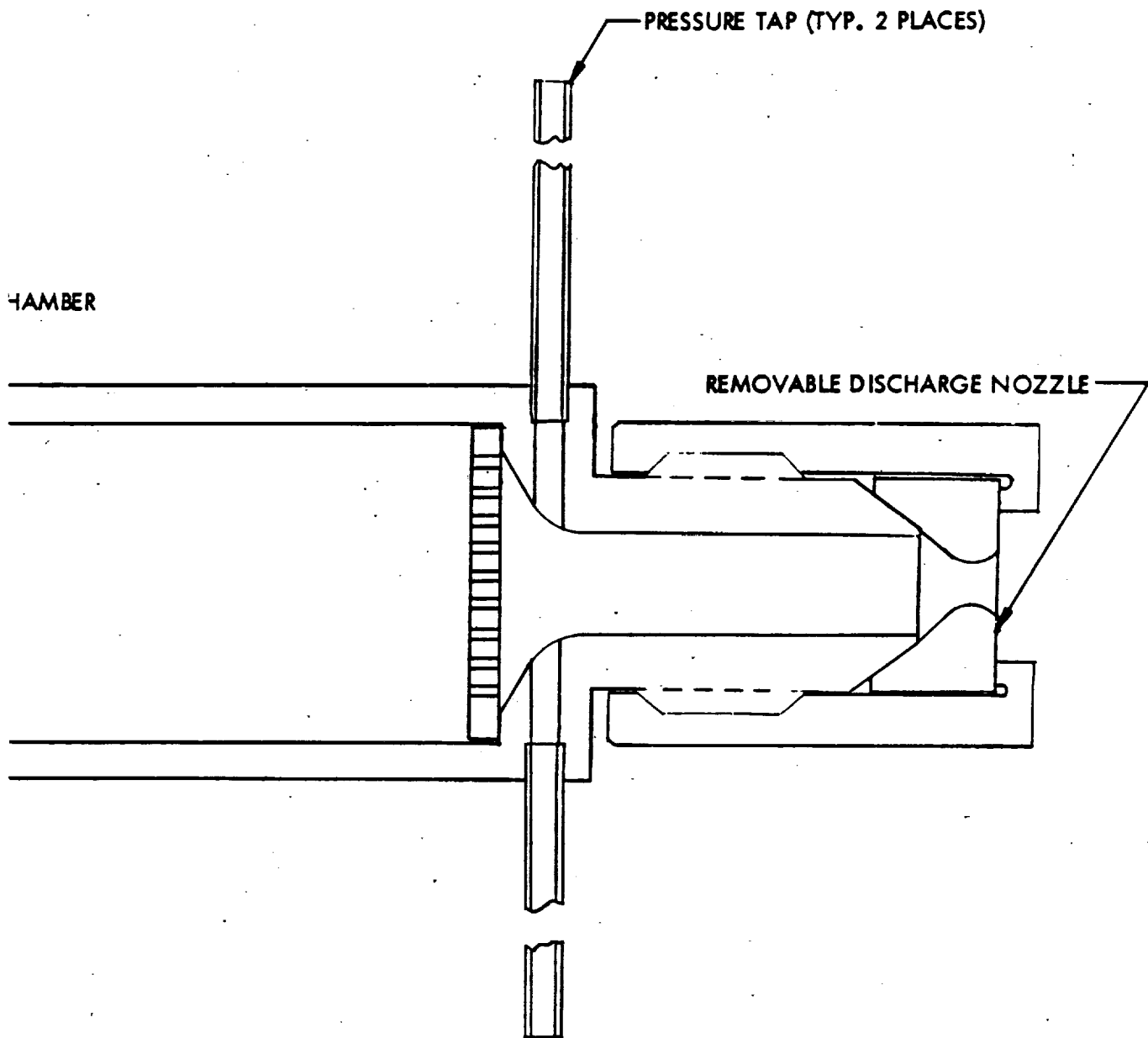
The chamber of 0.544 inches diameter is flanged at the upper end to permit removal and replacement of injector plates. The outlet of the reactor consists of an AN fitting to which various sized nozzles, machined in AN 929 fittings, are attached. Pressure taps are utilized to measure upstream and downstream chamber pressure and to take gas samples. Because of the smallness of the chamber no thermocouple taps are used on the engine.

An Eckel solenoid valve Model Number AF 56C-A53 is used as the propellant valve.

0.5 lbf INCH



ENGINE ASSEMBLY



5.0 TEST APPARATUS AND TEST PROCEDURES

5.1 Propellant Supply System

A schematic of the test cell setup for engine testing is shown in Figure 10. A line supply for each engine thrust level feeds off of a common hydrazine supply tankage. Flow meters are contained in series for each thrust level to obtain higher accuracy in measurement of flow rate. All valving is actuated remotely from the firing console. Teflon-lined stainless steel flexible lines are used to attach the propellant supply to the engine fire valve in order to provide a negligible resistance to the thrust measurement.

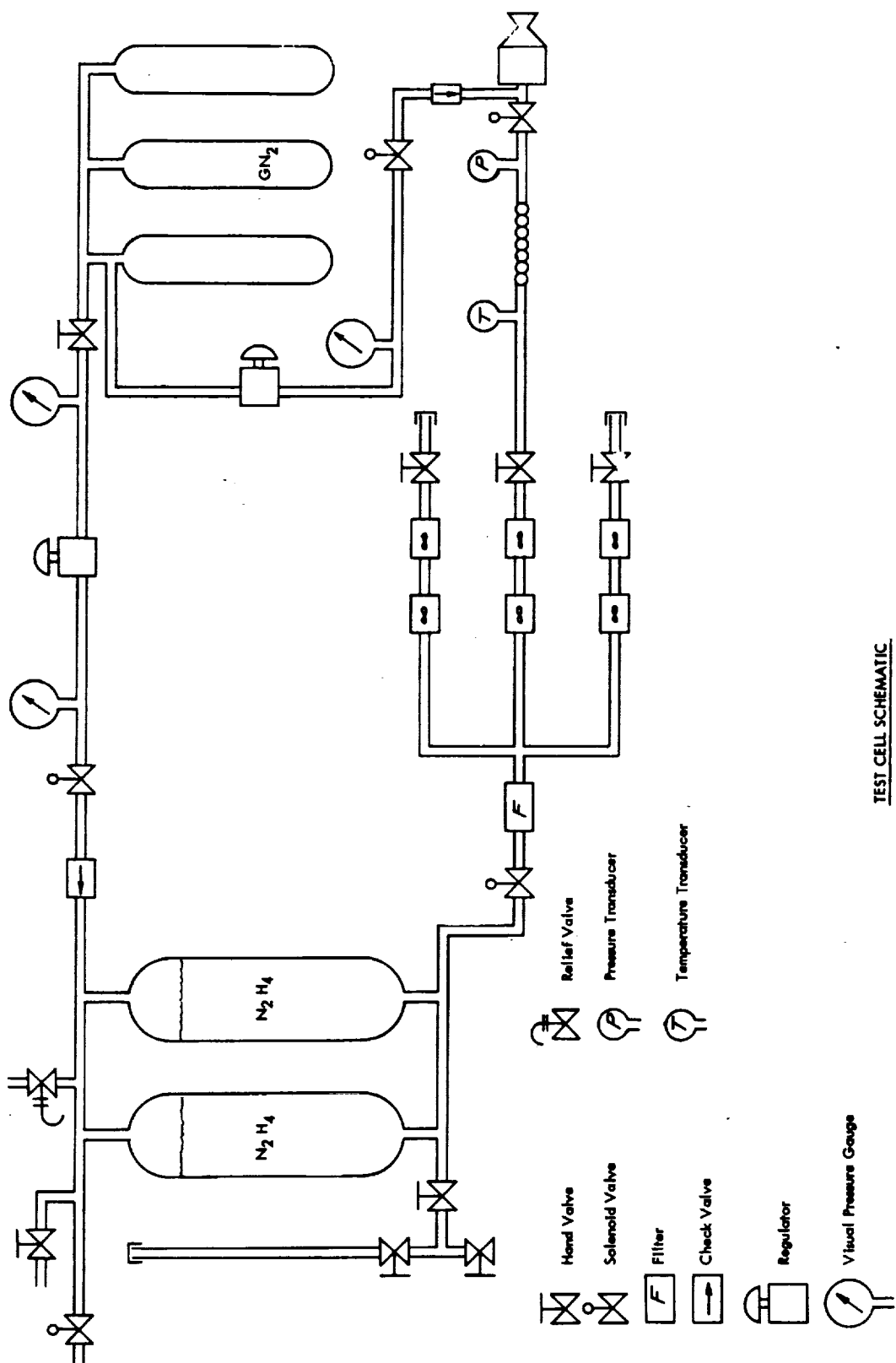
5.2 Thrust Stand

The thrust stands utilized for testing are of the parallelogram type. The stand consists of a reactor mount, suspended by four flexures from an inverted "L" shaped support. For the 0.5 and 5 lbf thrust stands (Figure 11) the flexures are stainless steel sheet stock 0.005 inches thick. For the 50 lbf engine thrust stand (Figure 12) Bendix Flexural Pivots are used. The axial thrust load is taken out by a Schaevitz-Bytrex load cell. The load from the thrust stand to the load cell is transmitted by a spherical load button acting on a flat plate in the 0.5 and 5 lbf thrust designs and by a flexure in the 50 lbf stand design. These designs eliminate application of side loads to the load cell to ensure high accuracy measurements.

Calibration of the stand is accomplished by application of known weights acting over a low friction pulley or a Bendix Flexural Pivot. The estimated friction error of the pulley is less than 0.06 percent of rated thrust.

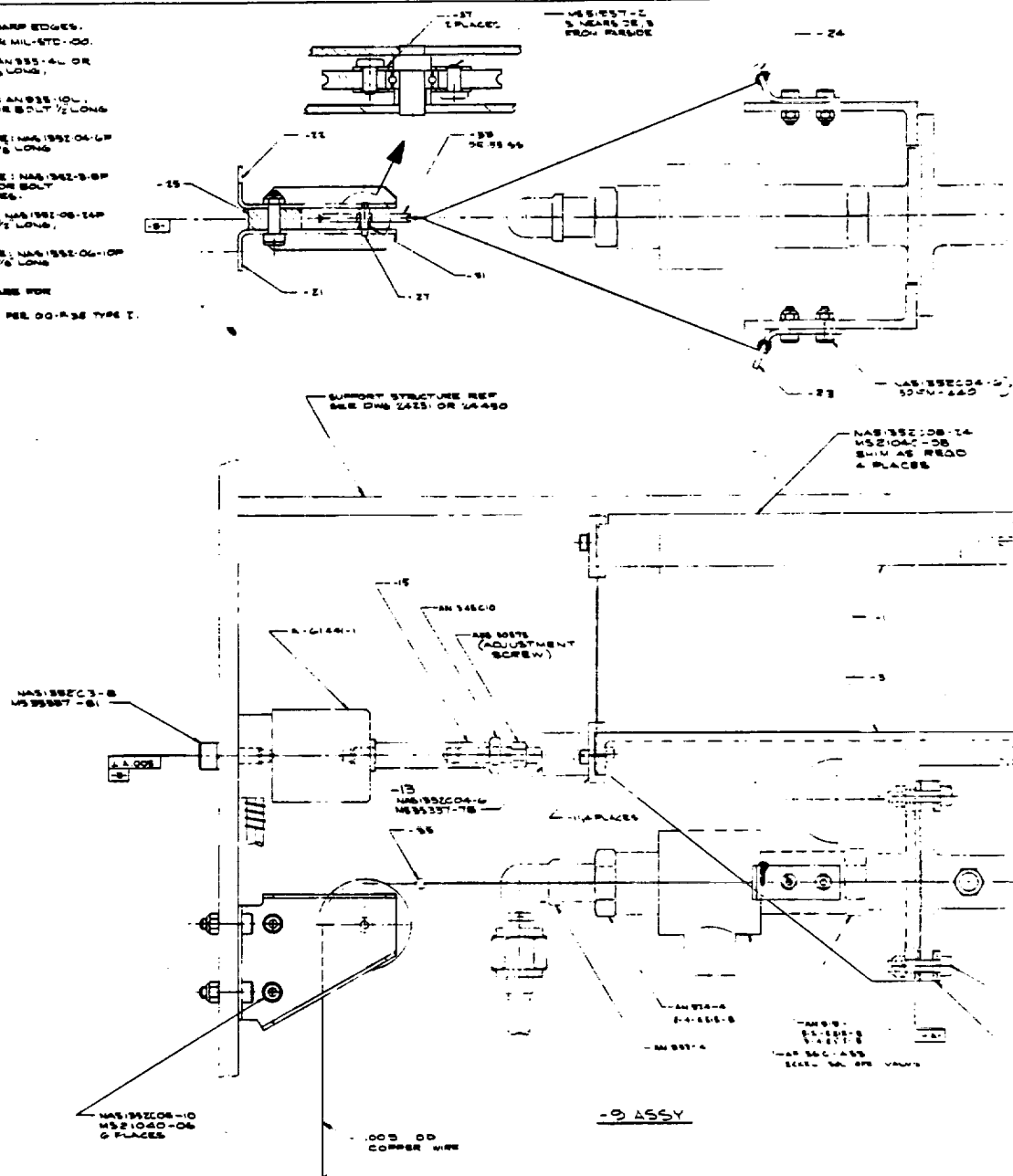
5.3 Instrumentation

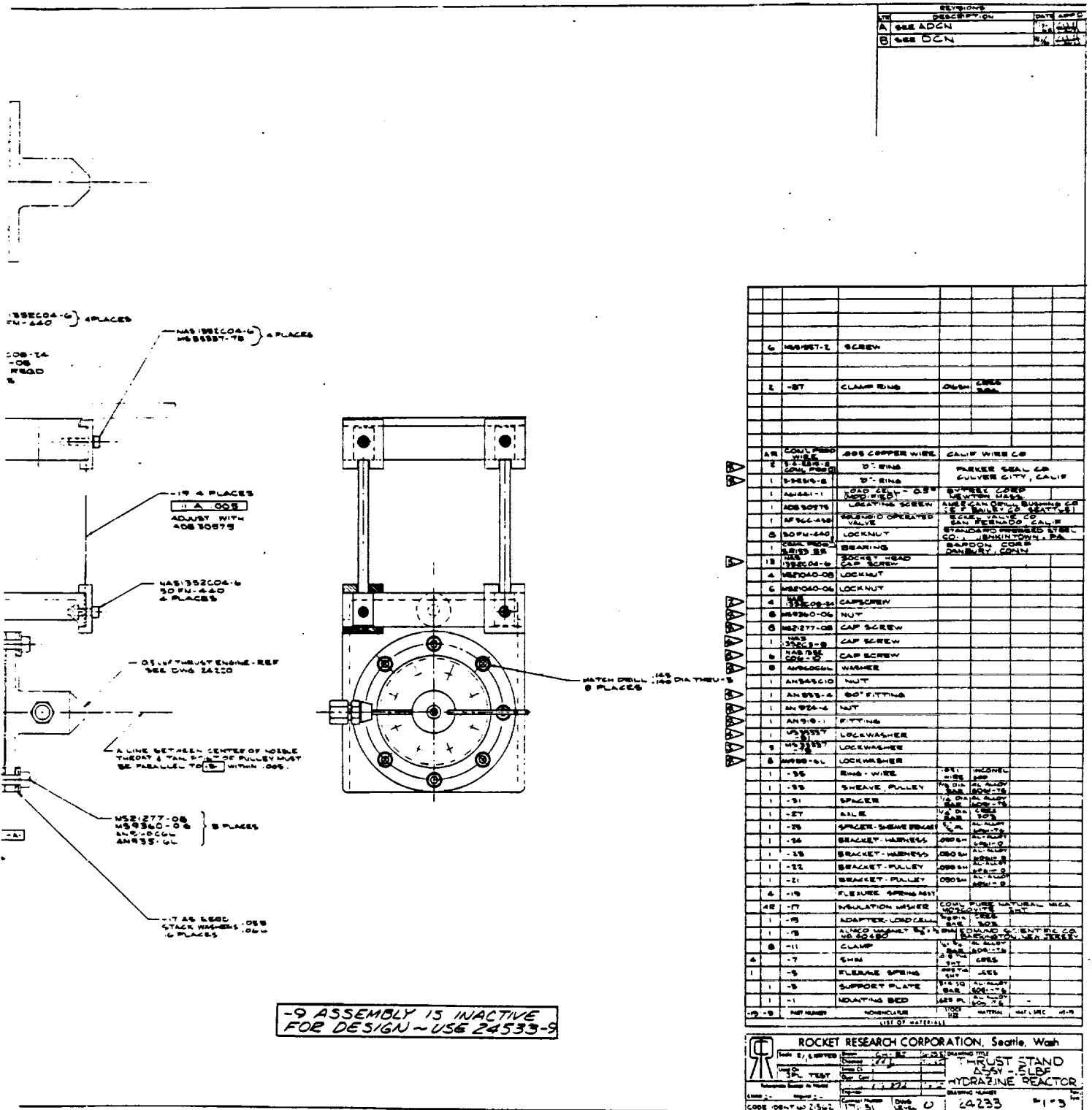
The contract specified that the reduced measurement error in pressure, flow rate and thrust measurements shall be less than 0.5 percent 3σ . In order to accomplish this high accuracy all measurement devices procured had a specified error source of not greater than 0.25 percent. The gauge types used in the testing are described below. High accuracy recording equipment is used to assure that the total measurement error is less than 0.5 percent 3σ .

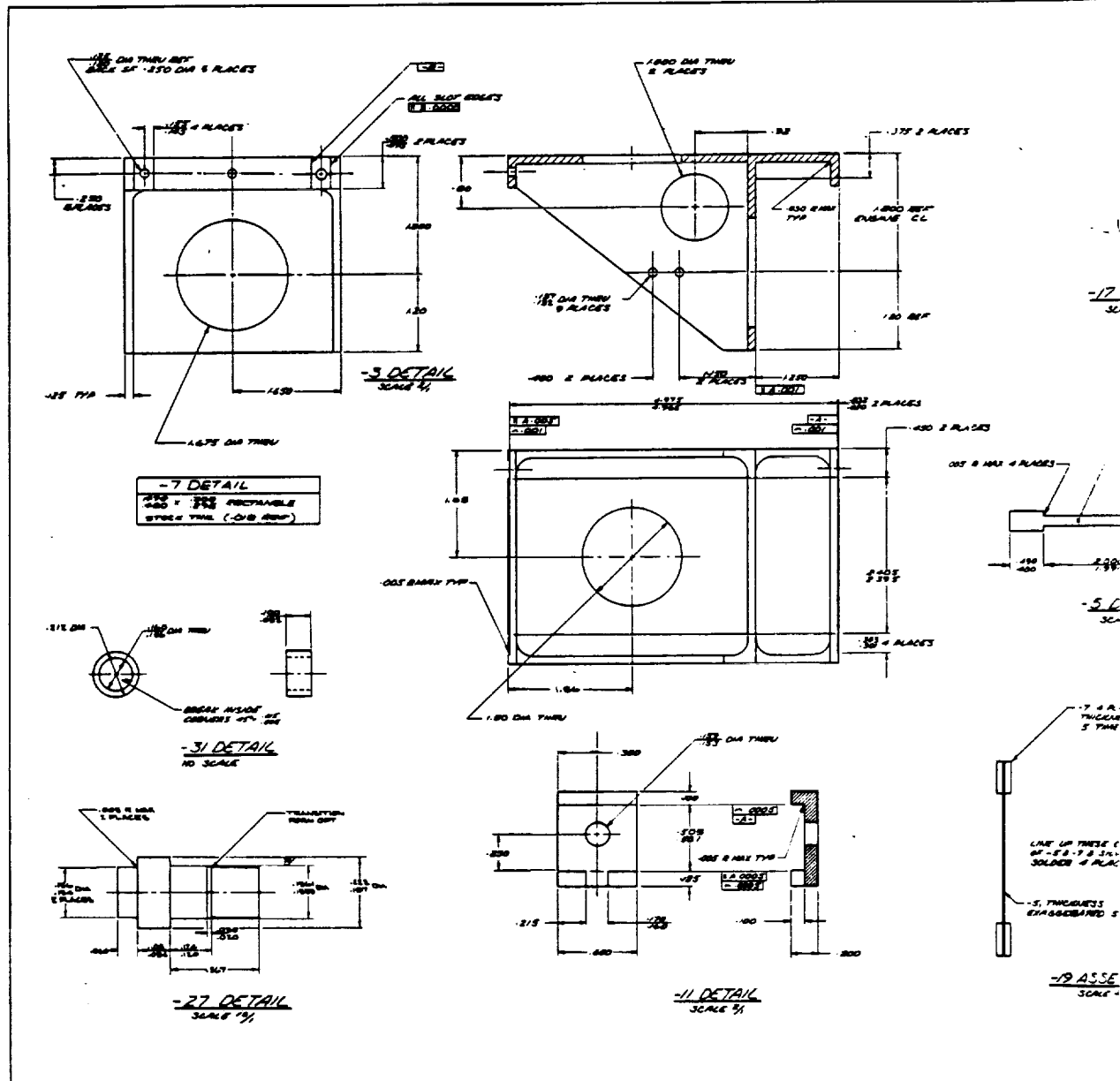


TEST CELL SCHEMATIC

- 1. REMOVE ALL BURRS & SHARP EDGES.
- 2. INTERPRET DRAWING PER MIL-STD-20.
- 3. ACCEPTABLE SUBSTITUTE: AN 835-4L OR ANY NO. 4-32 SCREW 3/8" LONG, CRSS. PREFERRED.
- 4. ACCEPTABLE SUBSTITUTE: AN 835-10L OR ANY NO. 10-32 SCREW OR BOLT 1/2" LONG, PREFERABLY CRSS.
- 5. ACCEPTABLE SUBSTITUTE: NA 951-06-16P OR ANY NO. 6-32 SCREW 3/8" LONG, PREFERABLY CRSS.
- 6. ACCEPTABLE SUBSTITUTE: NA 951-08-18P OR ANY NO. 8-32 SCREW 1/2" LONG, PREFERABLY CRSS.
- 7. ACCEPTABLE SUBSTITUTE: NA 951-06-16P OR ANY NO. 6-32 SCREW 3/8" LONG, PREFERABLY CRSS.
- 8. ENGINE MOUNTING HARDWARE FOR 1610 ENGINE ONLY.
- 9. PASSIVATE ALL CRSS PARTS PER QQ-A-353 TYPE I.



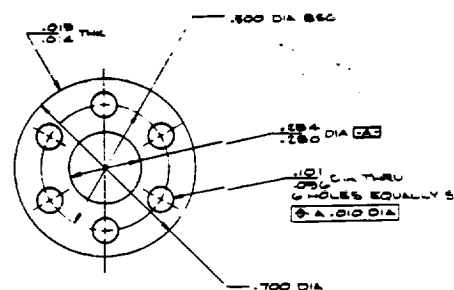




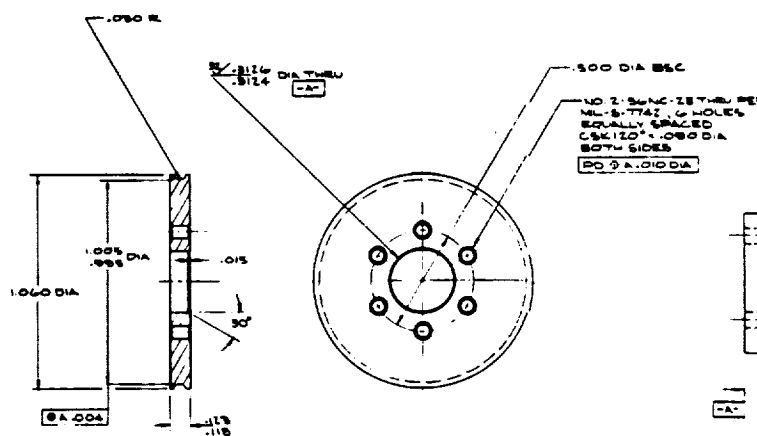
37.00

Preceding page blank

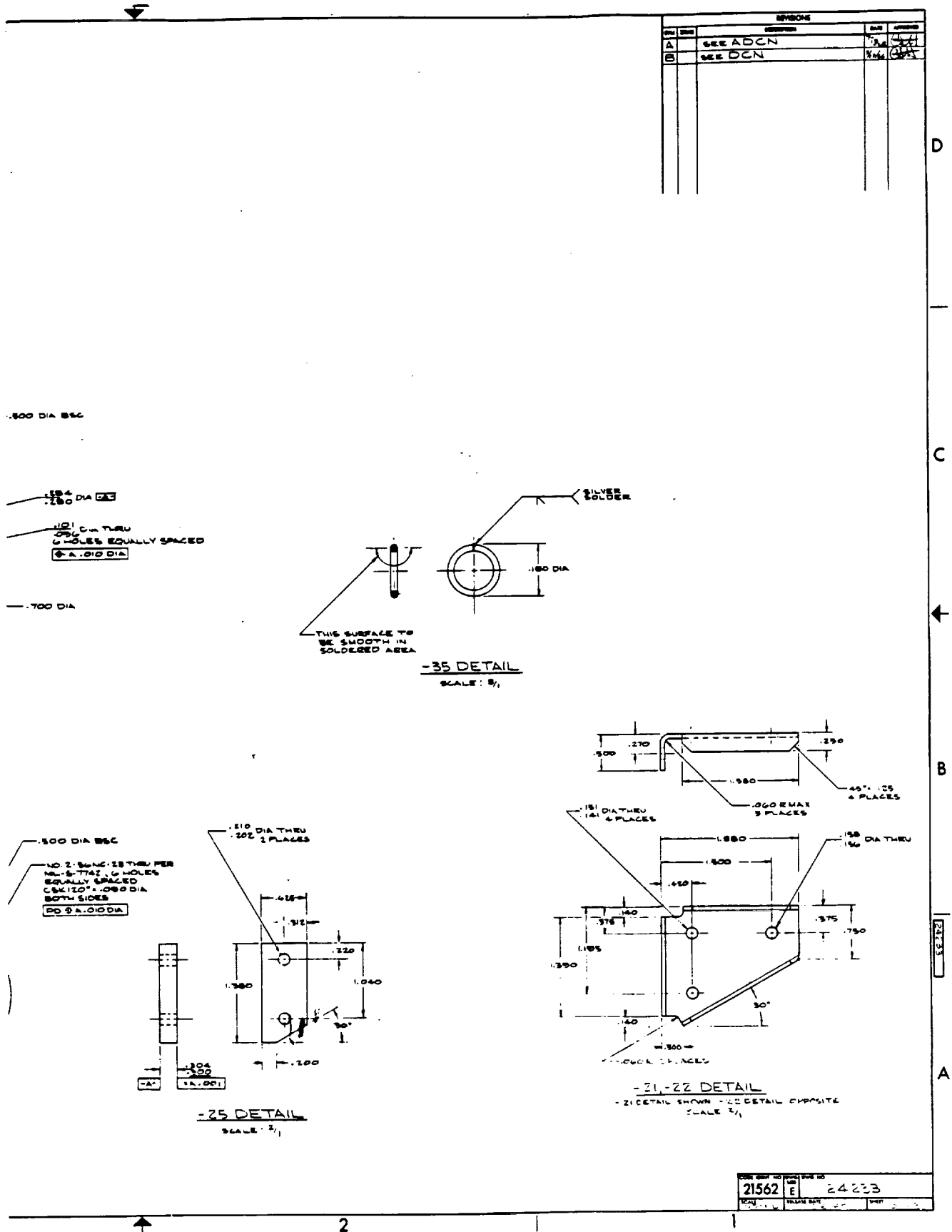


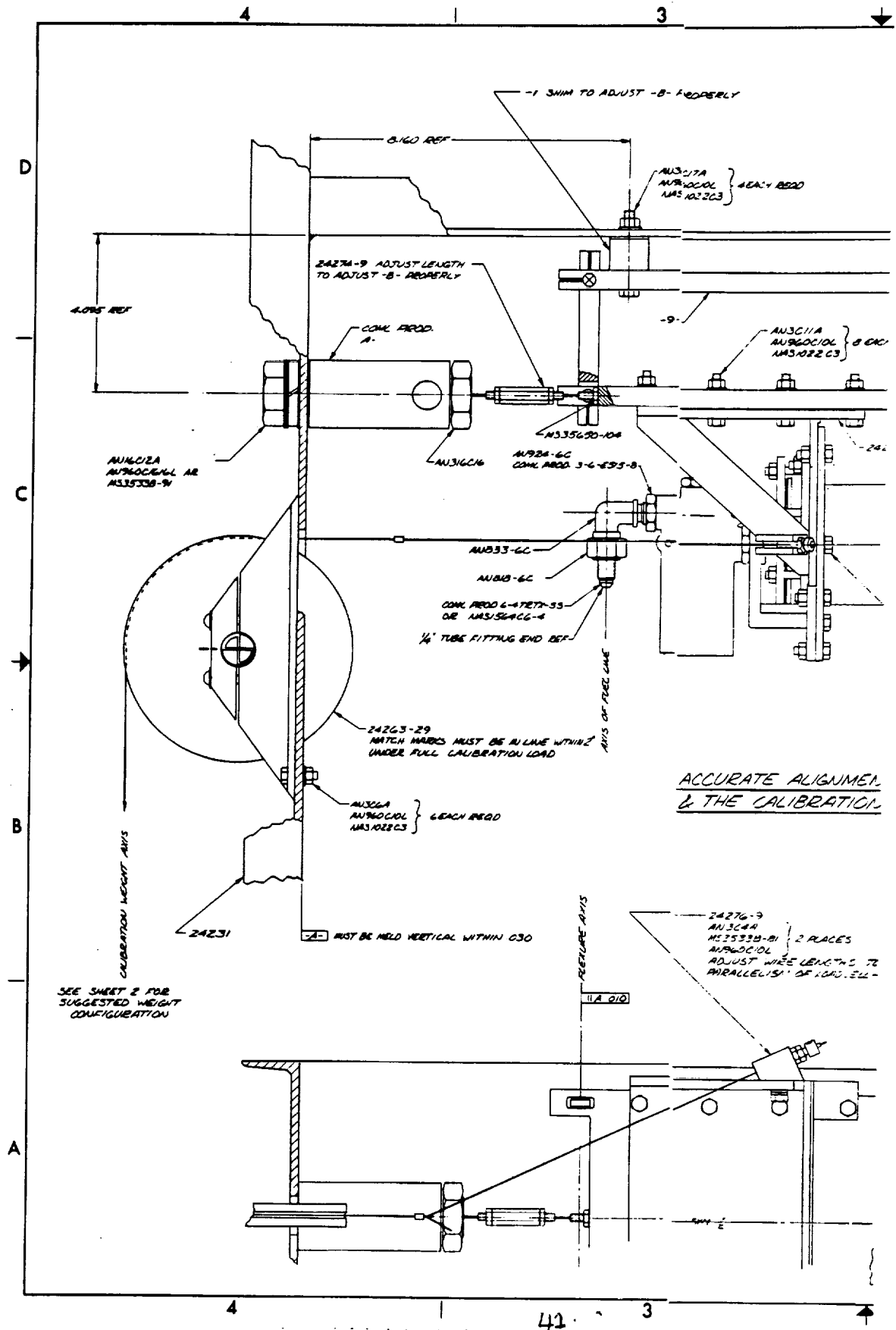


-37 DETAIL



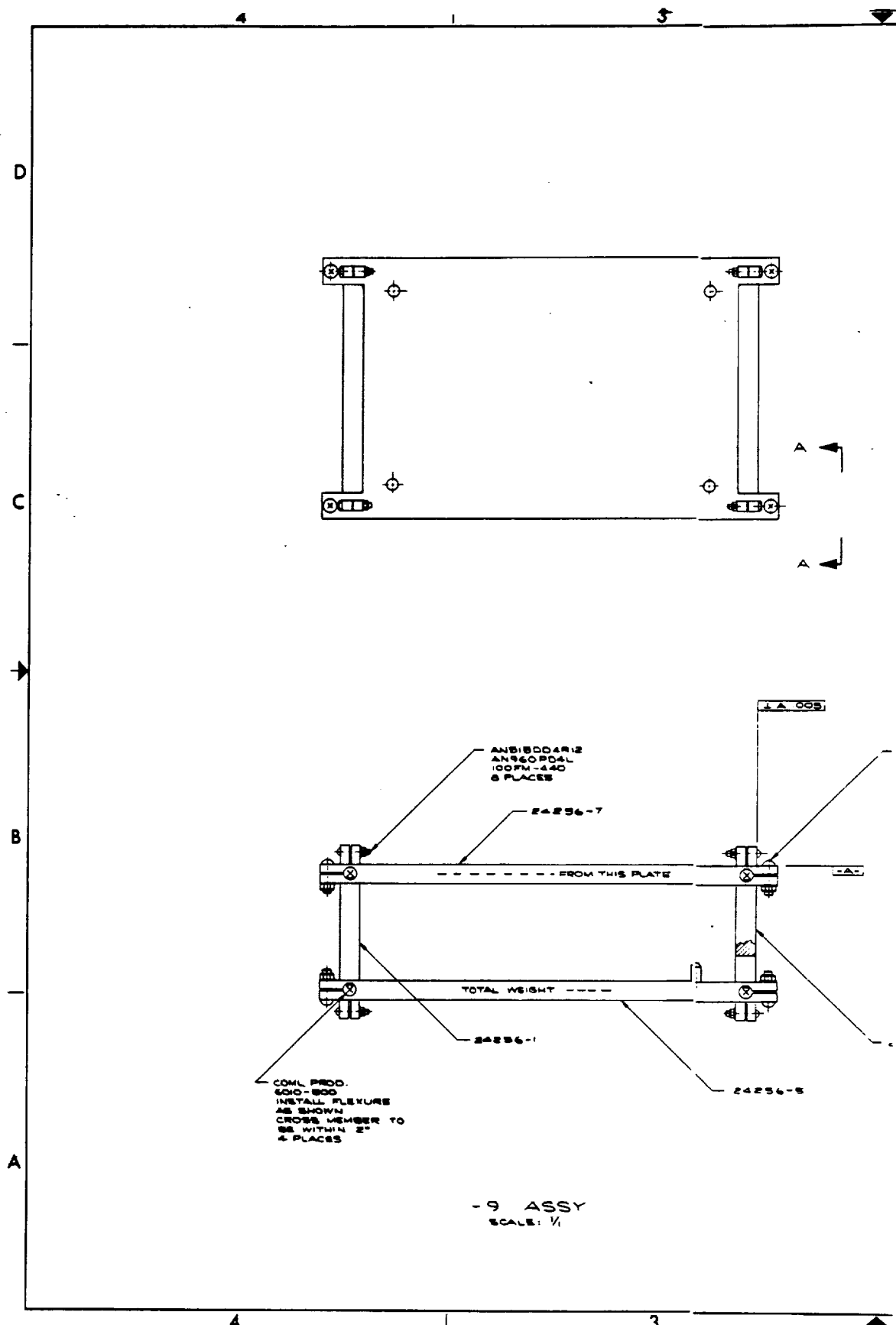
-33 DETAIL
SCALE: 1/4"





ACCURATE ALIGNMENT
2 THE CALIBRATION

Preceding page blank



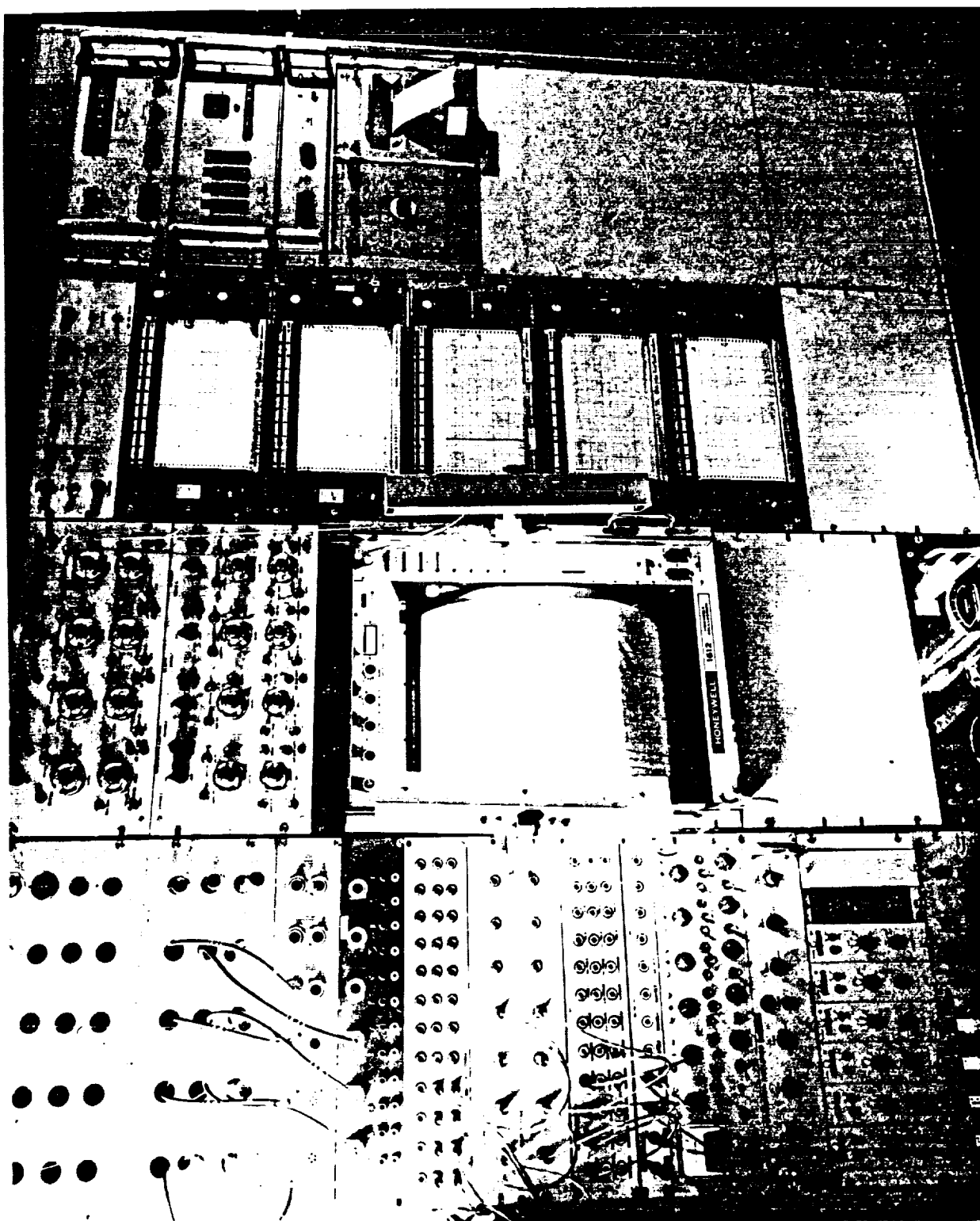
Instrumentation used for measurement of the indicated engine performance parameter is summarized below:

- a. Turbine flowmeters (two (2) in-series meters) manufactured by Cox Instrument Division, Lynch Corporation, were used for engine flow rate measurement. The following model numbers were used:
 - 1. 0.5 lbf Engine - Model No. LF6-00
 - 2. 5.0 lbf Engine - Model No. LF6-3
 - 3. 50 lbf Engine - Model No. AN8-6
- b. Alinco pressure transducers manufactured by M. B. Electronics are used for chamber pressure and tank pressure measurement. The following ranges and model numbers were used:
 - 1. 0 - 200 psia - Model No. 151-BAA-1
 - 2. 0 - 500 psia - Model No. 151-BAA-1
 - 3. 0 - 1500 psia - Model No. 151-AAA-1
- c. Load cells manufactured by Schaevitz-Bytrex Corporation are used for measurement of engine thrust. The following load cells were used:
 - 1. 0.5 lbf Engine - Model No. A-61441-1
 - 2. 5.0 lbf Engine - Model No. A-6144-4
 - 3. 50 lbf Engine - Model No. A-61441-8
- d. Catalyst bed temperature is measured using chromel-alumel thermocouples of 0.040 inches wire diameter with ungrounded tips. The same thermocouple is also used for propellant temperature measurement.

Three data recovery systems are utilized for recording of the data from the engine tests. All pressures, thrust, flow rate, and valve sequencing are recorded on a 36 channel Honeywell Model 1612 oscillograph. All pressure, thrust, and temperature measurements are recorded on Moseley strip charts. Additionally, pressure and temperature measurements are recorded and printed out on a Dymec Model 2010A digital system. The data recording system is shown in Figure 13.

5.4 Test Procedures

Prior to engine hot firings each injector was water flow calibrated to determine its pressure drop-flowrate characteristics. Additionally, random orifices



DATA RECORDING SYSTEM

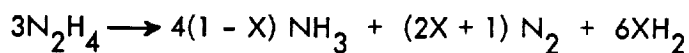
were individually sampled to assure that no gross maldistribution of flow existed from individual orifices. In no case did the flow out of any orifice deviate more than 5% from the average.

The catalyst bed was packed in a random dense manner (see Volume II, Section 5.0) in the chamber for all tests. The weight of catalyst packed was accurately measured and compared with the predicted values based on previous catalyst bed packing studies. If gross differences existed, the bed was repacked.

Each test was conducted under ambient temperature and pressure conditions. All tests represented steady state runs of 30 to 40 seconds duration.

For each test conducted during the study of reactor design variables, a gas sample of the decomposition products was obtained. Specifically, when the catalyst bed and gas temperature reached steady state, a gas sample, taken immediately downstream of the catalyst bed, was drawn into an evacuated Hoke gas sample cylinder. The gas was then analyzed for the mole percent of ammonia, nitrogen and hydrogen by use of a gas chromatograph.

The hydrazine decomposition can be expressed as:



Three mole ratios, i.e., ratio of ammonia to hydrogen, ammonia to nitrogen, and nitrogen to hydrogen may be related to fractional ammonia dissociation, X , on the basis of the above equation; this permits calculation of fractional ammonia dissociation from gas sample analysis data. Ammonia dissociation is reported as the average of that determined from the ammonia to hydrogen and ammonia to nitrogen mole ratios. The deviation between these two calculated values was, in most cases, less than 2%.

Periodically a sample of the catalyst was removed from the reactor and measurements were made of the carrier and active metal surface areas to determine changes with use. Carrier surface area was measured by nitrogen adsorption techniques and active metal surface area was measured by hydrogen chemisorption.

All granular and cylindrical pellet size catalyst used in the injector optimization testing was manufactured from the Harshaw Alumina Carrier. For the catalyst bed design parameter studies the granular catalyst was manufactured from the Reynolds Alumina Carrier.

6.0 INJECTOR OPTIMIZATION TEST RESULTS

6.1 Data Reduction Techniques

Data reduction for the injector optimization tests consisted of determination of engine ignition delay time, chamber pressure rise time to 80% of steady state value, chamber pressure decay time to 10% of steady state value, chamber pressure roughness, characteristic velocity, specific impulse, and thrust coefficient. In addition, catalyst bed, injector head, and propellant temperatures were measured during each test. The techniques used in the data reduction are explained in the ensuing paragraphs.

Ignition delay is defined as the time from entry of propellant into the chamber until the chamber pressure downstream of the catalyst bed attains 1% of its steady state value. On engine start, the feed pressure (measured just upstream of the propellant valve) drops off momentarily as the ullage volume between the valve and injector is filled. The point at which this pressure begins to rise after dropping off is defined as the time when propellant begins to enter into the chamber. Ignition delay is then the time increment between the beginning of feed pressure rise and downstream chamber pressure rise. This parameter is obtained from the oscillograph record.

Chamber pressure rise time is defined as the time from propellant entry into the chamber to achievement of 80% steady state chamber pressure. The 80% value is taken as a percentage of the steady state chamber pressure downstream of the catalyst bed expressed in absolute units. Rise time to 80% of steady state chamber pressure was selected in lieu of 90% because it appeared to be a more consistent parameter. During the engine testing rise times to 90% chamber pressure averaged 2.7 times those to 80%. Chamber pressure decay time is defined as the time from downstream chamber pressure start decay to 10% of the steady state value measured in psig units.

Chamber pressure roughness is defined as the peak-to-peak variations in the chamber pressure downstream of the catalyst bed. The data is taken off the oscillograph at a run time between 20 and 30 seconds unless otherwise noted.

Characteristic velocity is calculated from the equation:

$$c^* = \frac{P_{cd} A_t g}{\dot{w}}$$

Where:

- c^* = Characteristic velocity, ft/sec
- A_t = Engine throat area, in²
- g = Gravitational constant, 32.17 ft/sec²
- \dot{w} = Propellant flow rate, lbm/sec
- P_{cd} = Chamber pressure downstream of the catalyst bed, psia.

The engine throat area used in the calculations represents the average geometric area with corrections made for the thermal expansion and nonuniform flow conditions in the throat region caused by nozzle wall effects. The correction for thermal expansion was made assuming the throat diameter expands freely based on the metal temperature at the throat. The correction for nonuniform flow at the throat is treated by Rao (Reference 1) and results in a decrease in the geometric area of 0.75%. The flow rate used in the equation is an average of two flowmeters in series in the propellant supply line.

Engine specific impulse is calculated from the equation:

$$I_{sp} = \frac{F_m}{\dot{w}}$$

Where:

- I_{sp} = Engine specific impulse, lbf-sec/lbm
- F_m = Measured thrust, lbf
- \dot{w} = Propellant flow rate, lbm/sec

The propellant flow rate used in the above equation is again an average of two flowmeters in series.

The engine thrust coefficient is calculated from the equation:

$$C_f = \frac{F_m}{P_{cd} A_t}$$

Where:

- C_f = Engine thrust coefficient
- F_m = Measured thrust, lbf
- P_{cd} = Chamber pressure downstream of the catalyst bed, psia
- A_t = Engine throat area, in²

Again, the same corrections are applied to the throat area as discussed under the characteristic velocity calculations.

Characteristic velocity, specific impulse, and the thrust coefficient are all calculated from average values of measurements taken from 29 to 30 seconds into the test.

As a first step in determination of the effect of injector variables on cold bed response times, ignition delay, chamber pressure decay time, and chamber pressure roughness scatter diagrams of the data were plotted (Reference 2). In the scatter diagram each separate factor is plotted without considering any other factor. The scatter diagram points out significant trends without lengthy correlation analysis. Subsequently, statistical tests were made of the data for determination of levels of significance in trends noted from the scatter diagram. If a complete test matrix was completed, a factorial analysis of variance was performed on the data to determine levels of significance and to determine interactions which may exist between the injector variables (Reference 2). When a complete test matrix was not completed, "F" tests were conducted to determine levels of significance (Reference 2).

6.2 Test Results

6.2.1 0.5 lbf Showerhead Injector

Testing of the 0.5 lbf showerhead injector engine is summarized in Table IV. Tests were conducted at pressure drops of 15, 45, and 75 psid with the injector flush with the catalyst bed and at 15 and 45 psid with the injector 0.2 inches from the bed. For all of these tests, 20-25 mesh granular catalyst was used in the catalyst bed. The test results are plotted in a scatter diagram in Figure 14 and are described in the ensuing paragraphs.

TABLE IV
0.5 LBF ENGINE - TEST DATA SUMMARY - SHOWERHEAD INJECTOR

Test No.	Test Code (1)	Fuel Temperature °F	Initial Catalyst Bed Temperature °F	Ignition Delay ms.	Response Time ms.	Decay Time ms.	Injection Pressure psia	Chamber Pressure psia	Thrust lbf	Flow Rate lbm/sec	Steady-State Catalyst Bed Temperature °F	Characteristic Velocity ft/sec	Specific Impulse lbf-sec/lbm (2)	Thrust Coefficient (2)	Chamber Pressure Roughness % Peak-to-peak
171-31-2	15-0	59	59	4	80	---	165.0	137.1	0.354	0.002366	1428	4171	149.6	1.154	± 4.60
171-31-12	15-0	67	67	5	83	---	176.7	152.7	0.395	0.002620	1494	4195	150.8	1.156	± 4.30
171-31-13	15-0	65	66	10	118	167	173.0	150.7	0.391	0.002622	1560	4140	149.2	1.159	± 7.20
171-31-3	45-0	67	66	4	245	144	210.7	148.7	0.383	0.002550	1407	4193	150.2	1.152	± 2.50
171-31-4	45-0	64	66	10	454	144	210.7	149.5	0.382	0.002600	1424	4139	146.9	1.142	± 2.60
171-31-7	45-0	63	67	7	245	118	214.5	151.0	0.390	0.002613	1396	4160	149.4	1.155	± 2.68
171-31-8	45-0	63	68	10	285	128	213.2	150.5	0.393	0.002640	1409	4147	150.6	1.168	± 2.36
171-31-5	75-0	63	63	12	410	143	240.2	145.1	0.374	0.002561	1490	4078	146.1	1.152	± 1.90
171-31-6	75-0	63	63	22	637	116	242.7	147.5	0.382	0.002526	---	4203	151.2	1.157	± 1.60
171-31-9	75-0	69	71	15	510	140	242.7	147.2	0.381	0.002553	1472	4150	149.2	1.157	± 1.50
171-31-10	75-0	67	67	13	630	130	244.2	149.5	0.390	0.002559	1494	4205	152.4	1.166	± 1.65
171-31-11	75-0	65	65	18	550	118	241.0	146.7	0.381	0.002537	1481	4162	150.2	1.161	± 1.85
171-31-14	15-2	62	62	42	240	404	174.2	148.2	0.384	0.002548	1430	4186	150.7	1.158	± 3.6
171-31-15	15-2	62	64	26	160	---	172.7	150.9	0.391	0.002608	1506	4165	149.9	1.158	± 3.6
171-31-16	45-2	71	73	56	730	146	214.0	152.2	(3)	(3)	1486	(3)	(3)	(3)	± 13.2
171-31-17	45-2	68	71	23	680	387	210.2	150.9	(3)	(3)	1566	(3)	(3)	(3)	± 6.63

(1) First number refers to nominal injector pressure drop. Second number refers to distance of injector from top of catalyst bed.

(2) Nozzle Expansion Ratio is 3.5:1

(3) Chamber excursions too large to obtain steady-state data.

Examination of the scatter diagram in Figure 14 indicates that the cold bed response times increase as the injector pressure drop is increased. The average response time (average of data at each pressure drop) is plotted versus injector pressure drop in Figure 15. It is also noted from the scatter diagram that ignition delay increases as the injector pressure drop is increased. A plot of average ignition delay versus injector pressure drop is shown in Figure 16. Chamber pressure roughness declines as injector pressure drop is increased. This trend is shown in Figure 17. Chamber pressure decay time does not appear to be affected by injector pressure drop.

Significant changes in reactor operation were noted when the injector was moved 0.2 inches from the top of the catalyst bed. Cold bed response, ignition delay, and chamber pressure decay times increased markedly as is seen from the data in Table IV. At 15 psid pressure drop fairly smooth ($\pm 3.6\%$ peak-to-peak chamber oscillations) operation was obtained. However, at 45 psid injector pressure drop, chamber pressure oscillations were large. Because of these large oscillations in chamber pressure no tests were conducted at 75 psid injector drop.

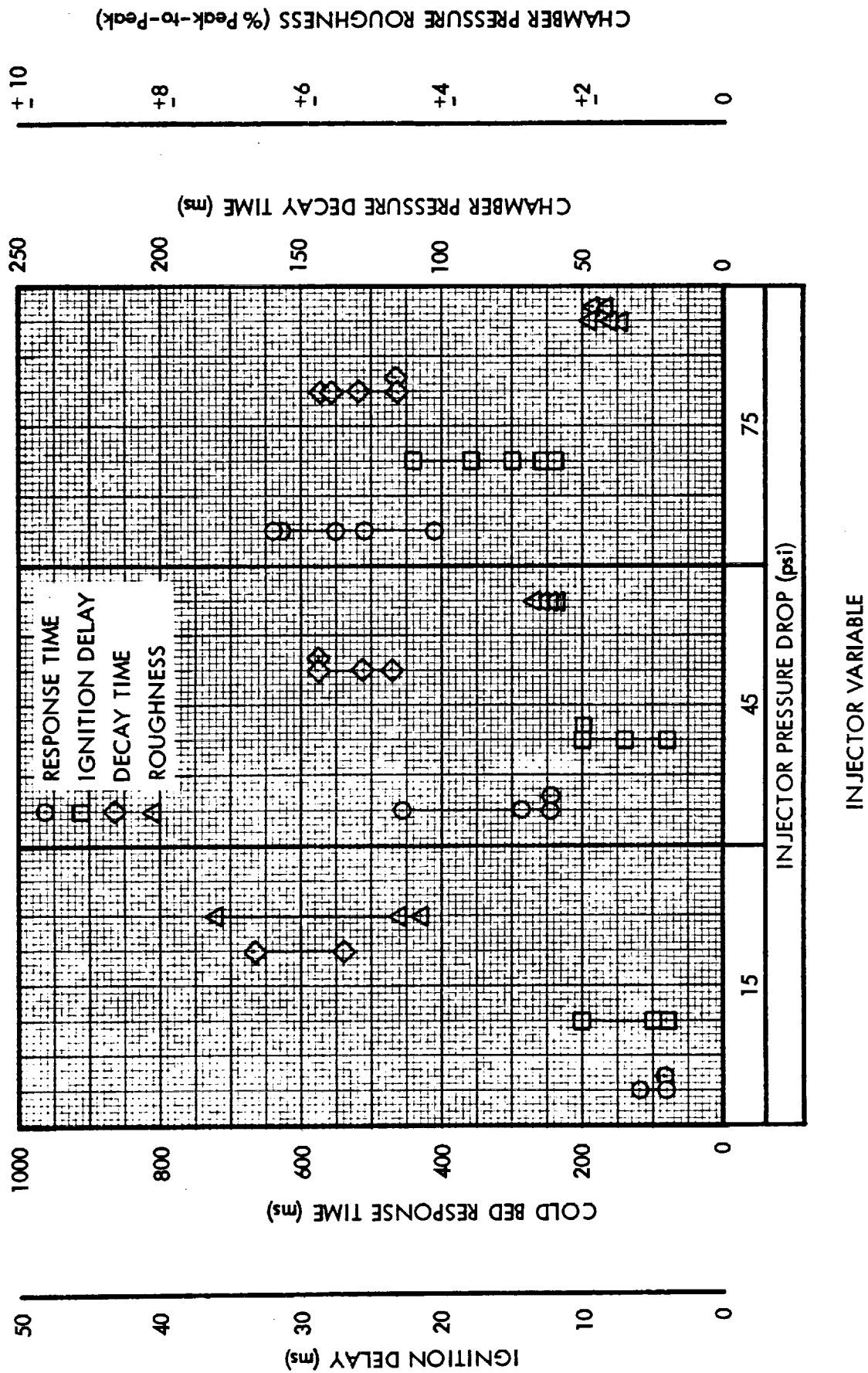
No observable change in performance was noted as the injector parameters were varied. Characteristic velocity averaged 4,164 feet per second, specific impulse averaged 149.7 lbf-sec/lbm, and the thrust coefficient averaged 1.157.

6.2.2 0.5 lbf Engine Rigimesh Injector

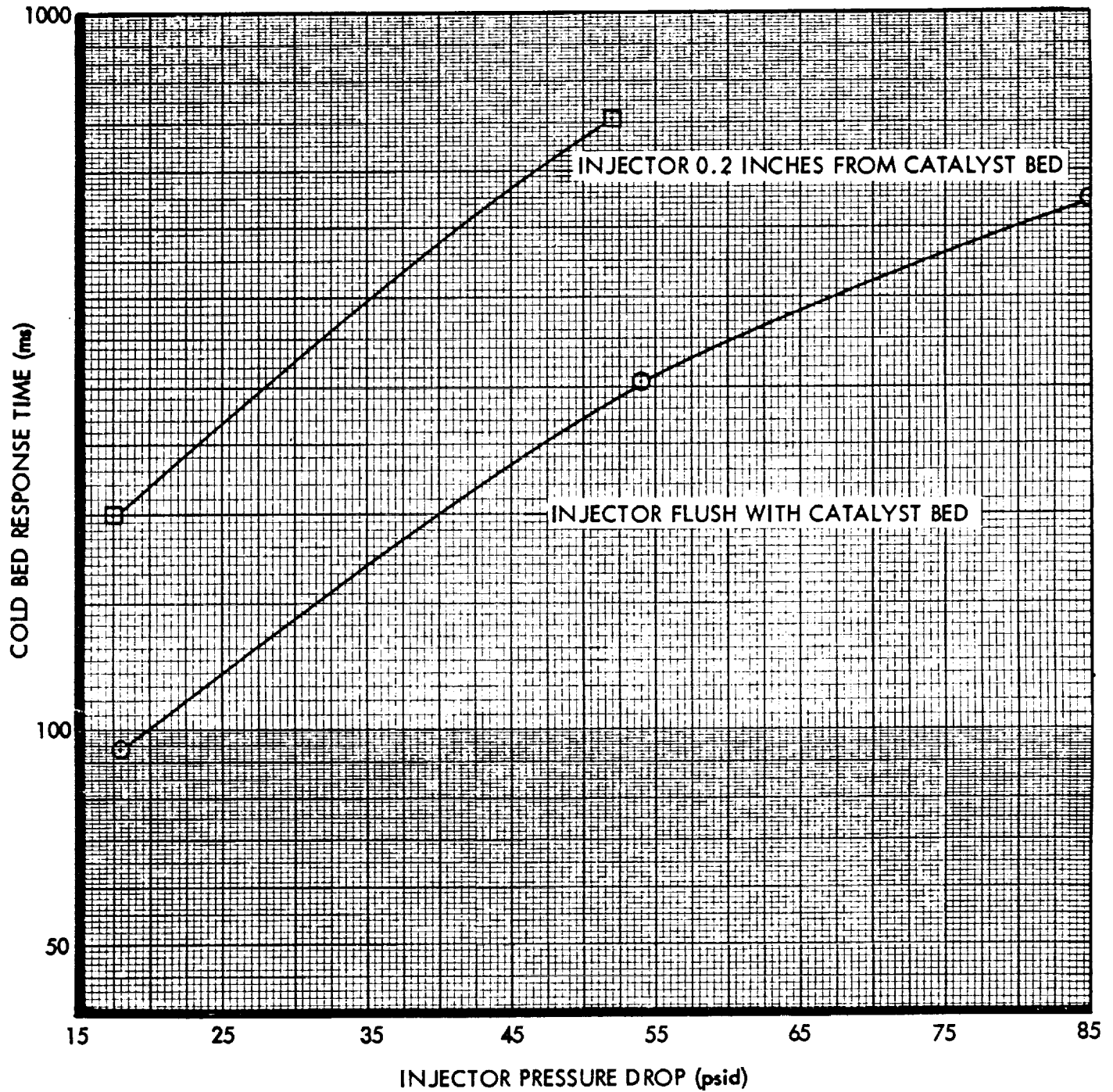
Testing of the 0.5 lbf rigimesh injector engine is summarized in Table V. Tests were conducted at pressure drops of 15, 45, and 75 psid with the injector flush with the catalyst bed and at 75 psid with the injector away from the catalyst bed. Data obtained from the testing is plotted in the scatter diagram in Figure 18. The results of this testing are described in the following paragraphs.

Examination of the scatter diagram indicates an increase in cold bed response time with pressure drop. The average response time is plotted in Figure 19, versus injector pressure drop. The scatter diagram in Figure 18 indicates ignition delay times are lower at 15 psid injector pressure drop

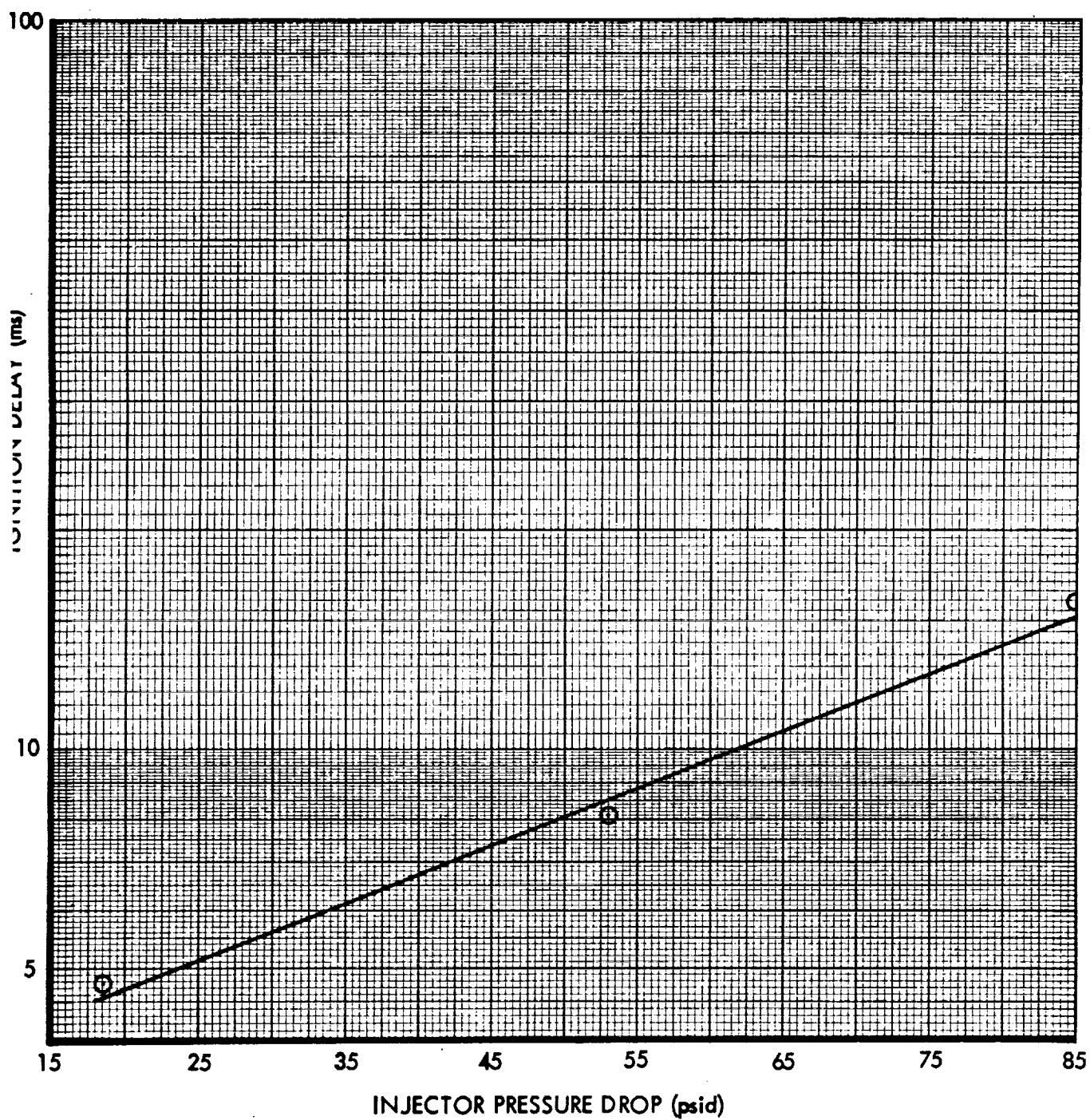
0.5 lbf ENGINE SHOWERHEAD INJECTOR SCATTER DIAGRAM



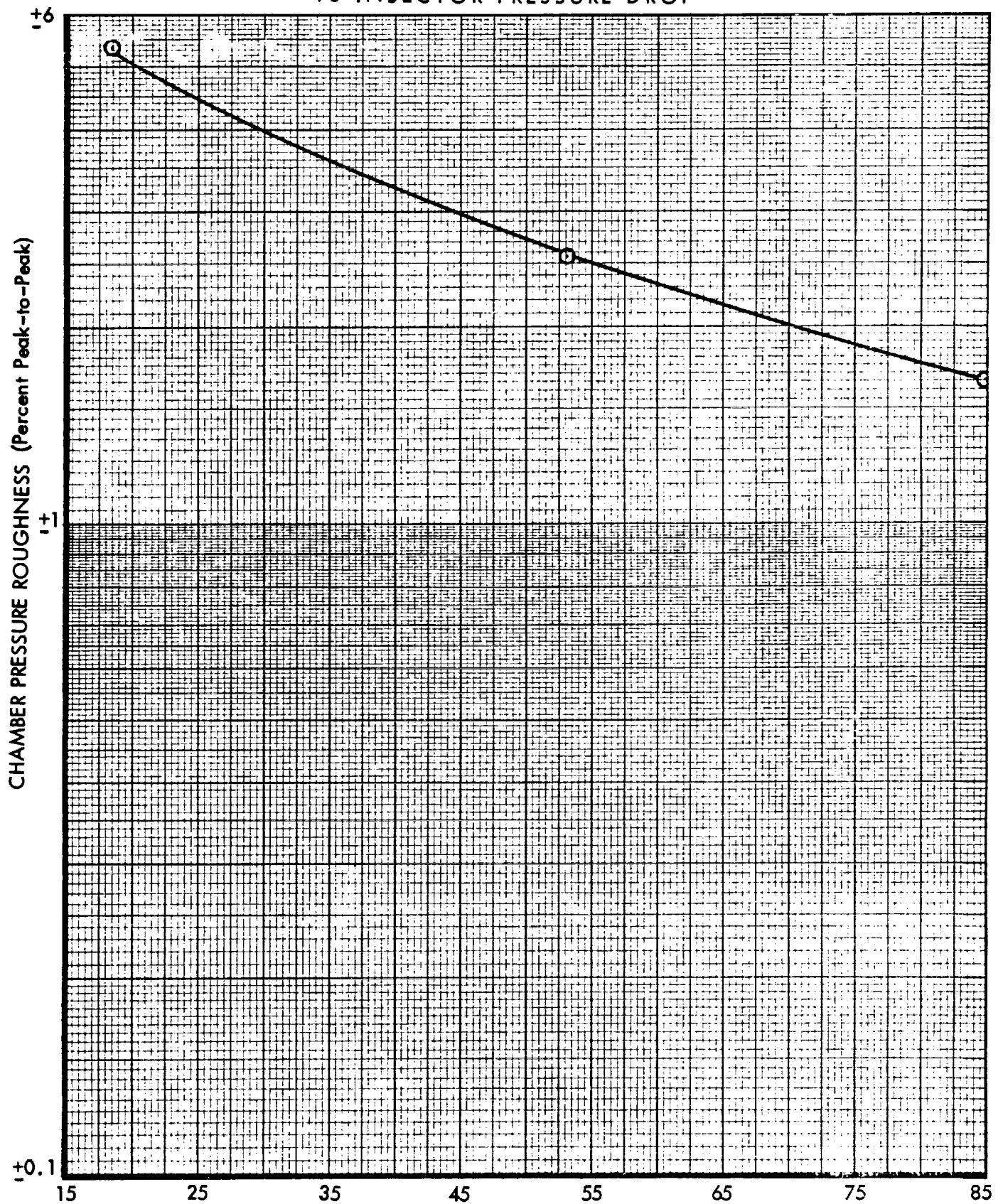
0.5 lbf ENGINE
SHOWERHEAD INJECTOR
AVERAGE COLD BED RESPONSE TIME
VS
INJECTOR PRESSURE DROP



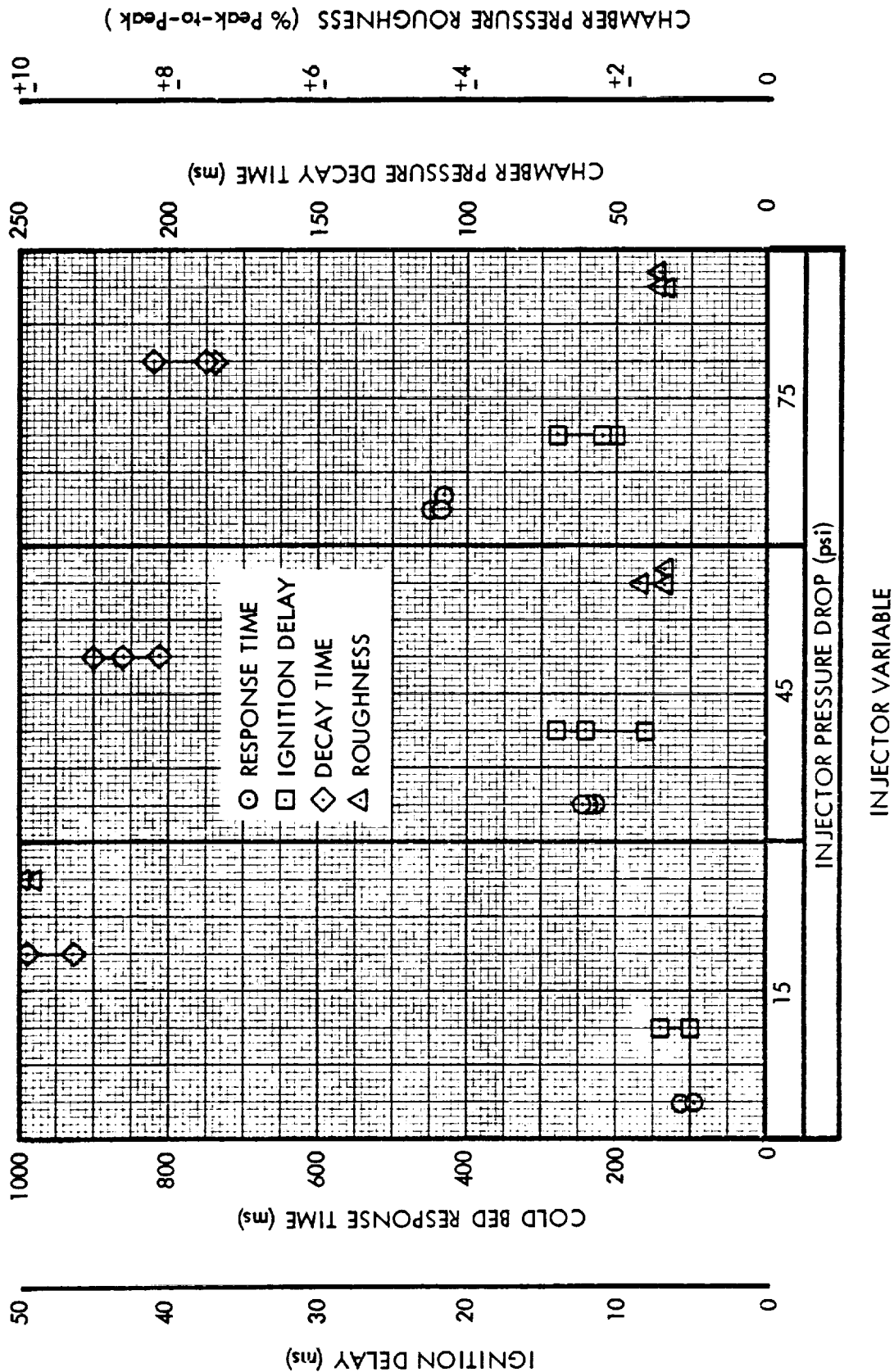
0.5 lbf ENGINE
SHOWERHEAD INJECTOR
AVERAGE IGNITION DELAY
VS
INJECTOR PRESSURE DROP



0.5 lbf ENGINE SHOWERHEAD INJECTOR
AVERAGE CHAMBER PRESSURE ROUGHNESS
VS INJECTOR PRESSURE DROP



0.5 lbf ENGINE RIGIMESH INJECTOR SCATTER DIAGRAM



0.5 lbf ENGINE RIGIMESH INJECTOR AVERAGE COLD BED
RESPONSE TIME VS INJECTOR PRESSURE DROP

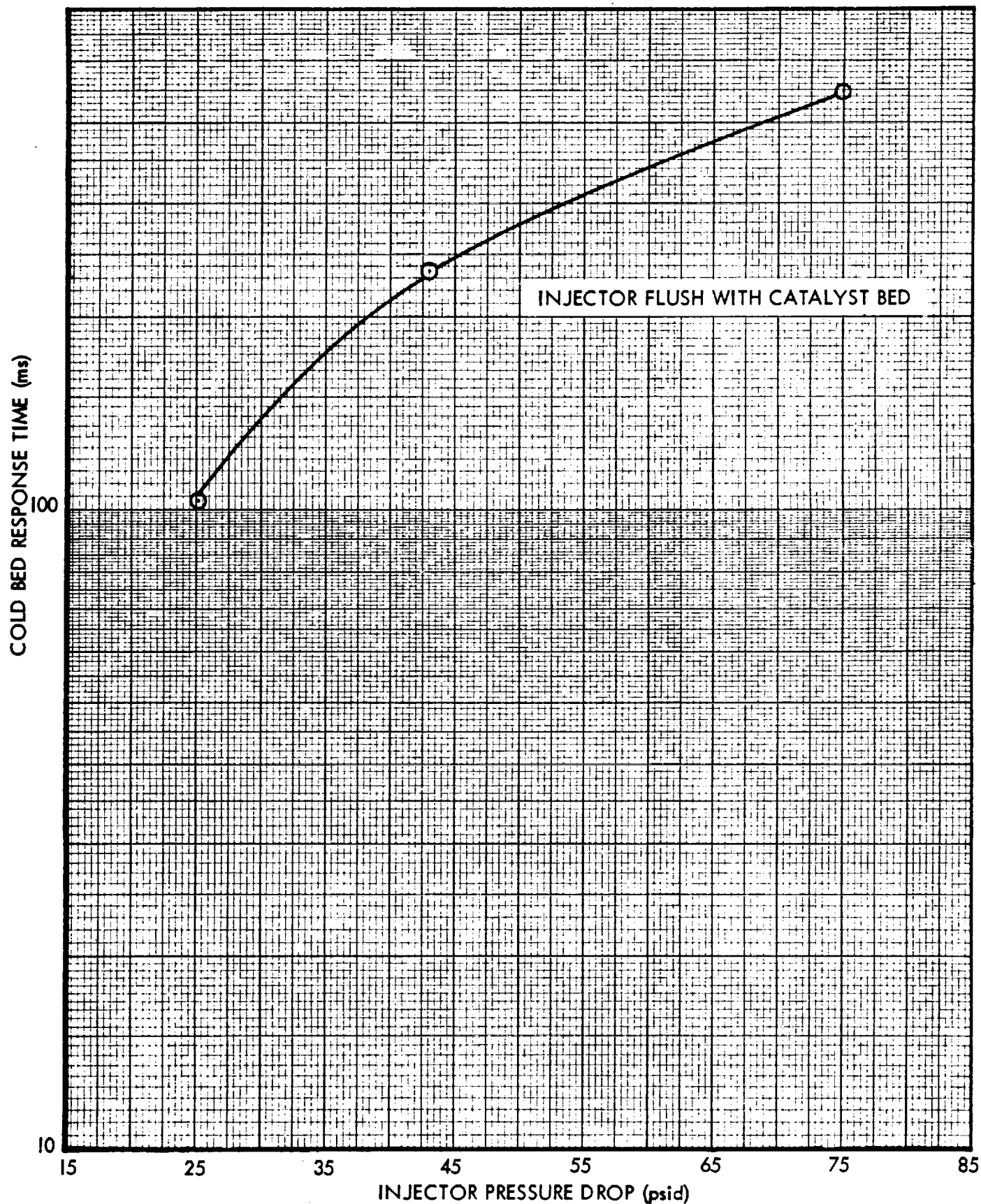


TABLE V
0.5 LBF ENGINE - TEST DATA SUMMARY - KIGIMESH INJECTOR

Test No.	Test Code	Fuel Temperature °F	Initial Catalyst Bed Temperature °F	Ignition Delay ms.	Response Time ms.	Decay Time ms.	Injection Pressure psia	Chamber Pressure psia	Turns lbf	Flow Rate lbn/sec	Steady-State Catalyst Bed Temperature °F	Characteristic Velocity ft/sec	Specific Impulse lbf-sec/lbm (4)	Thrust Coefficient (4)	Chamber Pressure Knockness % Pea -to-peak
171-31-83	15-0	55	57	7	95	232	181.0	152.3	(2)	(2)	1391	(7)	(2)	(2)	± 19.70
171-31-85	15-0	65	67	5	112	247	181.0	151.1	(2)	(2)	1381	(2)	(2)	(2)	± 20.00
171-31-80	45-0	61	61	8	235	225	198.1	161.4	0.426	0.002731	1400	4196	153.2	1.174	± 3.39
171-31-81	45-0	59	64	14	244	203	194.7	153.6	0.408	0.002714	1415	4149	151.1	1.165	± 2.72
171-31-82	45-0	59	61	12	270	215	195.1	150.2	0.405	0.002706	-----	4165	150.1	1.161	± 2.74
171-31-76	75-0	55	58	14	435	205	242.8	164.3	0.432	0.002910	1437	4188	152.4	1.176	± 2.74
171-31-77	75-0	55	57	11	431	135	233.4	155.5	0.413	0.002576	1460	4190	154.3	1.192	± 2.82
171-31-78	75-0	55	58	10	450	187	227.5	153.2	0.411	0.002628	1452	4190	154.1	1.183	± 2.87
171-31-86	75-2	65	67	45	(-)	(-)	24.7	(2)	(2)	(2)	1351	(2)	(2)	(2)	± 27.10

(1) First number refers to nominal injector pressure drop. Second number refers to distance of injector from row of catalyst bed.

(2) Chamber pressure excursions too large to obtain steady-state data.

(3) Start and shutdown erratic.

(4) Nozzle Expansion Ratio is 3.5:1

(average value 6 ms) than at 45 or 75 psid pressure drop (average value 12 ms). The scatter diagram also shows a decrease in chamber pressure decay time as injector pressure drop is increased. Very high chamber pressure oscillations were obtained with the 15 psid injector ($\pm 20\%$ peak-to-peak) while smooth operation (± 2.7 to $\pm 2.80\%$) was obtained at 45 psid and 75 psid.

Testing of the injector away from the catalyst bed produced very erratic operation and long response and tailoff times. Additionally, chamber pressure excursions of $\pm 27\%$ peak-to-peak occurred. This erratic operation may well be the result of the poor spray pattern out of the injector. The spray pattern was not axial and impingement of propellant on the chamber walls probably occurred giving rise to the erratic operation.

Characteristic velocity for the tests averaged 4,179 feet per second, specific impulse averaged 152.7 lbf-sec/lbm, and the thrust coefficient averaged 1.174.

In comparing the rigimesh injector test results with the showerhead injector, the following conclusion can be made:

- a. Cold bed response times are very similar
- b. Variations in ignition delay with pressure drop are not as large with the rigimesh injector as with the showerhead injector.
- c. The showerhead injector runs smoother than the rigimesh injector at all injector pressure drops, although at 45 psid the results are very similar.
- d. Decay times are higher with a rigimesh injector design than the showerhead.

6.2.3 5 lbf Engine Showerhead Injector

Testing on the 5 lbf engine with the showerhead injector was in accordance with the test matrix shown in Figure 1. The first test on the 5 lbf engine used a catalyst bed composed of 10-12 mesh granular particles. During the test, cyclic oscillations occurred in the chamber pressure of 20 to 50 psia at a frequency of 13 to 18 cps. Several variables were tested which could possibly have led to the instability noted. These variables included:

- a. Nonstable orifice characteristics
- b. Injector manifolding which could lead to (a) above
- c. Feed system coupling
- d. Channeling of flow in the catalyst bed
- e. Hydrazine boiling in the injector manifold
- f. Nonstable flame front in the catalyst bed
- g. Bed loading
- h. Catalyst particle size and/or porosity.

Testing covering the above variables resulted in elimination of the first five items as the cause of the instability. The instability was found to be due to a nonstable flame front in the catalyst bed. The flame front was stabilized by use of fine mesh catalyst on top of the catalyst bed. The fine mesh catalyst has a higher specific surface area and apparently stabilized the flame front near the top of the catalyst bed. The testing conducted on determination of the cause of the instability is described in the ensuing paragraphs.

During water flow calibrations of the showerhead injectors, it was noted that fully established turbulent streams were not being achieved and that stream breakup and oscillatory flow was occurring. Also, at certain pressure drops, approximately $\pm 5^\circ$, angular movement of the stream occurred. It was concluded that a possible "hydraulic flip" phenomena was taking place in the orifices. This phenomena was alleviated by increasing the orifice length to diameter ratio from 2.5 to 8.5, contouring the orifice entrance and decreasing the velocity in the line feeding the manifold from 15 to 4 feet per second. All three of the aforementioned changes were accomplished individually and changes were noted in stream properties with each change in the injector or manifold configuration. However, none of the changes had any significant effect on the operating characteristics of the engine.

Changing the number of orifices from 1 to 9, and therefore propellant mass distribution in the bed, did not affect the operation of the engine. Changing the injector pressure drop did not appear to result in any changes in engine

operation except for one test with a 75 psid injector which did run smoothly. However, this test could not be subsequently duplicated.

Three additional thermocouples were added in the catalyst bed to define the location of the flame front. For the majority of the tests, their locations were as follows:

T_{B1} - 0.5 inches from top of bed

T_{B2} - 0.88 inches from top of bed

T_{B3} - 1.35 inches from top of bed

T_{B4} - At the outlet of the bed.

On almost all tests instrumented in this fashion, the temperature reached steady state values within two to three seconds and was very stable with the upper bed temperature reading the highest value. For most of the tests, the thermocouples were located radially in the center of the bed. When the thermocouples were placed near the chamber wall (approximately 0.1 inches from the wall), the temperature measurements were not markedly different from the middle of the bed location, and based on this data, channeling of the flow down the chamber wall was eliminated as a possible cause of the instability.

Analysis and testing of other variables including feed system variations, reduction of propellant manifold volume, changes in manifold velocity, and changes in catalyst size from 10-12 mesh to 12-16 mesh did not produce significant changes in engine operation.

When 0.3 inches of 20-25 mesh catalyst was placed at the top of the catalyst bed, with the remainder of the bed 12-16 mesh catalyst, stable engine operation was obtained. The conclusion was that there was a flame front instability which was not observable from the thermocouple measurements. One would suspect that determination of a flame front instability from thermocouple measurements would be extremely hard to observe. The fine mesh catalyst apparently supplies sufficient additional catalyst external surface area to stabilize the flame front on ignition. The 0.3 inches of 20-25 mesh catalyst with the remainder of the catalyst bed composed of 12-16 mesh particles, was the bed configuration utilized for all injector optimization testing.

Subsequent to the instability testing, data was received from Shell Development Company which raised a question concerning the cause of the instability. Catalyst for the program was procured in mesh sizes ranging from 6 to 40. The catalyst in the 10 to 40 mesh size was manufactured at one time in a single lot. The average metal content of the lot was 32.8 percent which was within the specification limits of 32 to 34 percent. However, when the 10 to 40 mesh catalyst was screened into mesh sizes of 10 to 20, 20 to 30, and 30 to 40, the following metal contents were obtained by analysis of the catalyst:

10-20 mesh	25.6%
20-30 mesh	33.6%
30-40 mesh	42.0%

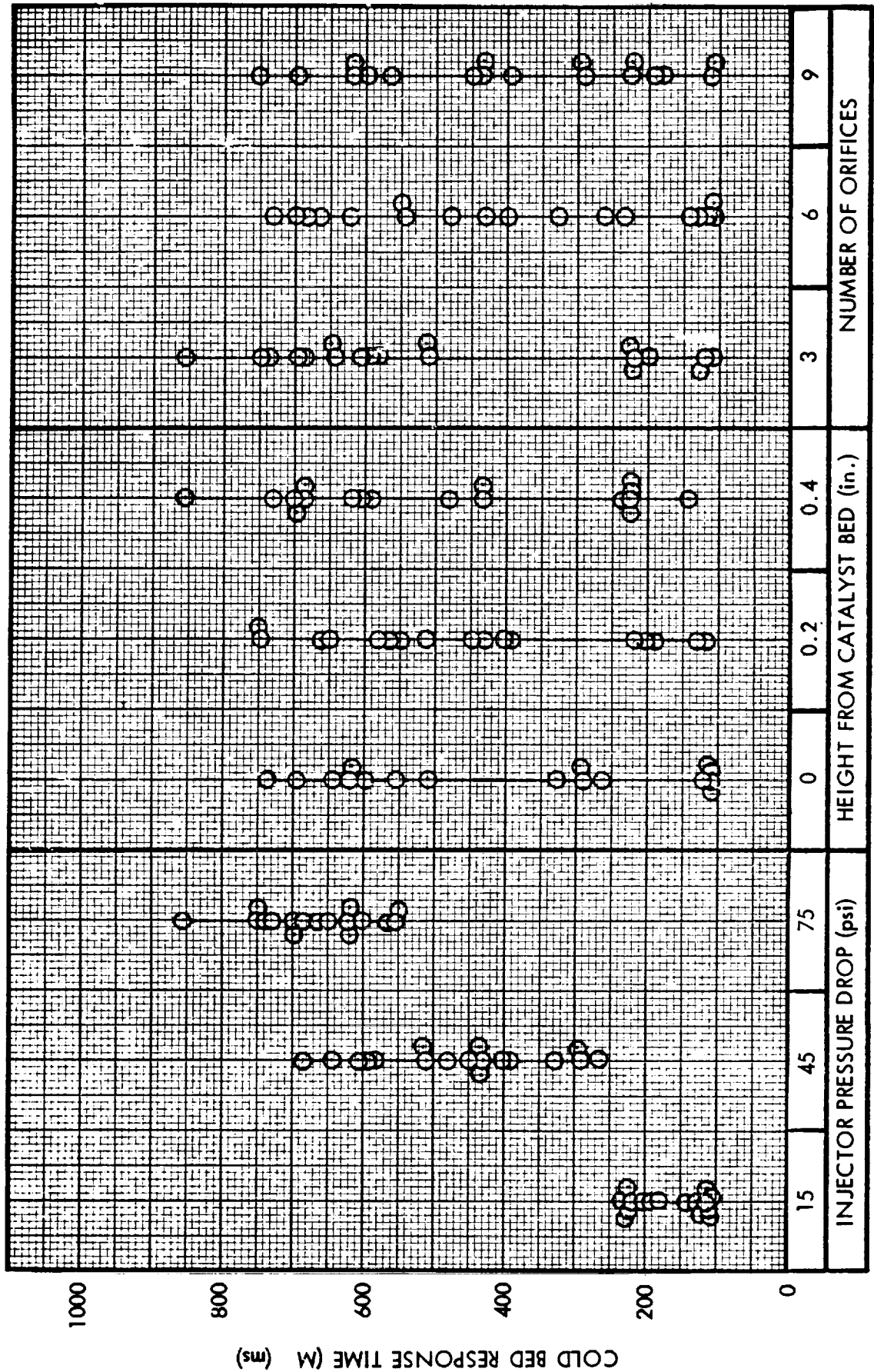
Plotting the above data and extrapolating to 10 to 12 and 12 to 16 mesh catalyst, which was used in the instability tests, gives metal contents of 22 and 25 percent respectively. It was thought that perhaps the reduced metal content led to a reduction in catalyst activity and was the cause of the instability. Subsequent testing on the 50 lbf engine with other catalyst proved this hypothesis to be wrong, since the same type of instability occurred. It is obvious that manufacture of catalyst over a wide range of mesh sizes should not be accomplished in a single lot of catalyst since the fine mesh catalyst appears to absorb the active metals faster than the coarser mesh catalyst.

The data obtained from the showerhead injector testing is summarized in Table VI. Scatter diagrams for the reactor variables of ignition delay, cold bed response time, chamber pressure roughness, and chamber pressure decay times are plotted in Figures 20 through 23 as a function of the injector variables. A factorial analysis of variance was performed on the data presented in each of the scatter diagrams. This allowed determination of which injector variable(s) has an effect on the reactor variable in question and also determination of interactions which exist between the injector variables. The results of these analyses are discussed in the ensuing paragraphs.

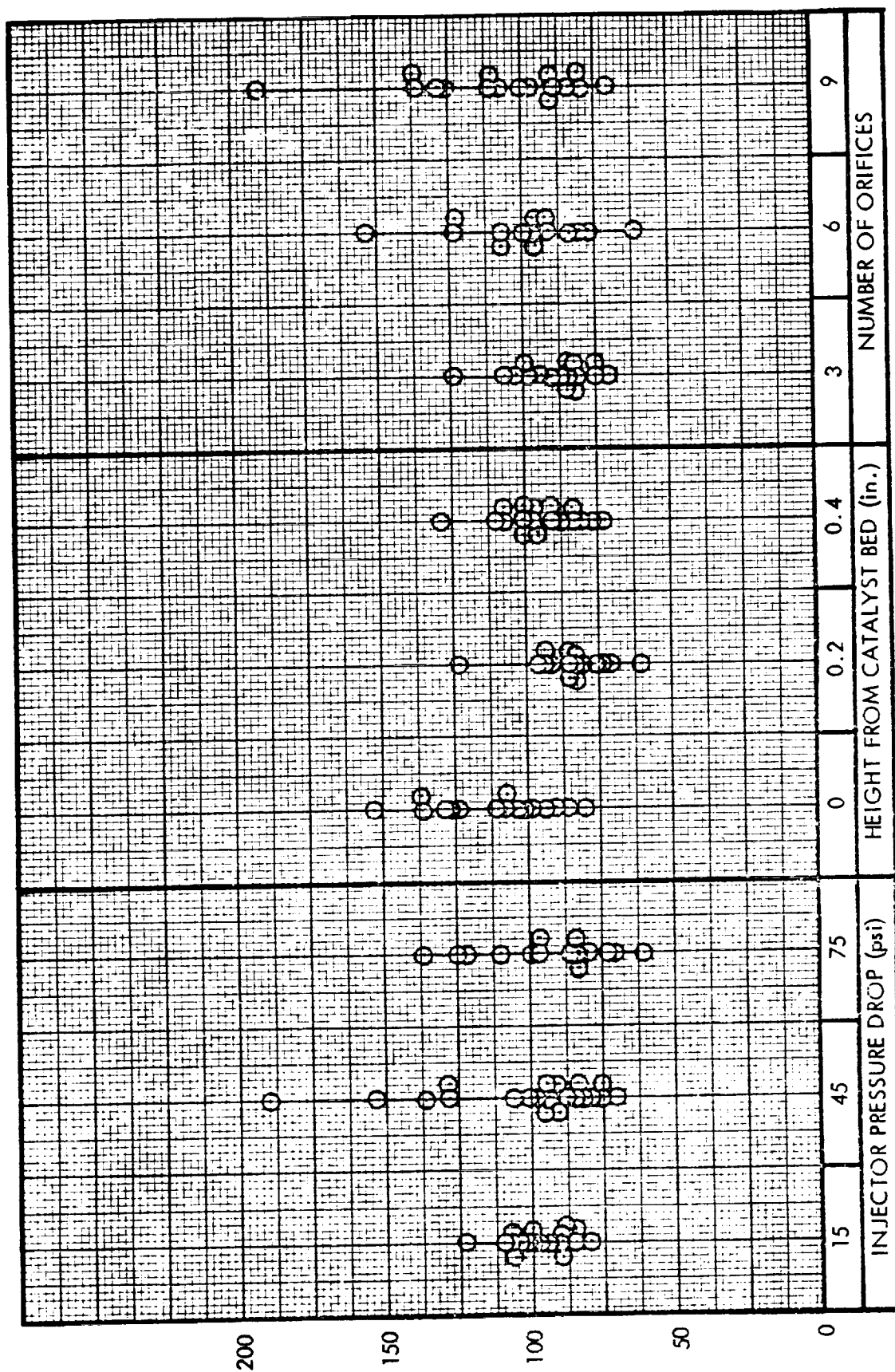
The analysis of variance conducted for the cold bed response time resulted in the following significant effects:

- a. Cold bed response time is affected by injector pressure drop

5 lb ENGINE SHOWERHEAD INJECTOR SCATTER DIAGRAM COLD BED RESPONSE TIME



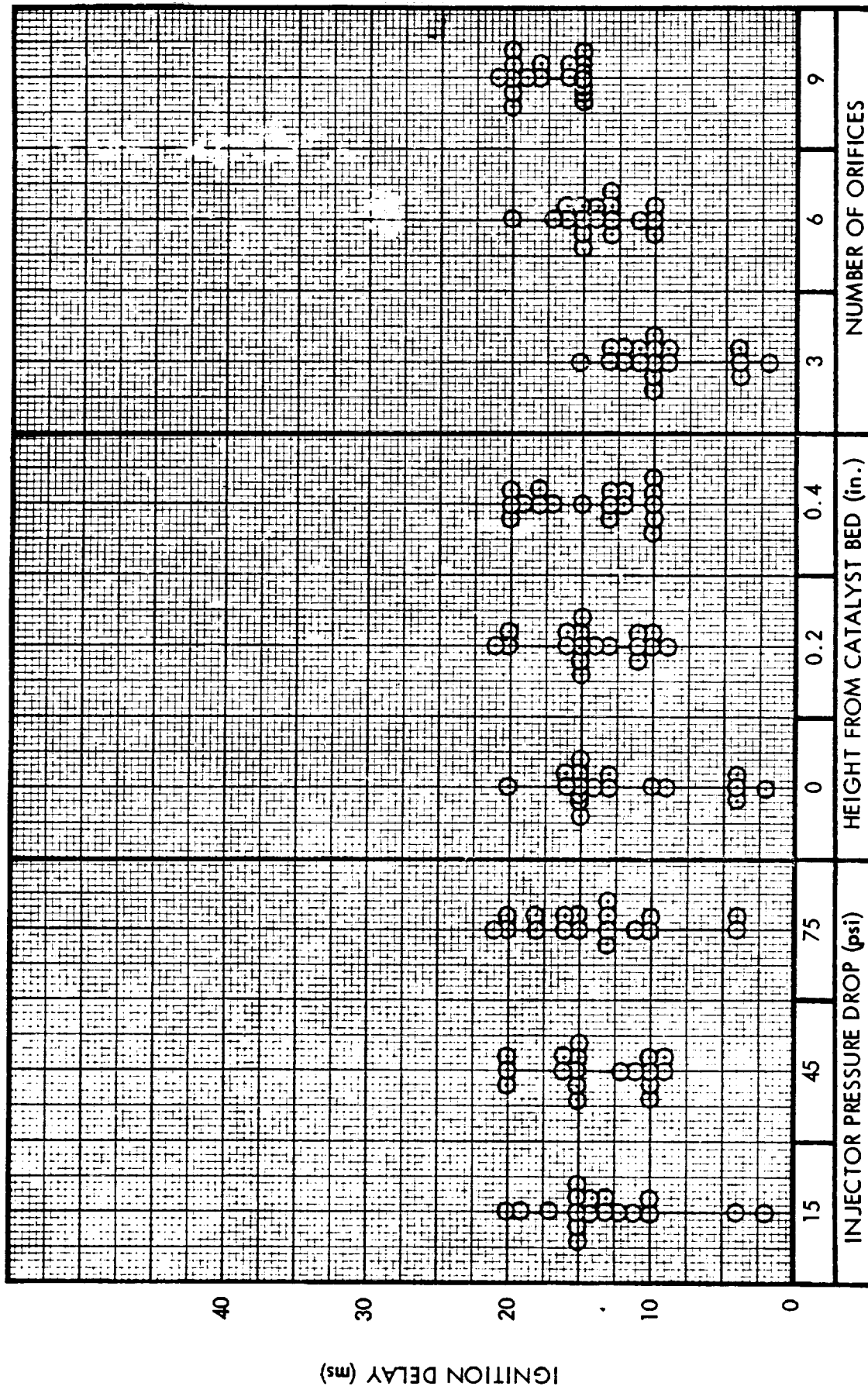
INJECTOR VARIABLE



INJECTOR VARIABLE

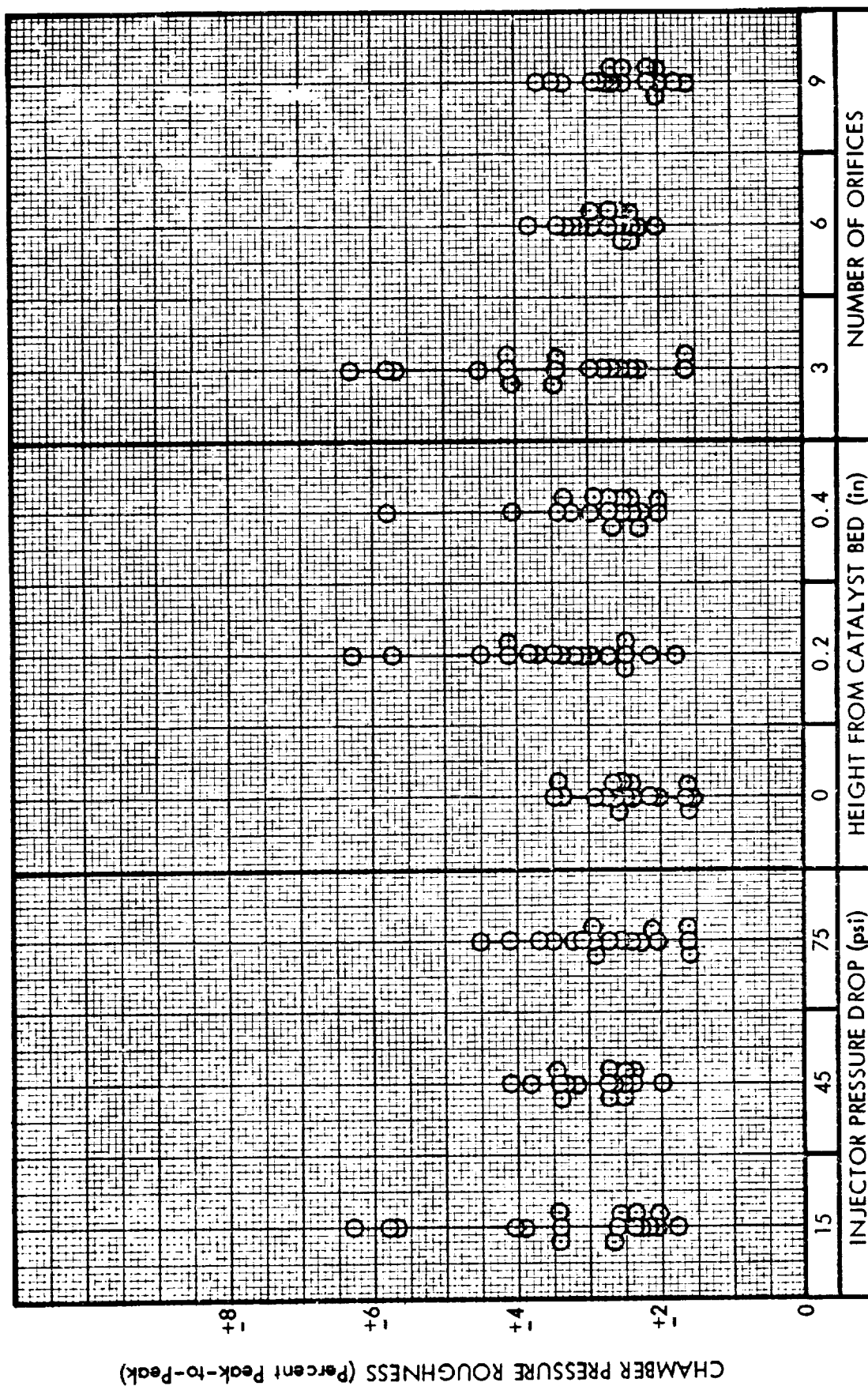
FIGURE 21

5 16f ENGINE SHOWERHEAD INJECTOR SCATTER DIAGRAM IGNITION DELAY



INJECTOR VARIABLE

5 1bf ENGINE SHOWERHEAD INJECTOR SCATTER DIAGRAM
CHAMBER PRESSURE ROUGHNESS



INJECTOR VARIABLE

TABLE VI
5 LBF ENGINE - TEST DATA SUMMARY - SHOWERHEAD INJECTOR

Test No.	Test Code	Fuel Temp. °F	Initial Catalyst Bed Temp. °F	Ignition Delay ms.	Response Time ms.	Decay Time ms.	Injection Pressure psia	Upstream Chamber Pressure psia	Downstream Chamber Pressure psia	Thrust lbf	Flow Rate lbm/sec	T _{c1} °F	T _{c2} °F	T _{c3} °F	T _{c4} °F	c ^a ft/sec	I _{sp} lbf-sec/lbm	Thrust Coefficient (2)	Chamber Pressure Roughness % Peak-to-peak
	(3)																		
171-31-74	81-1	62	66	4	115	90	177.1	160.4	143.5	3.210	0.02112	1580	1468	1403	1376	4140	151.9	1.181	±2.61
171-31-75	81-1	59	76	2	120	102	172.0	155.4	139.4	3.160	0.02060	1600	1468	1392	1372	4124	153.7	1.197	±3.41
171-31-196	81-2	38	45	10	510	128	205.3	158.5	147.3	3.333	0.02124	1649	1485	1381	1351	4225	156.9	1.195	±3.40
171-31-198	81-2	29	57	9	645	93	206.3	159.3	144.1	3.308	0.02091	1614	1460	1377	1347	4209	157.9	1.207	±3.46
171-31-71	81-3	66	70	4	694	86	246.9	169.7	154.3	3.520	0.02261	1574	1446	1415	1368	4158	155.8	1.203	±1.62
171-31-72	81-3	60	67	4	736	100	244.7	167.9	154.6	3.470	0.02226	1645	1516	1411	1385	4123	155.8	1.215	±1.62
171-31-96	81-4	57	58	13	112	107	178.9	159.4	144.2	3.260	---	1578	1463	1398	1372	---	---	1.195	±2.43
171-31-98	81-4	54	53	14	108	103	183.9	161.8	146.4	3.330	0.02155	1394	1355	1347	---	4111	154.5	1.209	±2.90
171-31-94	81-5	67	65	16	327	153	205.4	164.4	149.4	3.420	0.02206	1436	1394	1352	1342	4127	155.1	1.209	±2.34
171-31-95	81-5	54	56	15	262	98	201.9	160.5	140.4	3.250	0.02113	1623	1483	1410	1385	4122	153.9	1.202	±2.49
171-31-88	81-6	60	69	13	621	123	223.9	162.2	146.5	3.330	0.02164	1578	1446	1407	1381	4124	154.1	1.202	±2.05
171-31-91	81-6	58	65	20	555	80	247.1	169.4	157.2	3.620	0.02320	1735	1524	1437	1404	4129	156.0	1.215	±2.39
171-31-102	81-7	49	48	15	110	140	194.2	171.2	155.8	3.620	0.02208	1434	1394	1351	1341	4114	156.7	1.225	±2.57
171-31-103	81-7	52	54	15	107	114	187.1	165.6	150.6	3.450	0.02236	1459	1381	1355	1340	4104	154.4	1.209	±2.66
171-31-101	81-8	55	62	15	296	136	203.7	165.7	151.5	3.490	0.02234	1437	1394	1359	1340	4133	156.3	1.216	±1.98
171-31-199	81-8	40	51	15	290	190	194.3	161.0	146.8	3.348	0.02108	1446	1394	1338	1321	4244	158.8	1.204	±2.73
171-31-107	81-9	62	67	15	619	137	241.2	172.3	156.2	3.660	0.02310	1426	1400	1372	1352	4119	158.2	1.236	±1.60
171-31-108	81-9	53	57	16	600	125	210.4	---	140.6	3.160	0.02045	1416	---	---	---	4191	154.9	1.185	±2.13
171-31-187	81-10	49	51	10	202	85	187.1	173.3	153.5	3.520	0.02277	1781	1601	1446	1419	4107	154.6	1.211	±6.28
171-31-188	81-10	48	55	11	220	85	185.9	172.2	151.8	3.496	0.02245	1772	1605	1481	1415	4121	155.7	1.216	±5.70
171-31-185	81-11	42	52	9	514	75	208.3	165.8	146.8	3.352	0.02121	1772	1591	1446	1402	4218	158.1	1.205	±4.10
171-31-186	81-11	48	48	11	581	84	206.9	166.4	147.1	3.364	0.02144	1781	1609	1448	1420	4181	156.9	1.207	±2.72
171-31-190	81-12	45	52	13	748	83	236.3	168.3	154.1	3.540	0.02238	1763	1667	1494	1429	4195	158.2	1.218	±4.50
171-31-191	81-12	44	52	10	650	70	241.2	172.1	156.8	3.592	0.02276	1740	1740	1477	1424	4198	157.8	1.210	±4.10
171-31-109	81-13	65	66	14	120	94	185.4	166.5	150.6	3.428	0.02225	1603	1479	1437	1413	4122	154.1	1.202	±3.32
171-31-113	81-13	58	66	15	129	123	189.7	170.9	152.1	3.496	0.02256	1529	1481	---	---	1394	155.0	1.218	±2.47
171-31-114	81-14	62	64	15	400	94	199.0	160.8	144.7	3.316	0.02149	1591	1468	---	---	1396	154.7	1.209	±3.80
171-31-115	81-14	58	64	15	430	91	206.8	164.8	150.1	3.422	0.02241	1594	1481	---	---	1398	152.7	1.203	±3.16
171-31-116	81-15	55	59	11	663	61	243.2	170.3	154.1	3.581	0.02289	1627	---	---	---	1402	156.5	1.226	±3.08
171-31-117	81-15	50	53	16	550	96	241.5	168.5	152.6	3.531	0.02261	1605	1499	---	---	1405	156.2	1.221	±2.95
171-31-168	81-16	43	53	15	180	80	186.3	169.0	154.1	3.551	0.02251	1503	1503	1433	1411	4170	157.8	1.217	±1.79
171-31-169	81-16	43	58	15	189	88	186.1	168.4	153.2	3.520	0.02255	1516	---	---	---	1433	1407	1.213	±2.12

TABLE VI (cont'd)

Test No.	Test Code (3)	Fuel Temp. °F	Initial Catalyst Bed Temp. °F	Ignition Delay ms.	Response Time ms.	Decay Time ms.	Injection Pressure psia	Upstream Chamber Pressure psia	Downstream Chamber Pressure psia	Thrust lbf	Flow Rate lbm/sec	T _{c1} °F (1)	T _{c2} °F (1)	T _{c3} °F (1)	T _{c4} °F (1)	c* ft/sec	I _{sp} lbf-sec/lbm (2)	Thrust Coefficient	Chamber Pressure Roughness % Peak-to-Peak
171-31-172	81-17	43	52	20	395	70	196.1	165.6	150.4	3.432	0.02174	1583	1540	1448	1420	4215	157.9	1.208	+2.49
171-31-173	81-17	43	53	16	450	80	197.5	167.0	151.2	3.456	0.02179	1583	1538	1448	1420	4225	158.6	1.207	+2.48
171-31-174	81-18	40	49	20	564	83	241.7	174.1	156.2	3.588	0.02247	1516	1503	1437	1407	4236	159.7	1.213	+3.69
171-31-175	81-18	43	56	21	750	--	244.3	176.3	158.9	3.620	0.02283	1547	1516	1437	1415	4240	158.5	1.203	+3.47
171-31-210	81-19	41	56	13	277	106	178.3	163.7	151.5	3.470	0.02241	1864	1605	1455	1415	4120	154.9	1.209	+5.78
171-31-211	81-19	44	55	12	222	100	182.7	167.9	155.0	3.556	0.02266	1740	1573	1446	1407	4168	156.9	1.211	+4.03
171-31-212	81-20	47	55	12	606	87	208.1	163.4	150.0	3.428	0.02182	1721	1547	1442	1402	4188	157.1	1.207	+2.50
171-31-213	81-20	49	47	10	590	82	206.5	162.1	149.2	3.393	0.02173	1735	1560	1446	1407	4185	156.2	1.201	+2.35
171-31-208	81-21	42	52	15	685	84	239.7	168.7	155.8	3.608	0.02266	1717	1560	1459	1424	4190	159.2	1.223	+2.25
171-31-209	81-21	37	48	10	855	75	235.1	166.4	152.9	3.508	0.02231	1762	1568	1446	-----	4176	157.2	1.211	+2.94
171-31-205	81-22	41	46	10	235	96	180.5	162.3	147.9	3.373	0.02143	1645	1521	1459	1415	4206	157.4	1.204	+2.37
171-31-207	81-22	40	45	17	142	100	184.8	165.2	154.5	3.592	0.02238	1713	1591	1446	1415	4206	160.5	1.228	+2.26
171-31-200	81-23	45	45	10	480	107	201.7	163.2	147.3	3.352	0.02156	1602	1499	1452	1432	4163	155.5	1.201	+3.40
171-31-201	81-23	46	55	10	685	95	202.7	163.5	148.4	3.408	0.02185	1685	1516	1415	1393	4139	156.0	1.212	+2.70
171-31-202	81-24	46	44	13	730	83	240.7	174.7	159.3	3.664	0.02324	1658	1507	1429	1381	4177	157.7	1.214	+2.50
171-31-203	81-24	39	49	13	700	72	242.3	172.1	156.7	3.560	0.02256	1670	1516	1418	1407	4199	157.8	1.209	+2.70
171-31-218	81-25	53	53	19	225	90	179.3	160.7	149.3	3.352	0.02144	1472	1415	1398	1372	4192	156.3	1.200	+2.01
171-31-219	81-25	51	59	20	225	90	179.3	161.5	149.2	3.388	0.02162	1490	1459	1407	1381	4169	156.7	1.209	+2.01
171-31-216	81-26	53	59	20	432	100	193.1	161.7	149.3	3.400	0.02151	1503	1459	1415	1381	4261	158.1	1.194	+3.37
171-31-217	81-26	53	53	20	435	122	198.7	166.4	151.2	3.496	0.02211	1459	1424	1402	1381	4167	158.1	1.221	+2.65
171-31-214	81-27	49	42	18	618	110	234.9	167.9	155.0	3.523	0.02237	1490	1437	1398	1372	4222	157.7	1.202	+3.21
171-31-215	81-27	52	59	18	697	97	237.1	168.8	156.0	3.556	0.02262	1516	1459	1407	1383	4202	157.2	1.203	+2.90

(1) T_{c1}, T_{c2}, T_{c3}, and T_{c4} are steady-state temperature measurements located at 0.5, 0.88, 1.35, and 1.75 inches from the top of the catalyst bed.

(2) Nozzle Expansion Ratio is 4.55:1

(3) Refer to Figure 1 for identification of test code.

- b. Cold bed response time is affected by the height from the catalyst bed
- c. Cold bed response time is affected by the number of orifices.

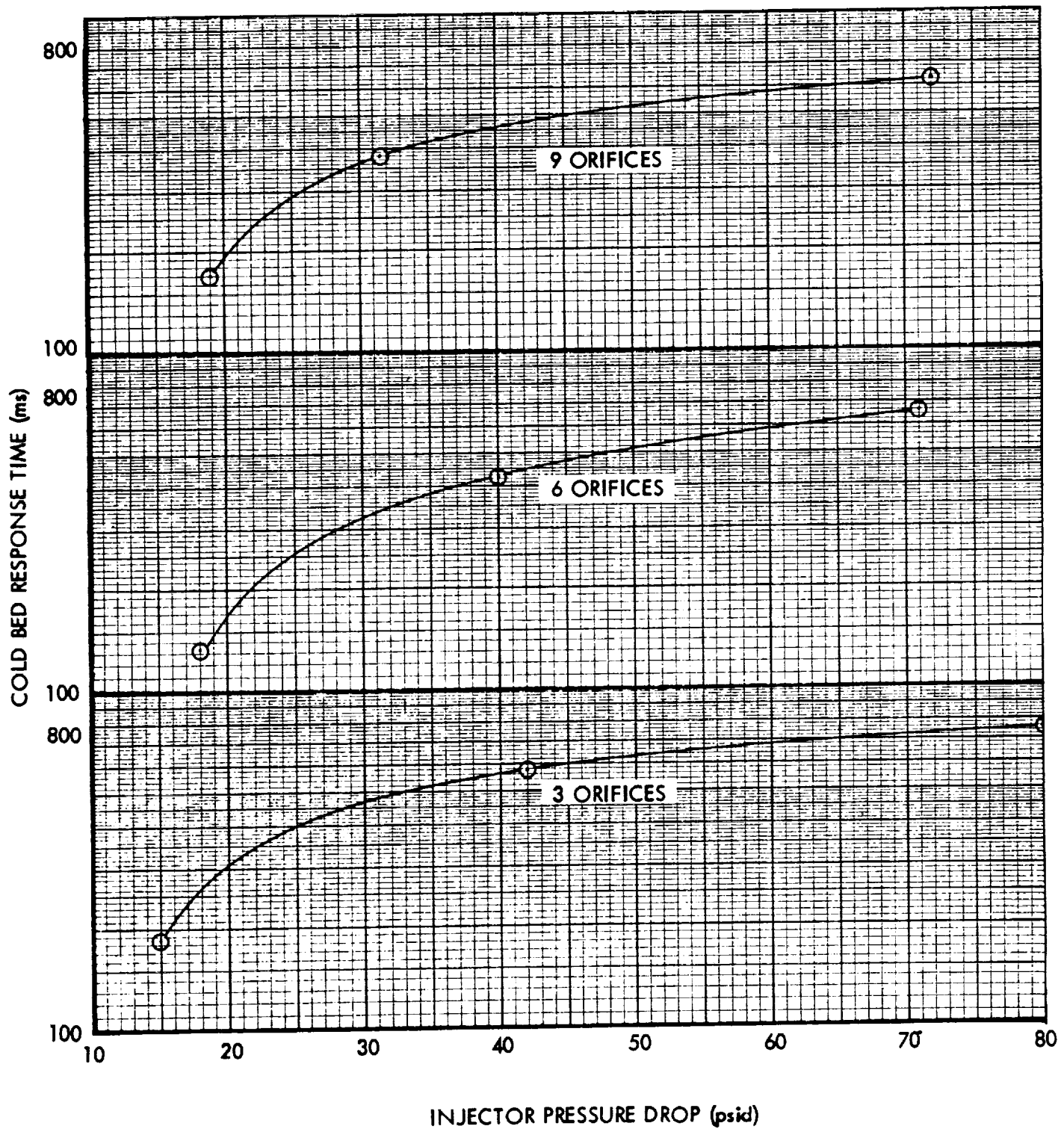
In Figure 24 cold bed response time data for all distances from the catalyst bed has been averaged at each pressure drop and is plotted versus injector pressure drop for the 3, 6, and 9 orifice injectors. An increase in cold bed response time with pressure drop is obvious from the curves.

Figure 25 is a plot of average cold bed response time (average of data at all pressure drops) versus distance from the catalyst bed for the 3, 6, and 9 orifice injectors. It is seen that cold bed response times increase as the injector is moved away from the catalyst bed. This effect is very small for the 3 orifice injector but it is significant for the 6 and 9 orifice injectors. Figure 26 is a cross plot of data in Figure 24 and depicts cold bed response time versus number of injector orifices for pressure drops of 20, 45, and 70 psid. It is seen that a minimum in cold bed response times exists with the 6 orifice injector at a pressure drop of 20 psid. At 45 and 70 psid pressure drop, the 6 and 9 orifice injectors have essentially the same response times which are both lower than the 3 orifice injector.

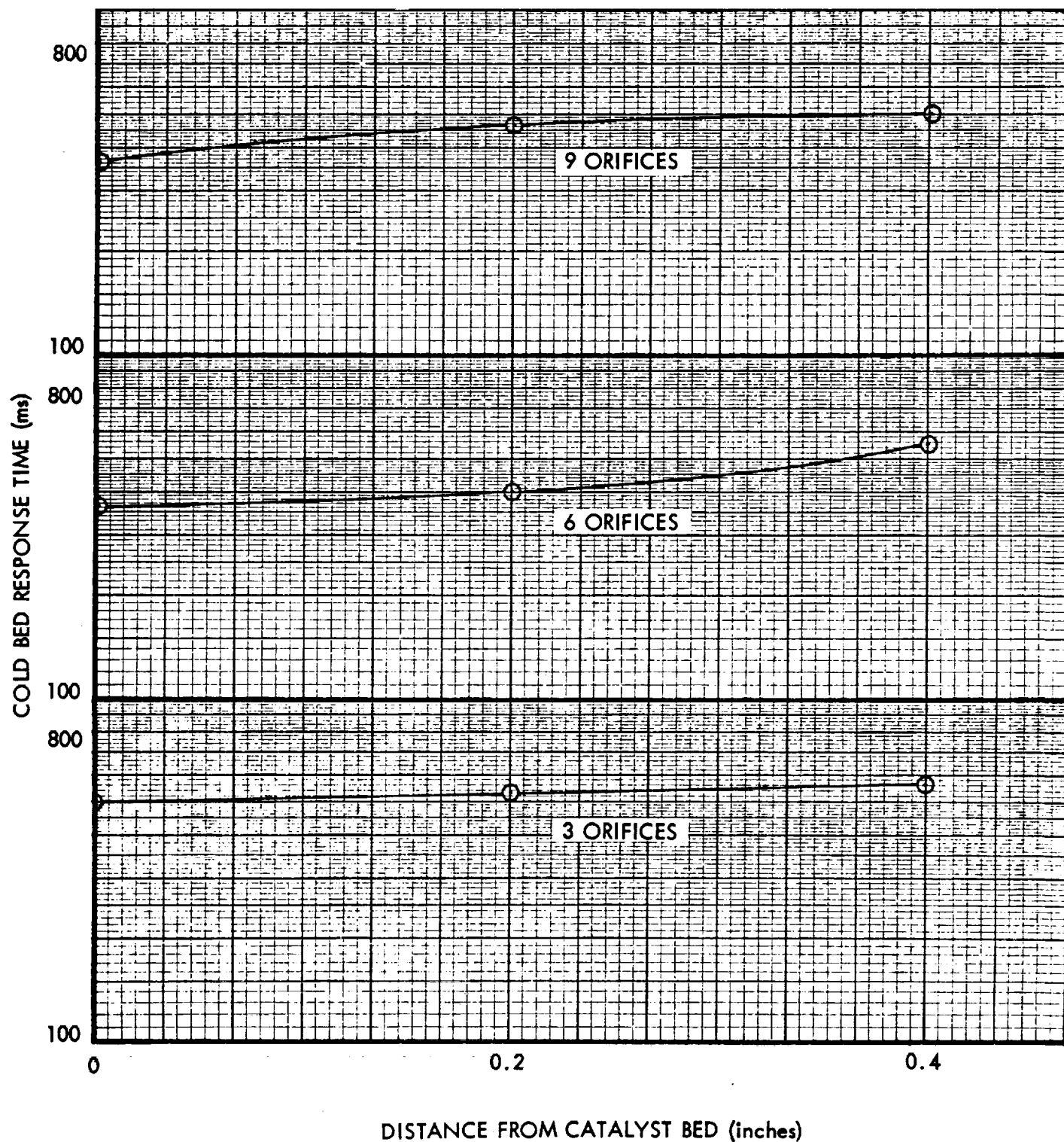
The analysis of variance conducted on the ignition delay data presented in the scatter diagram in Figure 22 resulted in the following observations:

- a. Ignition delay is affected by the number of injector orifices.
- b. Ignition delay is not affected by injector pressure drop.
- c. Ignition delay is affected by the distance of the injector from the catalyst bed.
- d. An interaction exists between the injector pressure drop and the injector distance from the catalyst bed.
- e. An interaction exists between the number of orifices and distance from the catalyst bed.
- f. An interaction exists between the number of orifices, injector pressure drop, and injector distance from the catalyst bed.

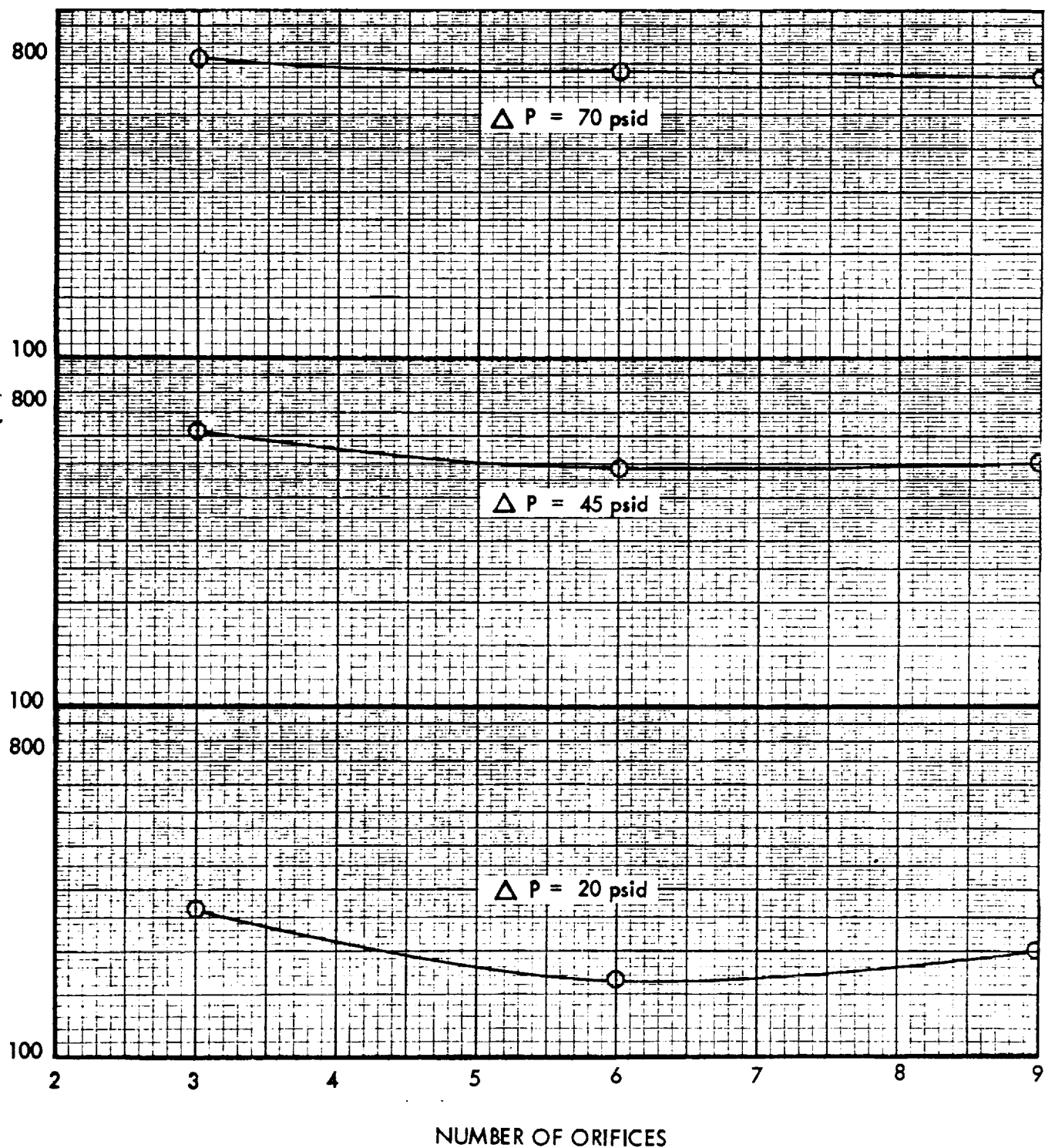
5 lbf ENGINE SHOWERHEAD INJECTOR AVERAGE COLD BED RESPONSE
TIME VS INJECTOR PRESSURE DROP



5 lbf ENGINE SHOWERHEAD INJECTOR AVERAGE COLD BED RESPONSE TIME VS DISTANCE FROM CATALYST BED



5 lbf ENGINE SHOWERHEAD INJECTOR AVERAGE COLD BED RESPONSE
TIME VS NUMBER OF ORIFICES



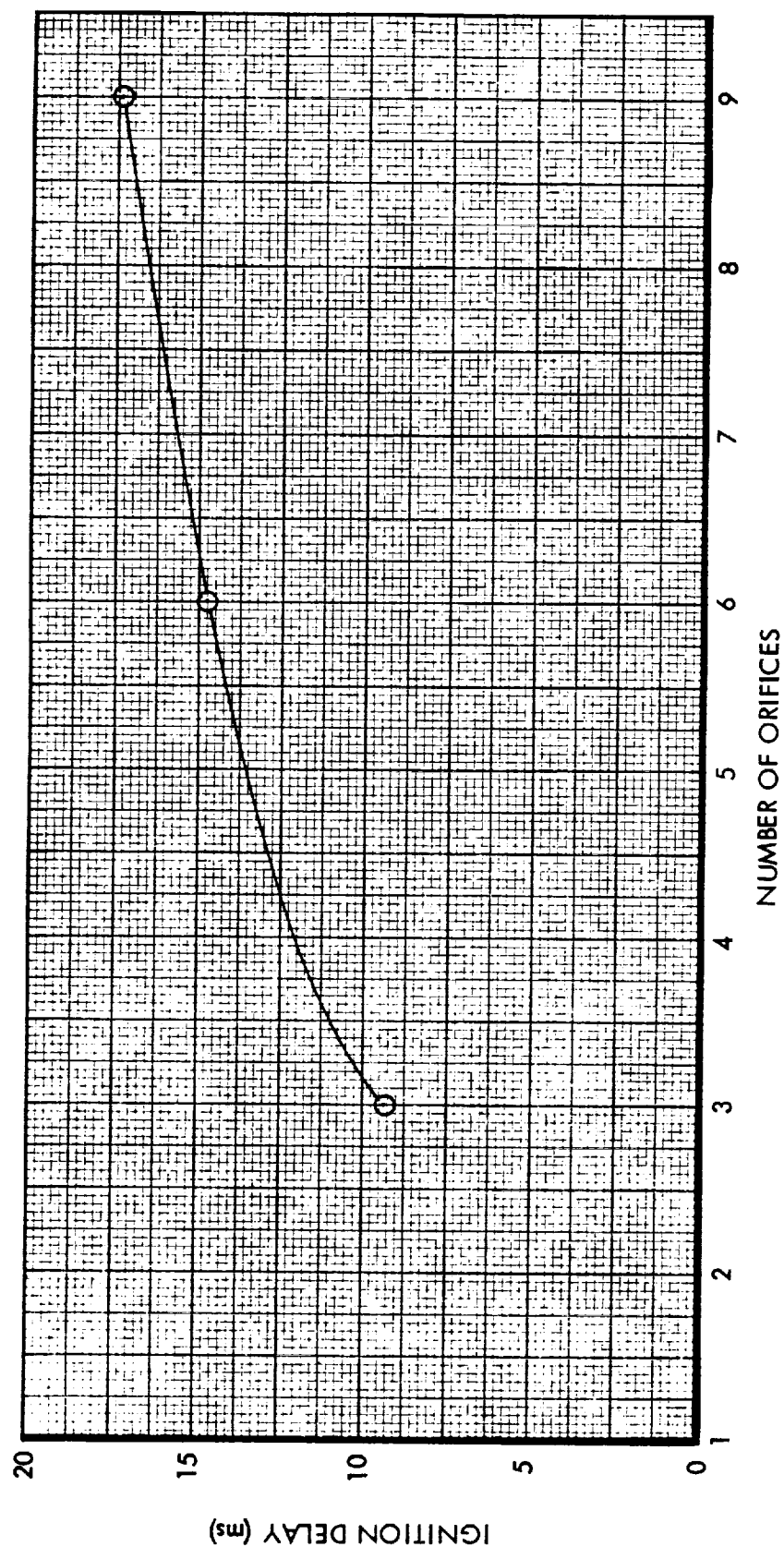
The interactions which exist between the injector variables make it difficult to come to definite conclusions regarding the effect of the variables on ignition delay. Figure 27 is a plot of average ignition delay versus the number of orifices. A definite increase in ignition delay is noted as the number of orifices is increased. The reason for this increase is not completely understood. With the 6 orifice injector, ignition delay decreases as the distance between the injector and the catalyst bed is increased. With the 3 and 9 orifice injectors ignition delay increases with distance from the catalyst bed. This information is presented in Figure 28, where ignition delay is plotted versus the distance of the injector from the catalyst bed for the 3, 6, and 9 orifice injectors.

The analysis of variance conducted on the chamber pressure decay time data presented in the scatter diagram of Figure 21 resulted in the following conclusions:

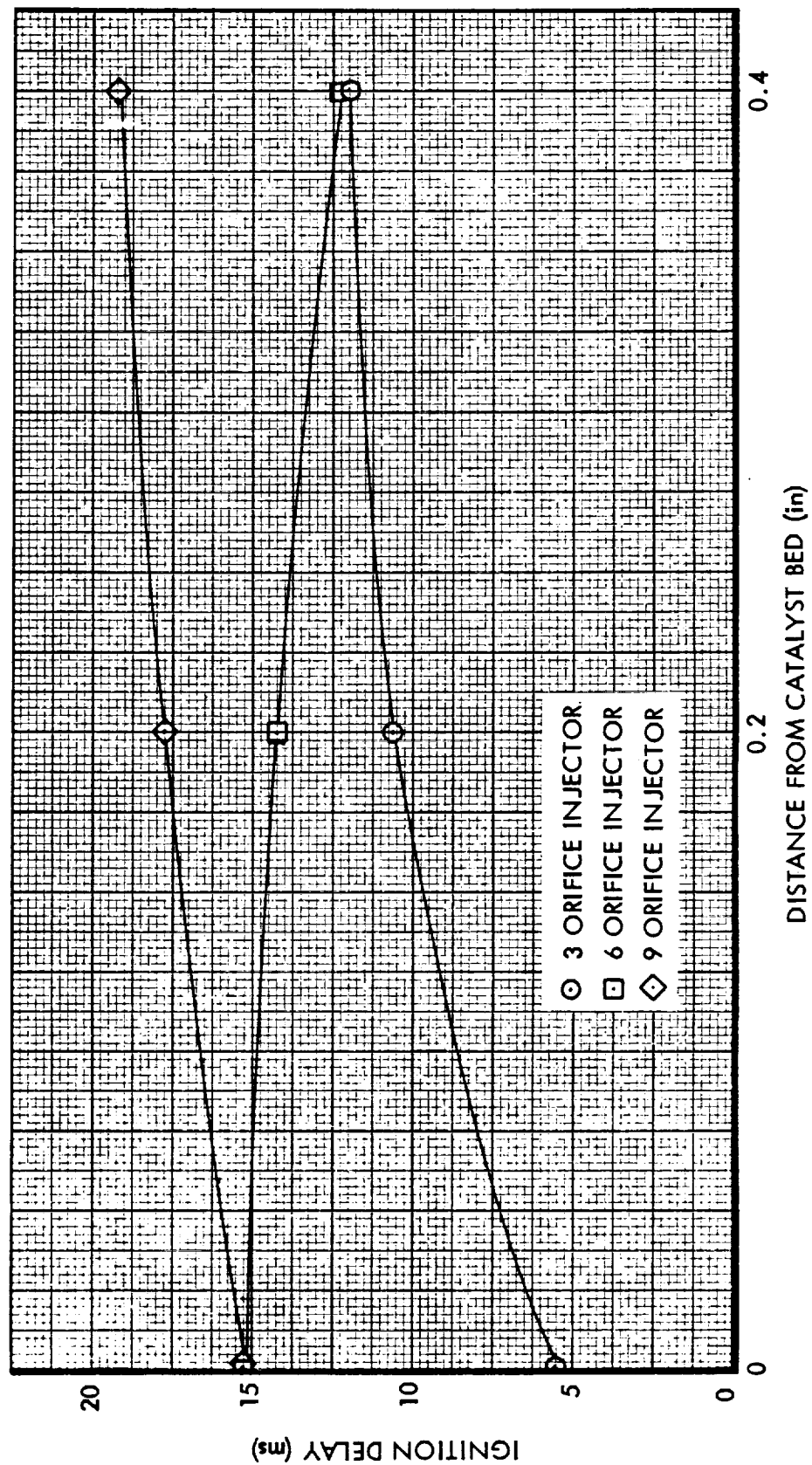
- a. Chamber pressure decay time is not affected by injector pressure drop.
- b. Chamber pressure decay time is significantly affected by the height from the catalyst bed.
- c. The number of injector orifices has an effect on the decay times.
- d. There is an interaction between the number of orifices and the distance from the catalyst bed.

In Figure 29 chamber pressure decay time is plotted versus the number of injector orifices for distances of the injector from the catalyst of 0, 0.2, and 0.4 inches. From this figure it is seen that the decay times increase with number of orifices with the injector flush and 0.4 inches from the catalyst bed. With the injector 0.2 inches from the bed the decay time is a maximum with the 6 orifice injector. The increase in decay time noted is probably due to the test configuration employed. As the number of orifices was increased, the propellant manifold diameter was increased to provide flow to the orifices. The manifold diameter was held only slightly larger than the orifice pattern diameter so that no areas of stagnant flow would exist in the manifold. Calculations indicate that the increase in holdup propellant volume as the number of

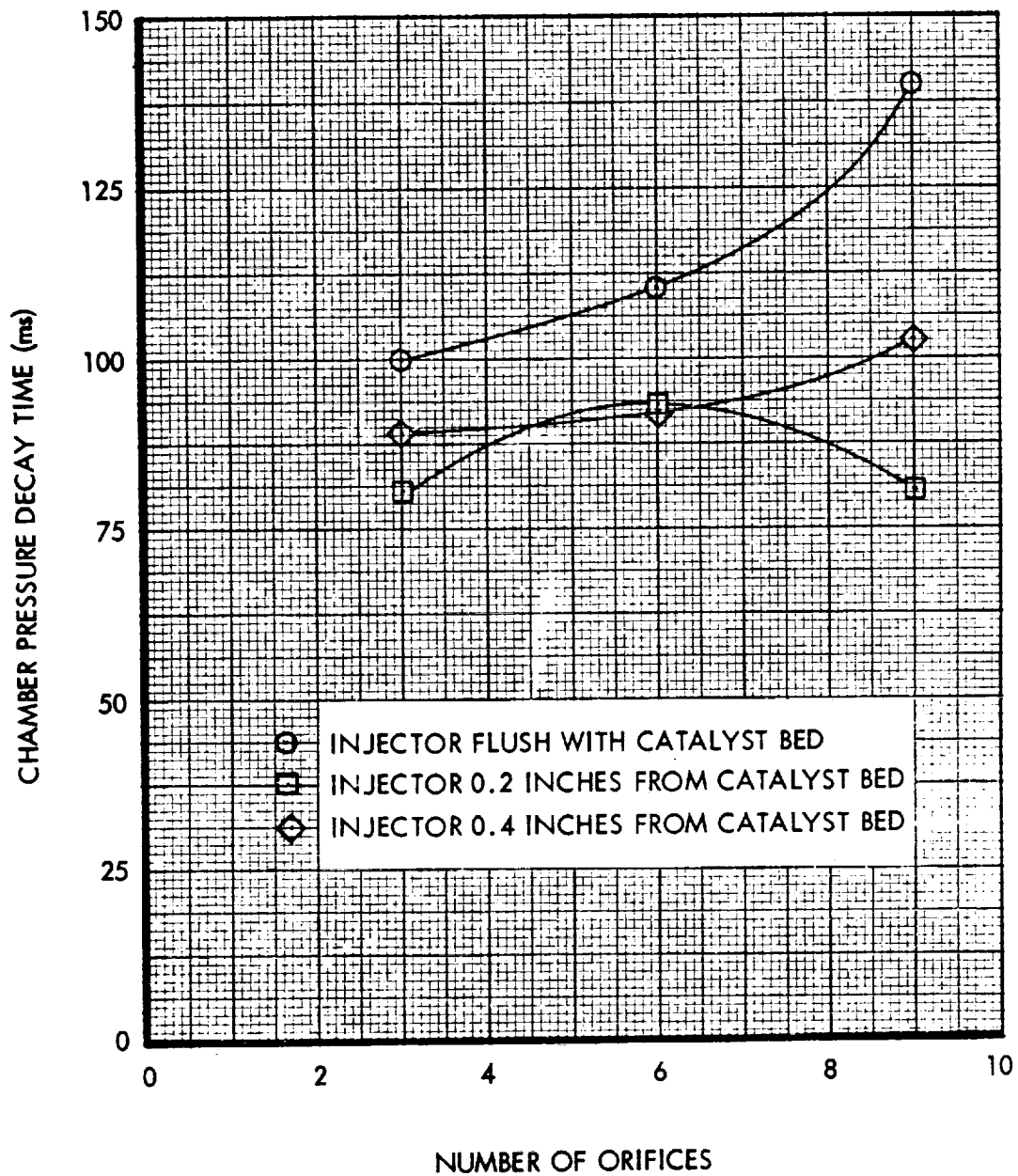
5 lbf ENGINE SHOWERHEAD INJECTOR
AVERAGE IGNITION DELAY
VS NUMBER OF ORIFICES



5 lbf ENGINE SHOWERHEAD INJECTOR
 AVERAGE IGNITION DELAY
 VS DISTANCE FROM CATALYST BED



5 Ibf ENGINE SHOWERHEAD INJECTOR AVERAGE CHAMBER
PRESSURE DECAY TIME VS NUMBER OF ORIFICES



orifices is increased is probably sufficient to account for the increase in tailoff noted. Thus it would appear that if the holdup propellant volume had been held constant, no change in decay time with number of orifices would have occurred. The main effect on decay time is then the distance from the catalyst bed wherein decay times are lower with a 0.2 inch void between the injector and the catalyst bed than with the injector flush or 0.4 inches from the bed.

The analysis of variance conducted on the chamber pressure roughness data shown in Figure 23 indicates that all injector variables have a significant effect on the chamber pressure roughness and that interactions exist between all variables. This makes any general conclusions about chamber pressure roughness impossible. However, the following trends are noted in the data:

- a. With the injector flush with the catalyst bed, chamber pressure roughness decreases slightly with increased injector pressure drop for all orifice patterns.
- b. With the injector 0.2 inches from the catalyst bed, roughness decreases with increased pressure drop for the 3 orifice pattern, is essentially constant for the 6 orifice pattern, and increases with pressure drop for the 9 orifice pattern.
- c. With the injector 0.4 inches from the catalyst bed the same trends in (b) above appear.
- d. Increasing the number of orifices from 3 to 6 lowers the chamber pressure roughness. Virtually no difference exists between the 6 and 9 orifice injectors.

In a few of the tests, some pressure spikes of approximately 50 to 60% of steady state chamber pressure occurred. In general these spikes would occur when the catalyst bed was freshly packed. Slight additional packing of the bed, which occurs during operation appeared to eliminate the spikes. These results indicate catalyst bed porosity has a definite effect on engine operation.

No variation in engine performance was noted when the injector pressure drop or number of orifices was varied. Slight increases in performance (0.5%) were noted when the injector was moved away from the bed, but it is not felt that this increase is significant. Characteristic velocity averaged 4,164 feet per second, specific impulse averaged 156.5 lbf-sec/lbm, and the thrust coefficient averaged 1.209 for the 54 tests tabulated in Table VI.

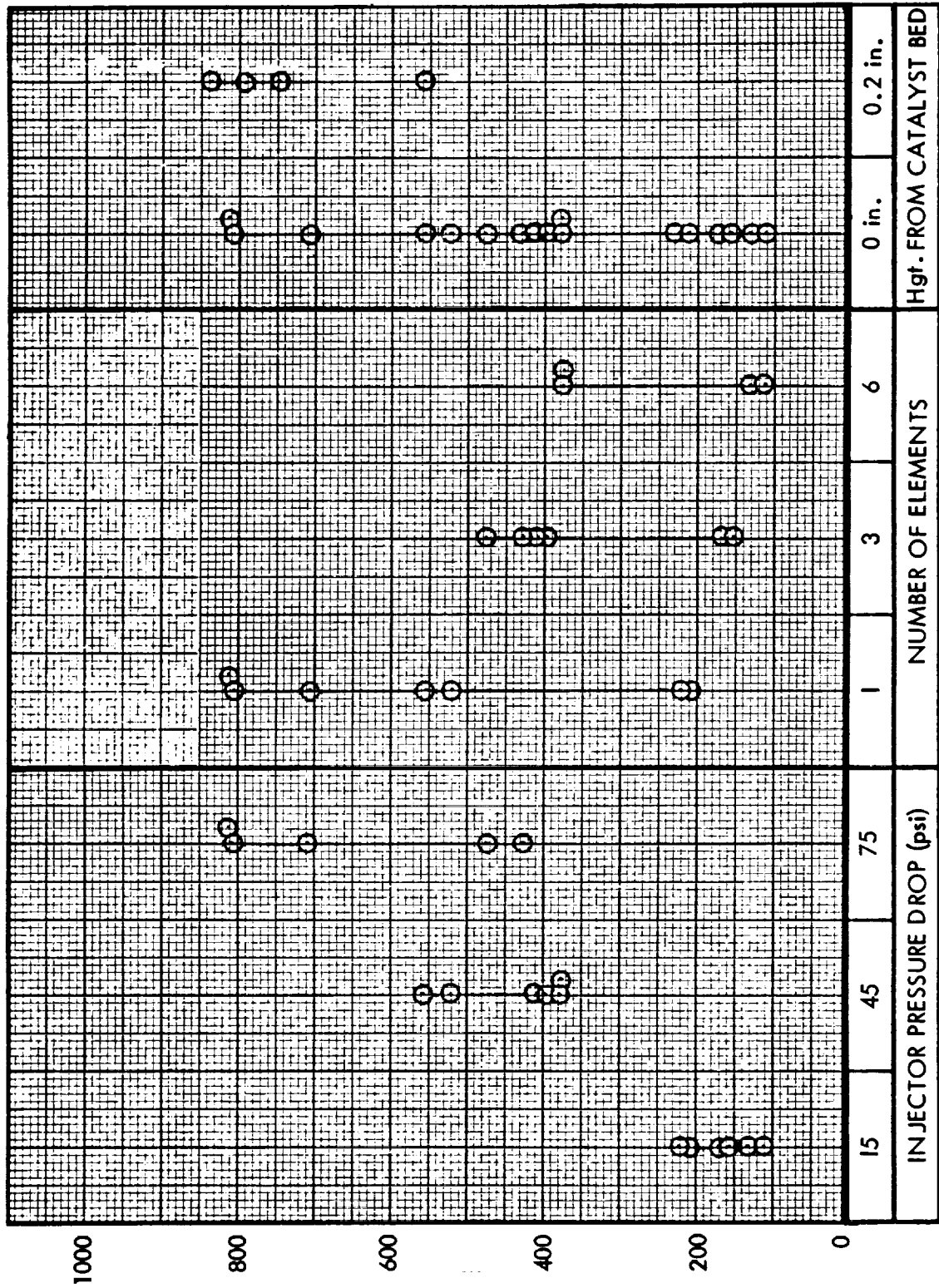
6.2.4 5 lbf Engine Rigimesh Injector

Testing of the rigimesh injector was conducted with 1, 3, and 6 element injectors each at 15, 45, and 75 psid pressure drop. Tests of each injector configuration were made with the injector flush with the catalyst bed and the 6 element injector was tested 0.2 inches away from the catalyst bed at 15 and 45 psid pressure drops. The test data obtained is summarized in Table VII. Scatter diagrams of the data for the reactor variables cold bed response time, ignition delay, chamber pressure decay time, and chamber pressure roughness are plotted in Figures 30 through 33.

From the scatter diagram in Figure 30, it is seen that cold bed response times increase with injector pressure drop. Figure 34 depicts cold bed response time plotted versus injector pressure drop for the 1, 3, and 6 element injectors. It is noted that the response times for the single element injector are significantly higher than those for the 3 and 6 element injectors. When the 6 element injector was moved 0.2 inches from the catalyst bed the start transient was very erratic and the response times increased by a factor of approximately 3. The cold bed response times with the rigimesh injector flush with the catalyst bed are similar to those with the showerhead injector.

The scatter diagram for ignition delay in Figure 31 indicates that ignition delay is affected by the number of orifices and injector distance from the catalyst bed. It is seen that the single element injector has ignition delay times all lower than the 3 and 6 element injectors. This same phenomena was noted with the showerhead injector and is not fully understood. Moving the injector away from the catalyst bed 0.2 inches produced marked increases in the ignition delay time.

5 1b ENGINE RIGIMESH INJECTOR SCATTER DIAGRAM COLD BED RESPONSE TIME



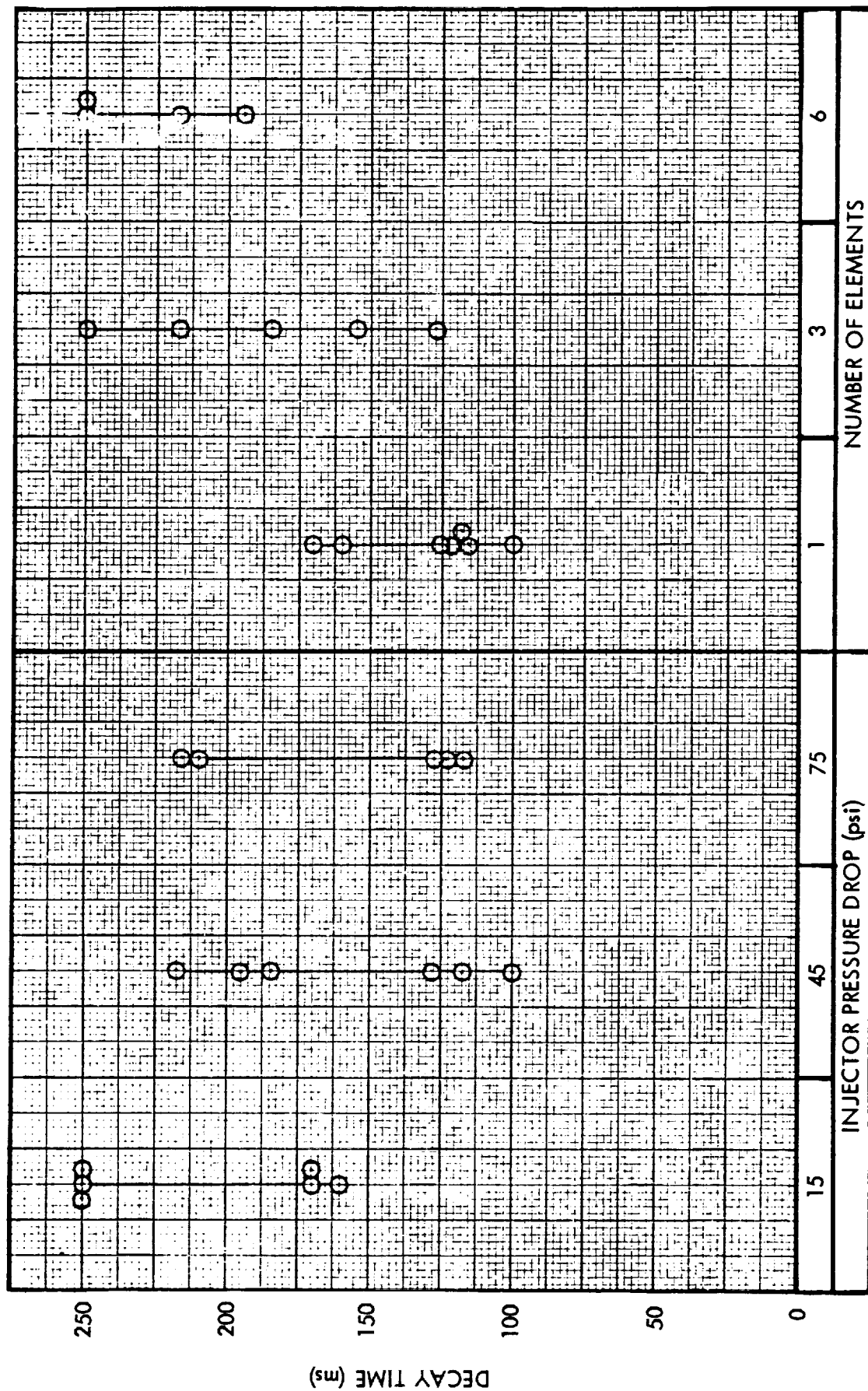
INJECTOR VARIABLE

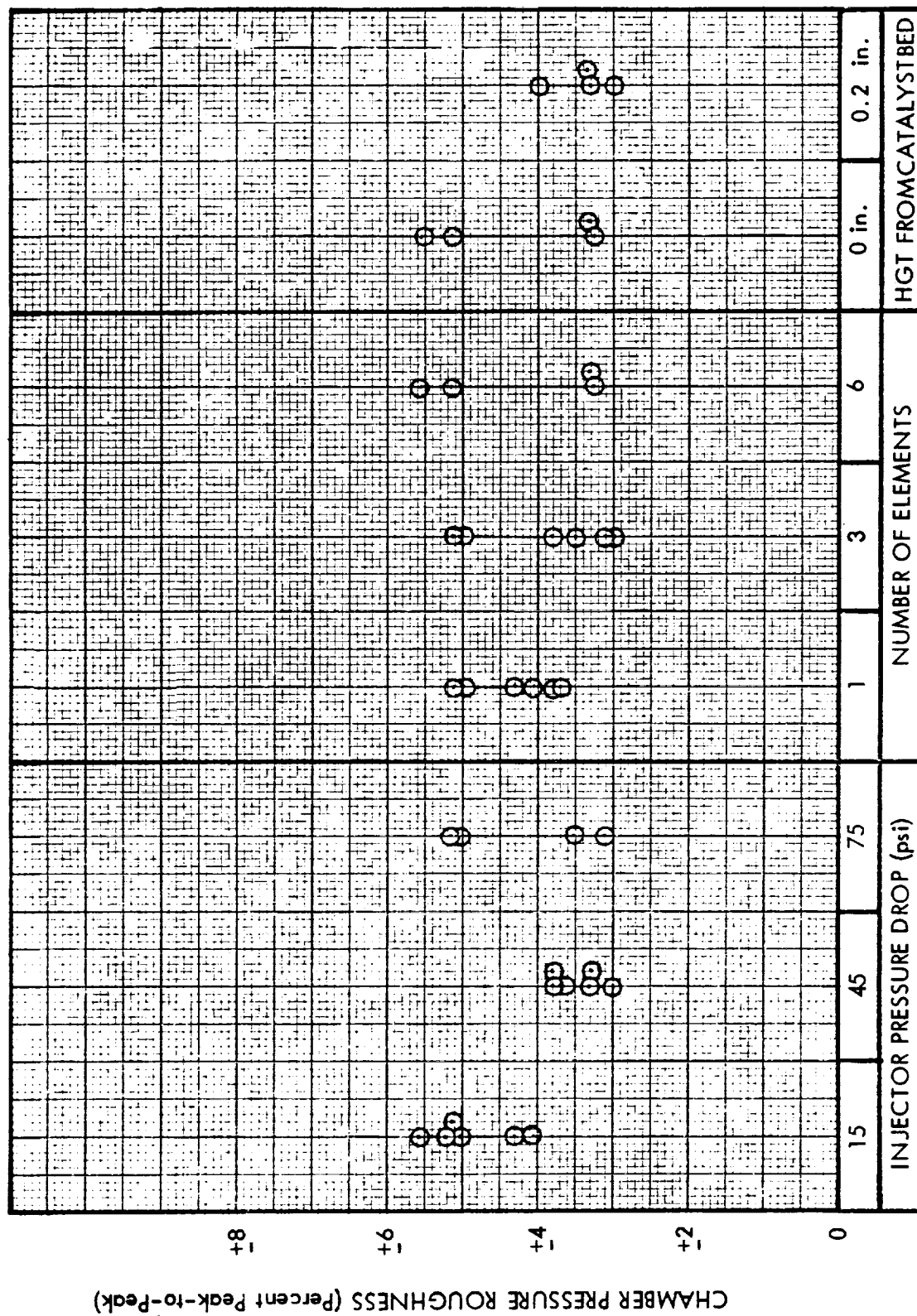


FIGURE 31

5 1bf ENGINE RIGIMESH INJECTOR SCATTER DIAGRAM DECAY TIME

09711





INJECTOR VARIABLE

5 lbf ENGINE RIGIMESH INJECTOR COLD BED RESPONSE TIME VS INJECTOR PRESSURE DROP

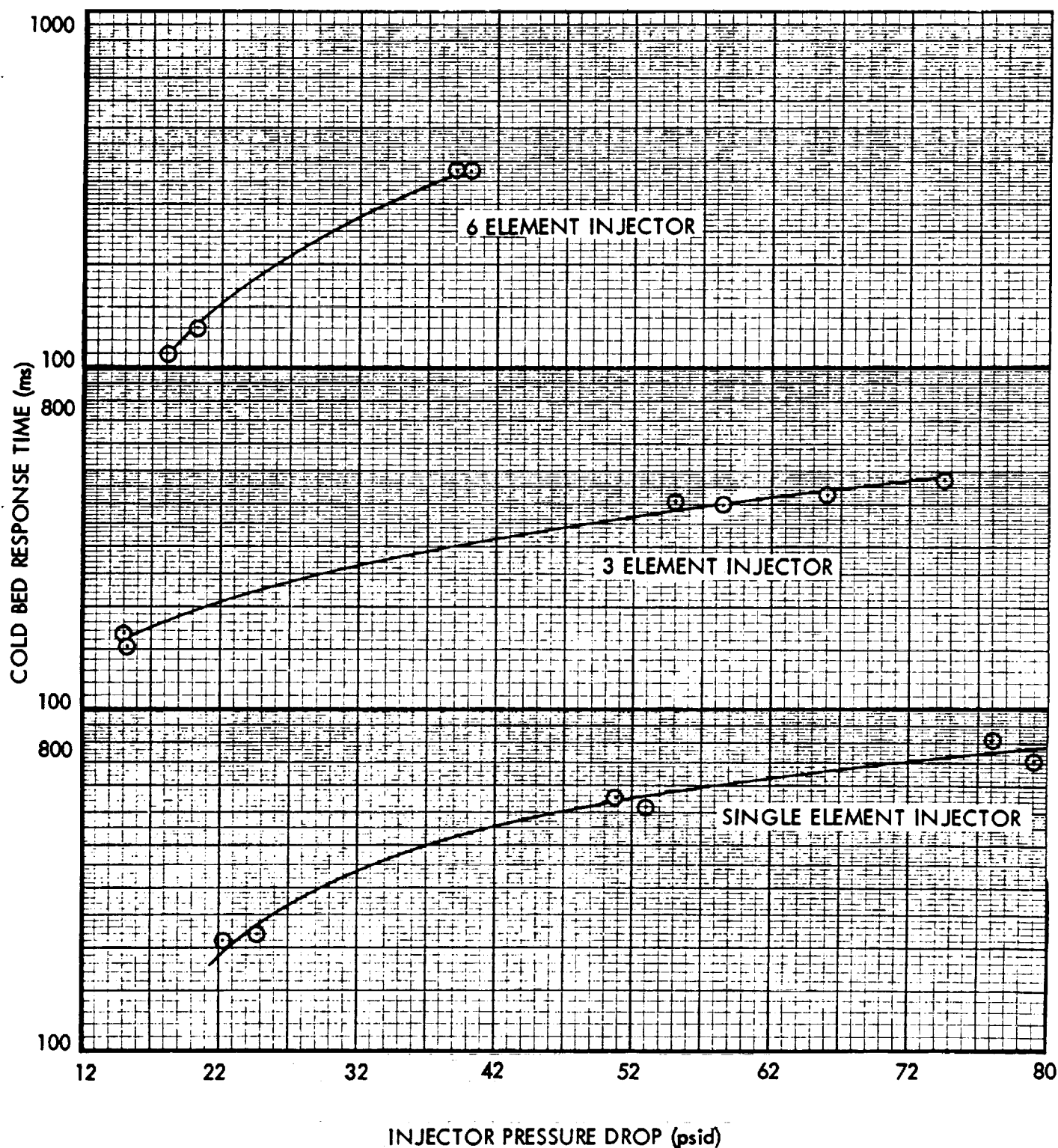


TABLE VII
5 LBF ENGINE - TEST DATA SUMMARY - RIGIMESH INJECTOR

Test No.	Test Code	Fuel Temp. °F	Initial Catalyst Bed Temp. °F	Ignition Delay ms.	Response Time ms.	Decay Time ms.	Injection Pressure psia	Upstream Chamber Pressure psia	Downstream Chamber Pressure psia	Thrust lbf	Flow Rate lbm/sec	T _{c1} °F (2)	T _{c2} °F (2)	T _{c3} °F (2)	T _{c4} °F (2)	c° ft/sec	I _{sp} lbf-sec/lb.m	Thrust Coefficient (3)	Chamber Pressure Roughness % Peak-to-peak
	(1)																		
171-31-166	15-0-1	40	42	11	210	170	178.8	155.3	145.3	3.291	0.02104	1605	1472	1398	1372	4207	156.4	1.196	± 4.30
171-31-167	15-0-1	40	47	10	220	160	192.5	167.9	154.8	3.556	0.02245	1623	1503	1394	1372	4201	158.4	1.213	± 4.04
171-31-159	45-0-1	46	49	10	520	117	216.1	170.9	153.6	3.519	0.02258	1735	1601	1463	1420	4145	155.9	1.210	± 3.71
171-31-160	45-0-1	41	45	10	554	100	209.1	164.8	150.3	3.428	0.02198	1694	1694	1490	1433	4167	156.0	1.204	± 3.79
171-31-176	75-0-1	42	45	12	707	118	245.9	167.0	149.7	3.452	0.02168	1411	1407	1359	1340	4207	159.2	1.218	± 5.01
171-31-177	75-0-1	45	47	14	810	123	244.1	162.2	145.7	3.340	0.02113	1503	1424	1368	1351	4202	158.1	1.210	± 5.05
171-31-178	75-0-1	42	42	13	805	127	242.5	163.3	145.0	3.347	0.02102	1494	1407	1359	1334	4204	159.3	1.219	± 5.07
171-31-170	15-0-3	44	50	29	152	250	179.7	161.6	149.5	3.420	0.02170	1364	1359	1334	1320	4198	157.6	1.208	± 5.01
171-31-171	15-0-3	45	55	27	167	160	182.5	162.7	146.5	3.352	0.02150	1437	1437	1364	1338	4153	155.9	1.208	± 5.12
171-31-155	45-0-3	53	55	18	398	128	232.5	169.4	155.6	3.584	0.02278	1690	1525	1424	1402	4162	157.3	1.216	± 3.80
171-31-156	45-0-3	47	50	17	403	185	223.7	162.6	149.7	3.431	0.02191	1667	1516	1415	1390	4163	156.6	1.210	± 3.00
171-31-157	75-0-3	49	50	18	472	210	242.9	173.0	160.4	3.715	0.02316	1735	1536	1424	1402	4220	160.4	1.223	± 3.50
171-31-158	75-0-3	49	53	16	427	217	230.3	162.1	146.3	3.282	0.02138	1749	1543	1424	1402	4170	153.5	1.184	± 3.71
171-31-161	15-0-6	51	56	16	110	250	174.1	150.5	134.1	2.996	0.01962	1503	1446	1385	1359	4164	152.7	1.180	± 5.59
171-31-162	15-0-6	47	55	18	130	250	181.3	161.6	145.1	3.280	0.02122	1459	1437	1381	1359	4166	154.6	1.195	± 5.17
171-31-164	45-0-6	48	50	21	375	218	20.13	162.6	152.3	3.480	0.02218	1450	1394	1347	1334	4197	156.9	1.203	± 3.27
171-31-165	45-0-6	45	57	20	375	190	200.7	162.1	150.9	3.460	0.02180	1446	1394	1359	1338	4218	158.7	1.211	± 3.31
171-31-182	15-2-6	40	36	28	555	810	185.5	157.4	144.1	3.264	0.02050	1394	1346	1329	1299	4263	158.5	1.196	± 3.99
171-31-183	15-2-6	41	55	35	790	1150	185.9	149.7	134.3	2.988	0.01899	1338	1340	1359	1297	4309	157.4	1.175	± 3.35
171-31-180	45-2-6	48	51	23	832	---	203.1	165.4	150.1	3.428	0.021341	1429	1381	1329	1329	4286	160.6	1.206	± 3.00
171-31-181	45-2-6	48	59	22	745	700	202.5	165.4	151.2	3.453	0.021443	1394	1351	1381	1316	4297	161.0	1.206	± 3.30

(1) First number refers to nominal injector pressure drop. Second number refers to distance of injector from catalyst bed. The third number refers to the number of injector elements.

(2) T_{c1}, T_{c2}, T_{c3}, and T_{c4} are steady-state temperature measurements located 0.5, 0.88, 1.35, and 1.75 inches from the top of the catalyst bed.

(3) Nozzle Expansion Ratio is 4.55:1

The scatter diagram for chamber pressure decay time in Figure 32 indicates an increase in decay time with number of rigimesh elements. As was explained with the showerhead injector this is thought to be due to increased manifold propellant holdup as the number of elements increased. When the injector was moved 0.2 inches from the catalyst bed, the decay times increased by a factor of 3 to 5 as is seen from the data in Table VII.

From the scatter diagram in Figure 33 it is seen that chamber pressure roughness decreases as pressure drop is increased. In general, the rigimesh injector gave higher chamber pressure roughness at all conditions than did the showerhead injector. The engine ran fairly smooth with the injector 0.2 inches from the catalyst bed, once the start transient was over. During the start transient rough and erratic operation was obtained.

No change in engine performance was noted during the tests when the injector parameters were varied. Characteristic velocity averaged 4,183 feet per second for the 18 tests. Specific impulse averaged 156.8 lbf-sec/lbm and the thrust coefficient averaged 1.206. These performance numbers are almost identical to those obtained with the showerhead injector.

6.2.5 50 lbf Engine Showerhead Injector

The first test on the 50 lbf engine was conducted with the showerhead injector utilizing a catalyst bed composed entirely of $1/8 \times 1/8$ inch cylindrical pellets. Chamber pressure oscillations of ± 40 psia peak-to-peak at a frequency of 10 cps occurred throughout the test. The instability was similar to that noted on initial tests with the 5 lbf engine. A series of tests was conducted with various sizes and bed lengths of granular catalyst at the top of the catalyst bed. This testing is summarized in Table VIII. Stable start transient and steady state operation were achieved when 0.2 inches of 25-35 mesh catalyst was used on the top of the catalyst bed. The remainder of the catalyst bed (2.48 inches) was composed of $1/8 \times 1/8$ inch cylindrical pellets.

Tests conducted with the showerhead injector consisted of tests with 20, 40, and 60 orifice injectors at pressure drops of 15, 45, and 75 psid with each orifice pattern. Each pressure drop and each orifice pattern

TABLE VIII
SUMMARY OF 50 LBF ENGINE CATALYST PARTICLE SIZE STUDIES

Test No.	INJECTOR TYPE	CATALYST BED CONFIGURATION	TEST RESULTS
171-31-118	20 Hole Showerhead 45 psid pressure drop	Entire bed composed of 1/8" x 1/8" cylindrical pellets.	Chamber pressure oscillations of ± 40 psia occurred throughout test of 5 seconds duration. Frequency of oscillations was 10 cps.
171-31-119	20 Hole Showerhead 45 psid pressure drop	0.3 inches of 16-20 mesh catalyst on top of bed. Remainder of bed 1/8" x 1/8" cylindrical pellets.	Chamber pressure oscillations of ± 5 psia occurred one second after start. Frequency of oscillations was 20 cps. Oscillations would damp out and then reappear. Test duration was 5 seconds.
171-31-120	20 Hole Showerhead 45 psid pressure drop	0.36 inches of 12-16 mesh catalyst on top of bed. Remainder of bed 1/8" x 1/8" cylindrical pellets.	Chamber pressure oscillations of ± 18 psid occurred 0.6 seconds after start and remained throughout the test of 21 seconds duration. Frequency of oscillations was 18 cps.
171-31-121	20 Hole Showerhead 45 psid pressure drop	0.36 inches of 16-20 mesh catalyst on top of bed. Remainder of bed 1/8" x 1/8" cylindrical pellets.	Chamber pressure oscillations of $\pm 5-6$ psid occur 0.8 seconds after start. Oscillations tend to damp out and stable operation is achieved at end of 30 second test. Frequency of oscillations is 23.5 cps.
171-31-122	20 Hole Showerhead 45 psid pressure drop	0.4 inches of 16-20 mesh catalyst on top of bed. Remainder of bed 1/8" x 1/8" cylindrical pellets.	Chamber pressure oscillations varying from ± 4 to ± 8 psid occurred 1.5 seconds after start and remained for the total test of 30 seconds duration. Frequency of oscillations was 25 cps.
171-31-123	20 Hole Showerhead 45 psid pressure drop	0.2 inches of 25-35 mesh catalyst on top of bed. Remainder of bed 1/8" x 1/8" cylindrical pellets.	Chamber pressure oscillations of ± 4 psia at a frequency of 20 cps occurred for first 5 seconds of test. The oscillations then damped out to ± 3 psia of random oscillations for remainder of test of 23 seconds duration.
171-31-124	20 Hole Showerhead 45 psid pressure drop	Same as Test No. 171-31-123. Bed not unpacked from previous test.	Chamber pressure oscillations of ± 4 to ± 8 psia occurred for first 3 seconds of test at frequency of 20 cps. The oscillations then damped out to ± 3 to 4 psia of random oscillations for remainder of test of 21 seconds duration.
171-31-125	20 Hole Showerhead 45 psid pressure drop	Same as Test No. 171-31-123. Bed not unpacked from previous test.	Stable operation throughout test of 5 seconds duration. Random oscillations of ± 3 psid.

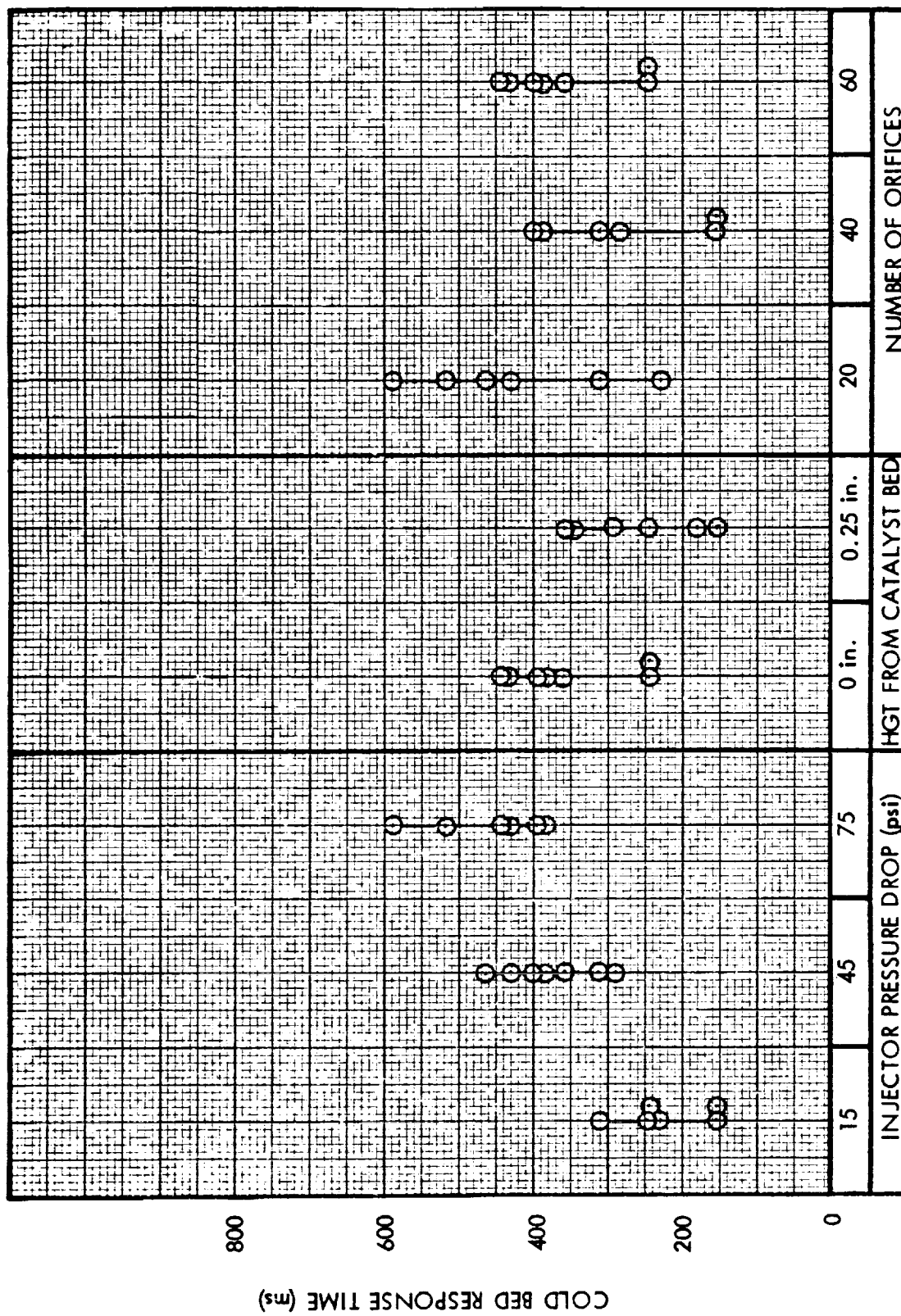
was tested with the injector flush with the top of the catalyst bed. The 60 hole pattern injector was tested at 15, 45, and 75 psid with the injector 0.25 inches from the top of the catalyst bed. The test data obtained from this testing is summarized in Table IX.

Scatter diagrams for the reactor variables of ignition delay, response time, chamber pressure roughness, and chamber pressure decay time are plotted in Figures 35 through 38 as a function of the injector variables.

Examination of the scatter diagram in Figure 35 indicates an increase in cold bed response time as the injector pressure drop is increased. Cold bed response time is plotted versus injector pressure drop in Figure 39. The scatter diagram also indicates that the response time with the 40 orifice injector is lower than that with the 20 or 60 orifice injectors. Statistical analysis was applied to this data to determine whether the differences were significant. This analysis concluded that with a confidence level of 90% the differences were significant. A confidence level of 95% gave a negative result of significance, which probably is due to the small number of the sample. Figure 40 is a cross plot of the data in Figure 39 and depicts average cold bed response time versus the number of orifices. It is seen that a minimum exists with the 40 orifice injector at each pressure drop studied. The data in the scatter diagram indicates a possible decrease in response time when the injector is moved 0.25 inches from the catalyst bed. Statistical analysis of this data indicated no significant difference at the 90% confidence level.

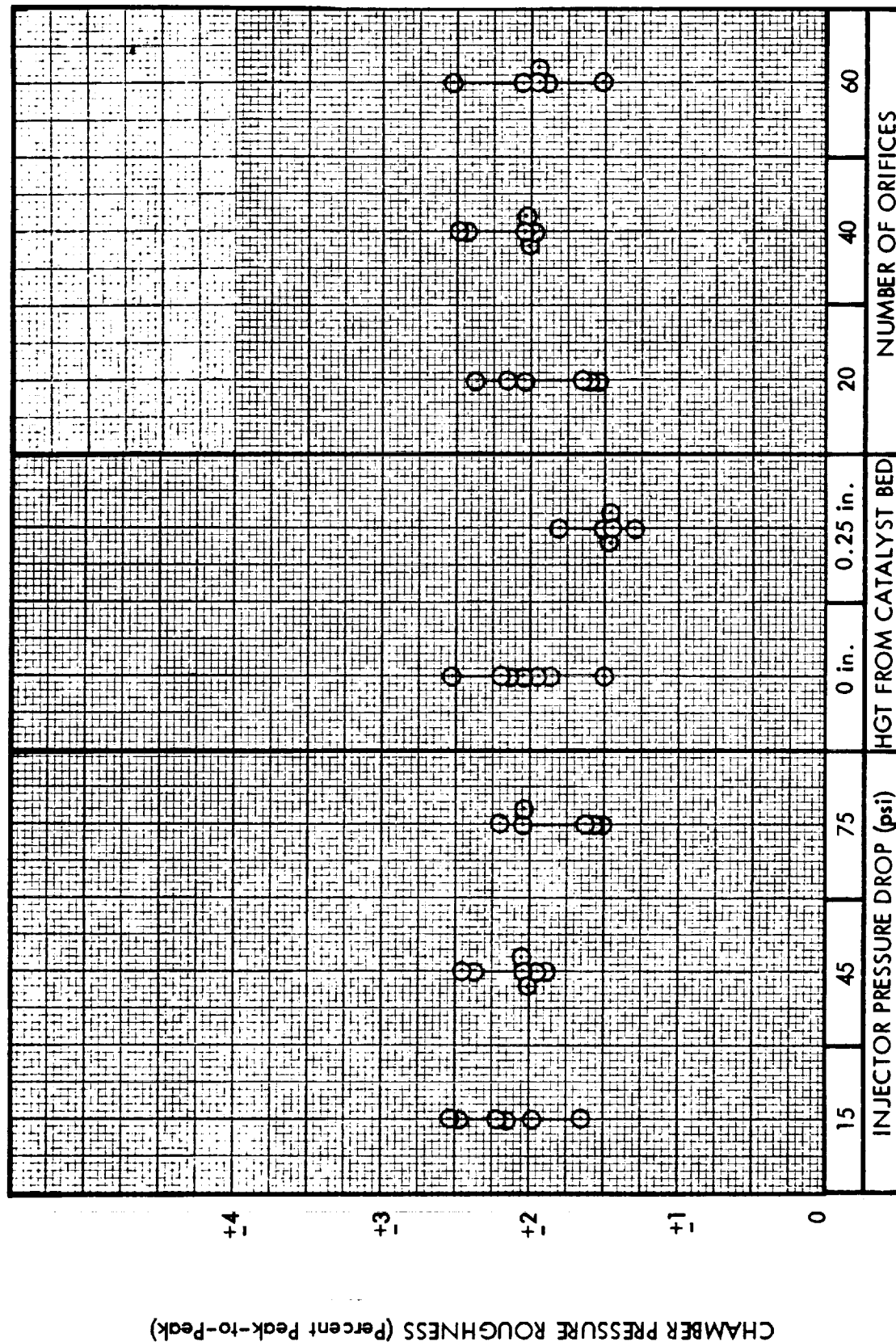
No significant difference was noted in ignition delay, chamber pressure roughness, or chamber pressure decay time as the injector parameters were varied. Chamber pressure roughness decreased slightly with increased pressure drop and when the injector was moved 0.2 inches from the catalyst bed, but the differences are not significant. This is seen in Figures 41 and 42 where chamber pressure roughness is plotted as a function of injector pressure drop.

There was no observable change in engine performance as the injector parameters were varied. The average characteristic velocity for the 27 tests tabulated in Table IX is 4,237 feet per second. Specific impulse averaged 158.1 lbf-sec/lbm and the thrust coefficient averaged 1.201.

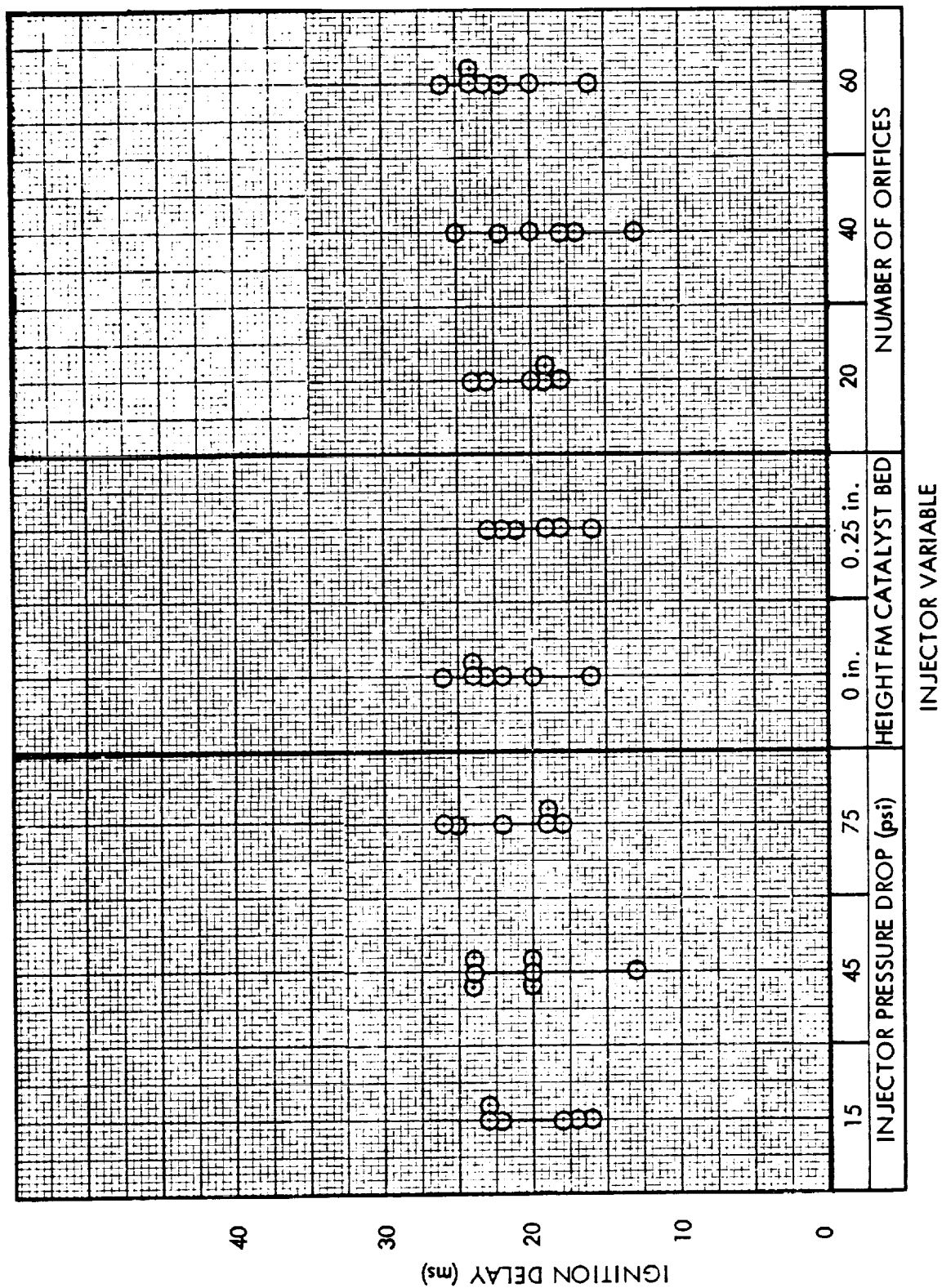


INJECTOR VARIABLE

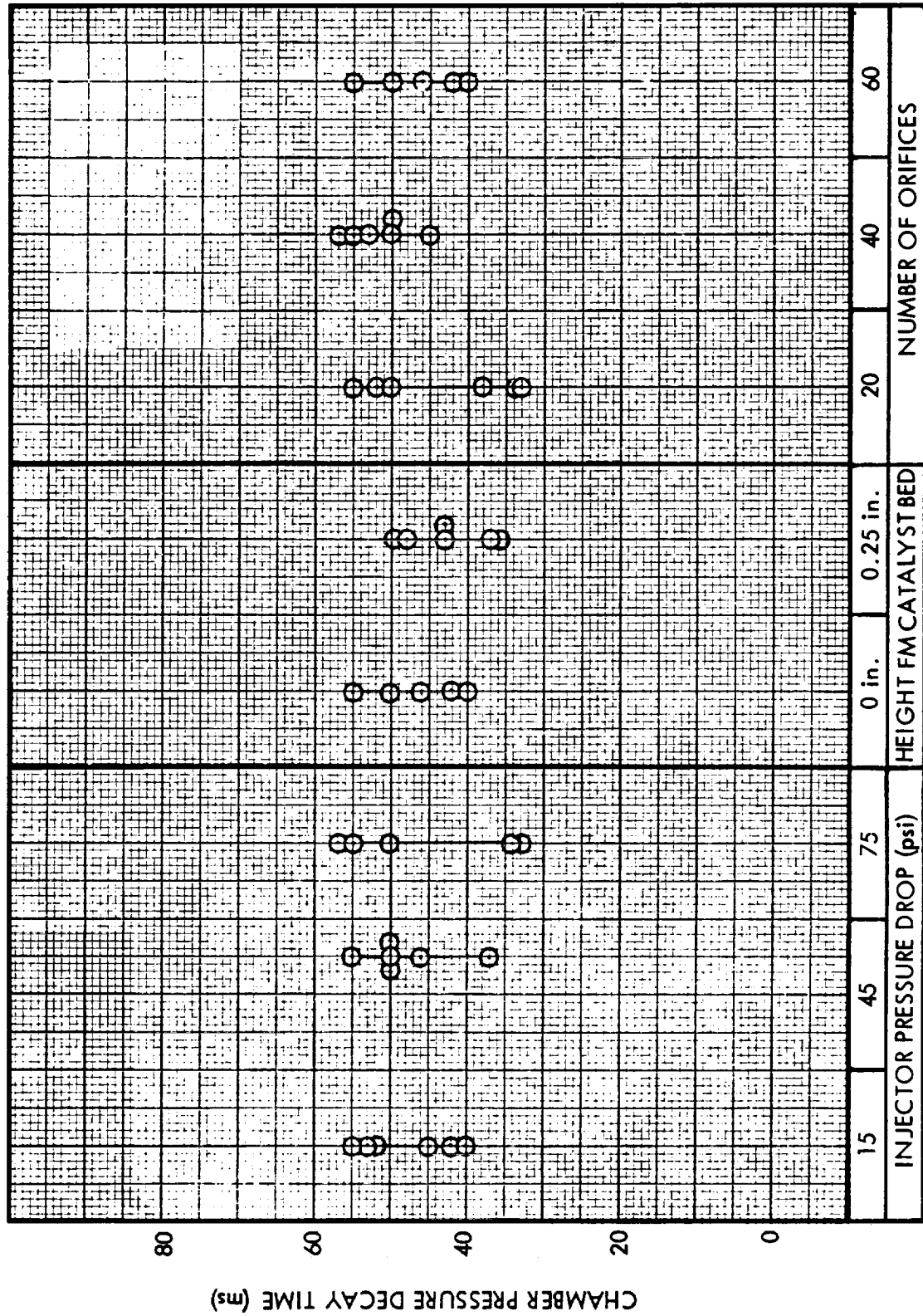
50 lbf ENGINE SHOWERHEAD INJECTOR SCATTER DIAGRAM CHAMBER PRESSURE ROUGHNESS



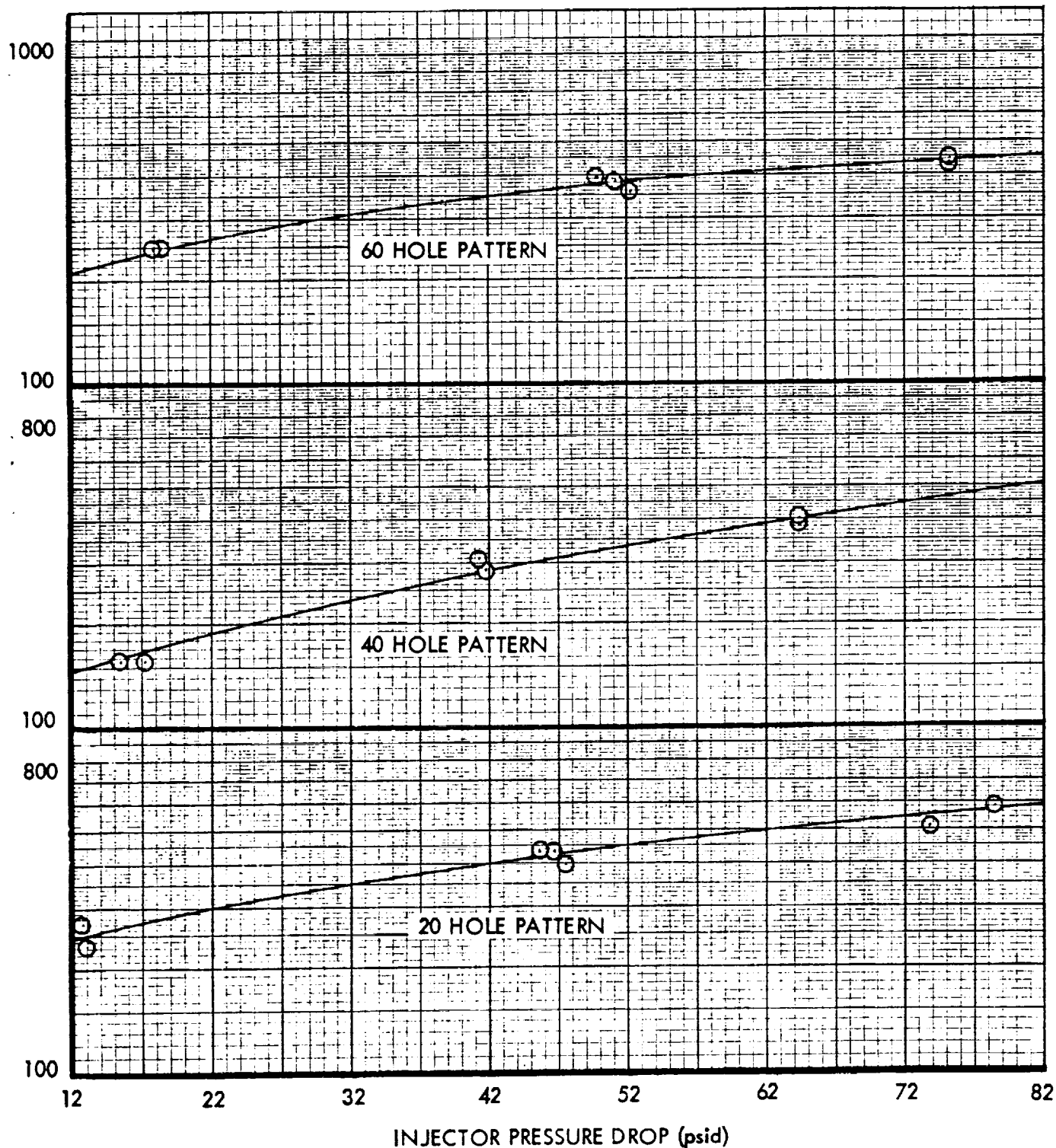
INJECTOR VARIABLE



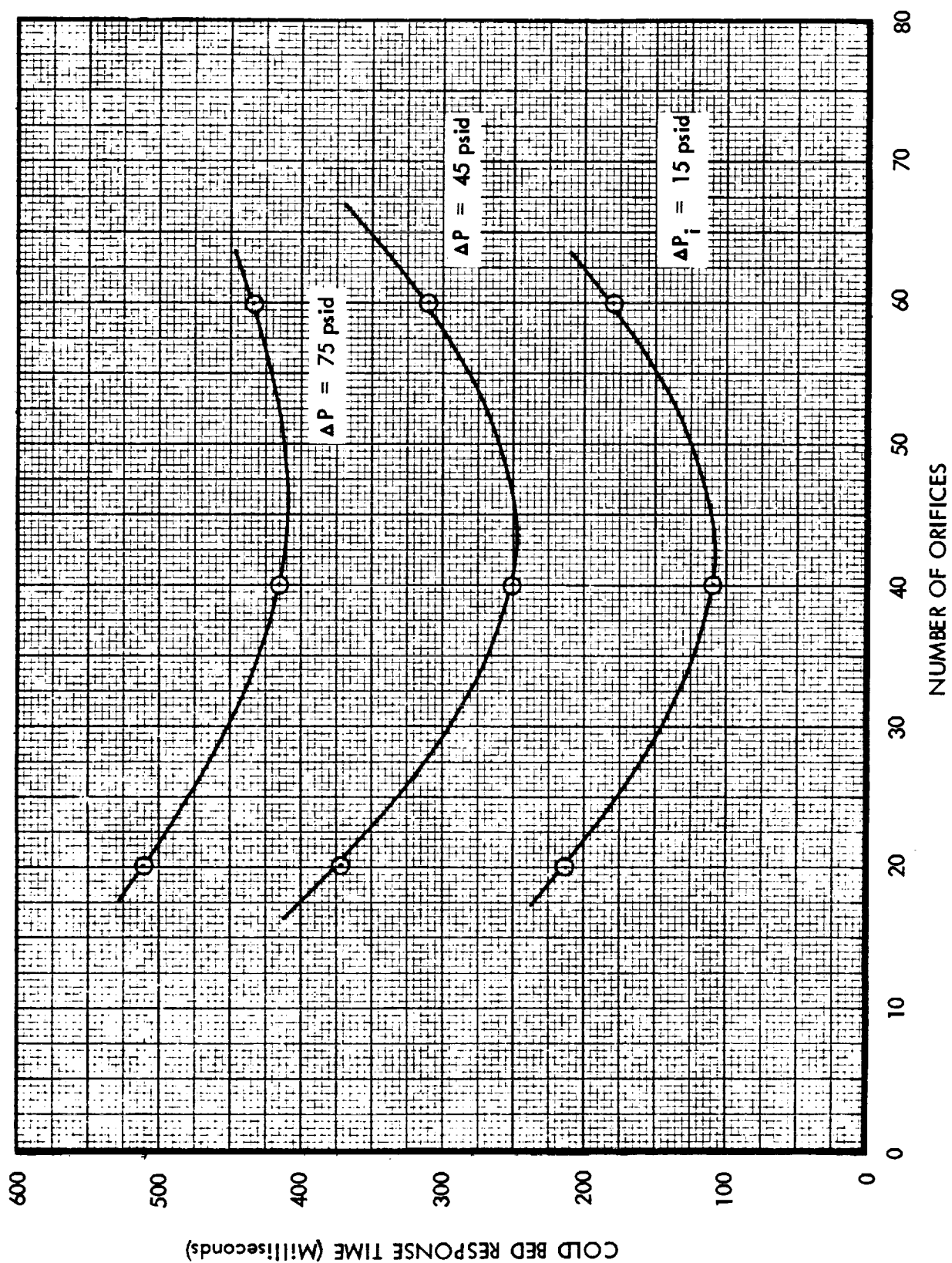
50 lbf ENGINE SHOWERHEAD INJECTOR SCATTER DIAGRAM



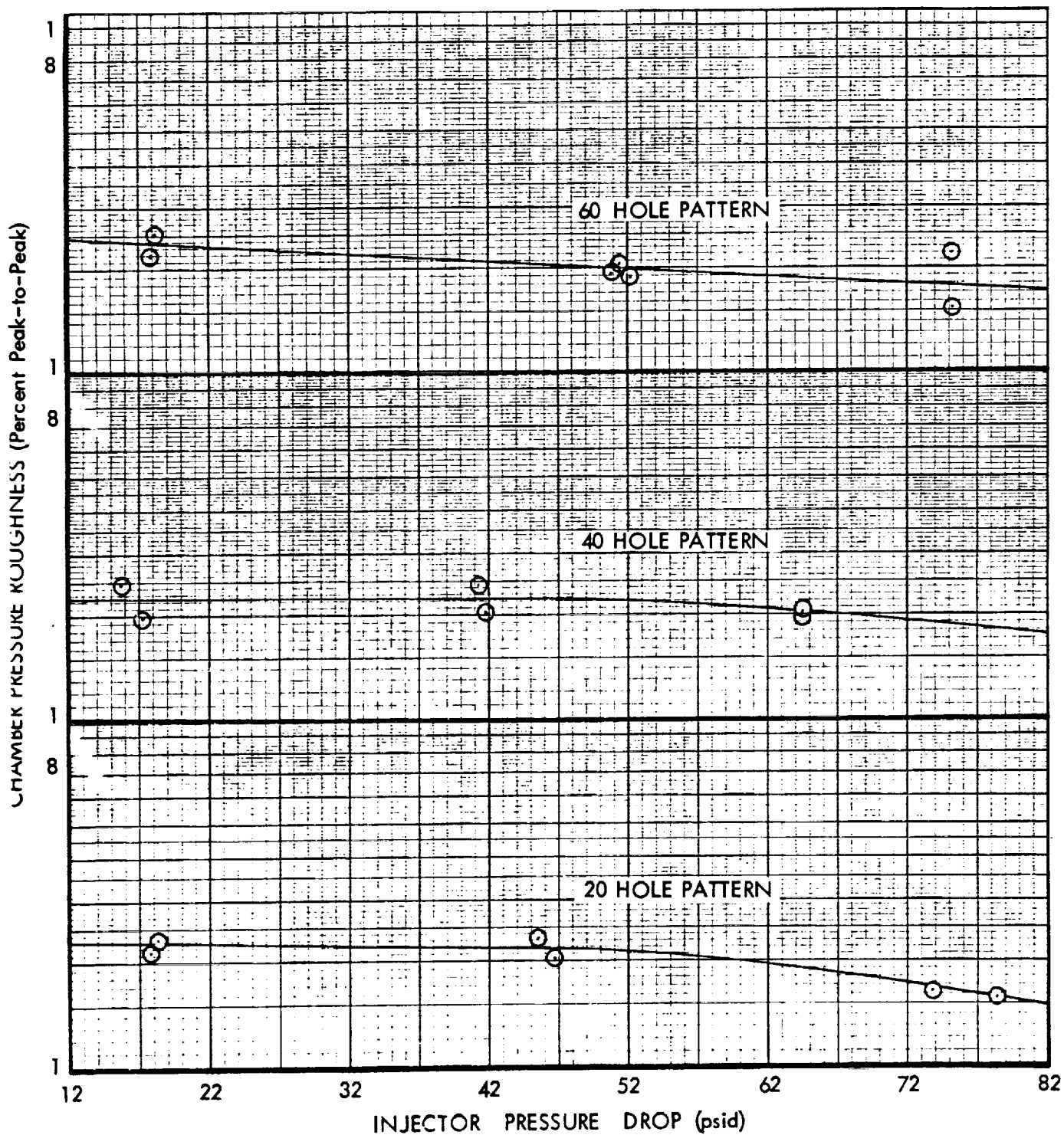
50 lb ENGINE SHOWERHEAD INJECTOR COLD BED RESPONSE DATA VS INJECTOR PRESSURE DROP



50 lbf ENGINE SHOWERHEAD INJECTOR COLD BED
RESPONSE TIME VS INJECTOR PRESSURE DROP



50 lbf ENGINE SHOWERHEAD INJECTOR CHAMBER PRESSURE ROUGHNESS VS INJECTOR PRESSURE DROP



50 Ibf ENGINE 60 HOLE SHOWERHEAD INJECTOR CHAMBER PRESSURE ROUGHNESS VS INJECTOR PRESSURE DROP

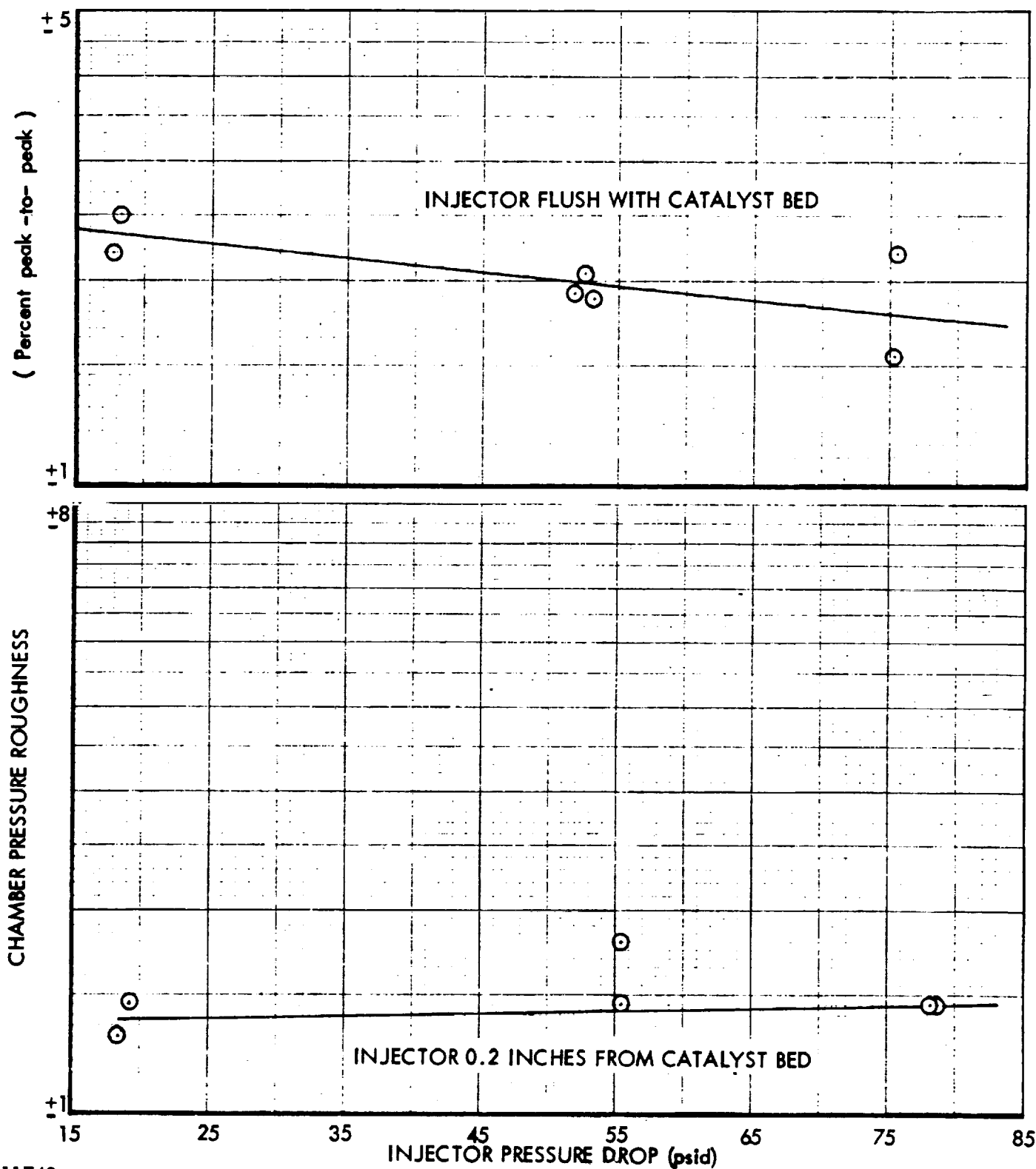


TABLE IX
50 LBF ENGINE - TEST DATA SUMMARY - SHOWERHEAD INJECTOR

Test No.	Injector Pressure Drop Temperature	Fuel Temperature	Initial Catalyst Temperature	Ignition Delay	Response Time	Tailoff Time	Upstream Chamber Pressure	Downstream Chamber Pressure	Thrust	Flow Rate	c*	Specific Impulse	C _F	Chamber Pressure Roughness	Test Code
	psid	°F	°F	ms.	ms.	ms.	psia	psia	lbf	lbm/sec	ft. sec	lbf-sec/lbm (1)	(1)	% Peak-to-peak	(2)
171-21-145	12.7	45	73	18	312	62	175.7	151.6	35.00	0.22107	4243	156.32	1.200	± 1.65	15-0-20
171-31-146	13.1	46	63	23	230	65	177.6	152.7	35.27	0.22479	4203	156.90	1.201	± 2.13	15-0-20
171-31-126	46.7	51	59	24	430	60	167.5	147.7	34.08	0.21365	4278	159.51	1.200	± 2.03	45-0-20
171-31-127	45.7	52	--	20	465	47	167.9	144.1	33.41	0.21106	4242	158.30	1.200	± 2.36	45-0-20
171-31-128	47.7	51	59	--	---	--	172.4	148.2	34.03	0.21591	4247	157.61	1.194	± 1.22	45-0-20
171-31-142	78.5	45	66	19	590	44	185.9	160.1	37.40	0.23395	4234	159.86	1.215	± 1.56	75-0-20
171-31-143	73.9	46	68	19	519	43	180.1	154.2	35.90	0.22569	4228	159.07	1.210	± 1.62	75-0-20
171-31-133	13.6	57	68	17	155	63	170.4	145.1	33.88	0.21122	4251	160.40	1.214	± 2.18	15-0-40
171-31-134	17.1	53	86	22	155	55	177.3	152.3	35.47	0.22331	4226	156.45	1.209	± 1.96	15-0-40
171-31-131	41.2	66	76	13	311	60	172.4	147.4	33.93	0.21529	4237	157.60	1.197	± 2.45	45-0-40
171-31-132	41.7	53	56	20	287	60	172.8	149.2	34.30	0.21687	4257	158.16	1.195	± 2.01	45-0-40
171-31-129	64.5	57	57	25	396	65	171.6	148.4	33.96	0.21583	4255	157.35	1.191	± 2.03	75-0-40
171-31-130	64.5	58	64	18	388	67	172.0	148.7	34.20	0.21557	4268	158.67	1.196	± 2.03	75-0-40
171-31-140	17.9	46	67	21	247	52	177.1	149.7	34.40	0.21938	4222	156.81	1.195	± 2.19	15-0-60
171-31-141	18.3	36	64	16	247	50	180.4	150.7	34.68	0.21276	4205	156.37	1.196	± 2.52	15-0-60
171-31-135	49.7	51	67	24	398	--	174.3	145.7	33.73	0.21202	4252	159.09	1.204	± 1.93	45-0-60
171-31-136	52.1	53	58	24	359	56	174.2	141.4	34.38	0.21730	4226	158.21	1.204	± 1.89	45-0-60
171-31-137	51.1	55	60	20	386	65	173.3	146.5	33.63	0.21471	4222	156.63	1.194	± 2.05	45-0-60
171-31-138	75.3	55	53	26	437	60	177.8	151.2	34.83	0.22063	4240	157.65	1.198	± 1.52	75-0-60
171-31-139	75.3	42	44	22	442	--	177.2	150.3	34.70	0.22089	4210	157.09	1.200	± 2.19	75-0-60
171-31-152	19.5	51	70	19	156	59	176.7	156.9	36.20	0.22927	4255	157.89	1.200	± 1.43	15-25-60
171-31-153	18.5	48	83	16	179	58	172.6	153.2	35.55	0.22348	4242	159.07	1.206	± 1.30	15-25-60
171-31-147	55.6	49	57	22	292	53	176.1	153.7	35.55	0.2245	4256	158.35	1.203	± 1.79	45-25-60
171-31-148	55.6	50	62	18	248	53	174.7	153.1	35.65	0.22444	4221	159.64	1.211	± 1.47	45-25-60
171-31-149	78.4	51	73	23	355	46	175.9	154.1	35.60	0.22472	4243	158.42	1.201	± 1.46	75-25-60
171-31-150	77.4	51	68	20	427	230	177.8	152.7	35.30	0.22383	4221	157.71	1.202	± 2.29	75-25-60
171-31-151	78.9	50	72	21	344	47	175.9	155.4	36.00	0.22608	4253	159.24	1.204	± 1.45	75-25-60

(1) Nozzle Expansion Ratio 4.03:1

(2) First number refers to nominal injector pressure drop. Second number refers to injector distance from catalyst bed. Third number refers to number of orifices.

Examination of the test data in Table IX indicates that test number 171-31-150 has appreciably longer rise and tailoff times than do tests 171-31-149 and 171-31-151 even though all three tests were with the same injector. For test 171-31-150, a 10 x 10 mesh screen of 0.025 inches wire diameter was placed on top of the 60 mesh screen used as the upper bed support. The addition of the 10 mesh screen apparently supplied volume where hydrazine could collect and resulted in the longer observed rise and tailoff times.

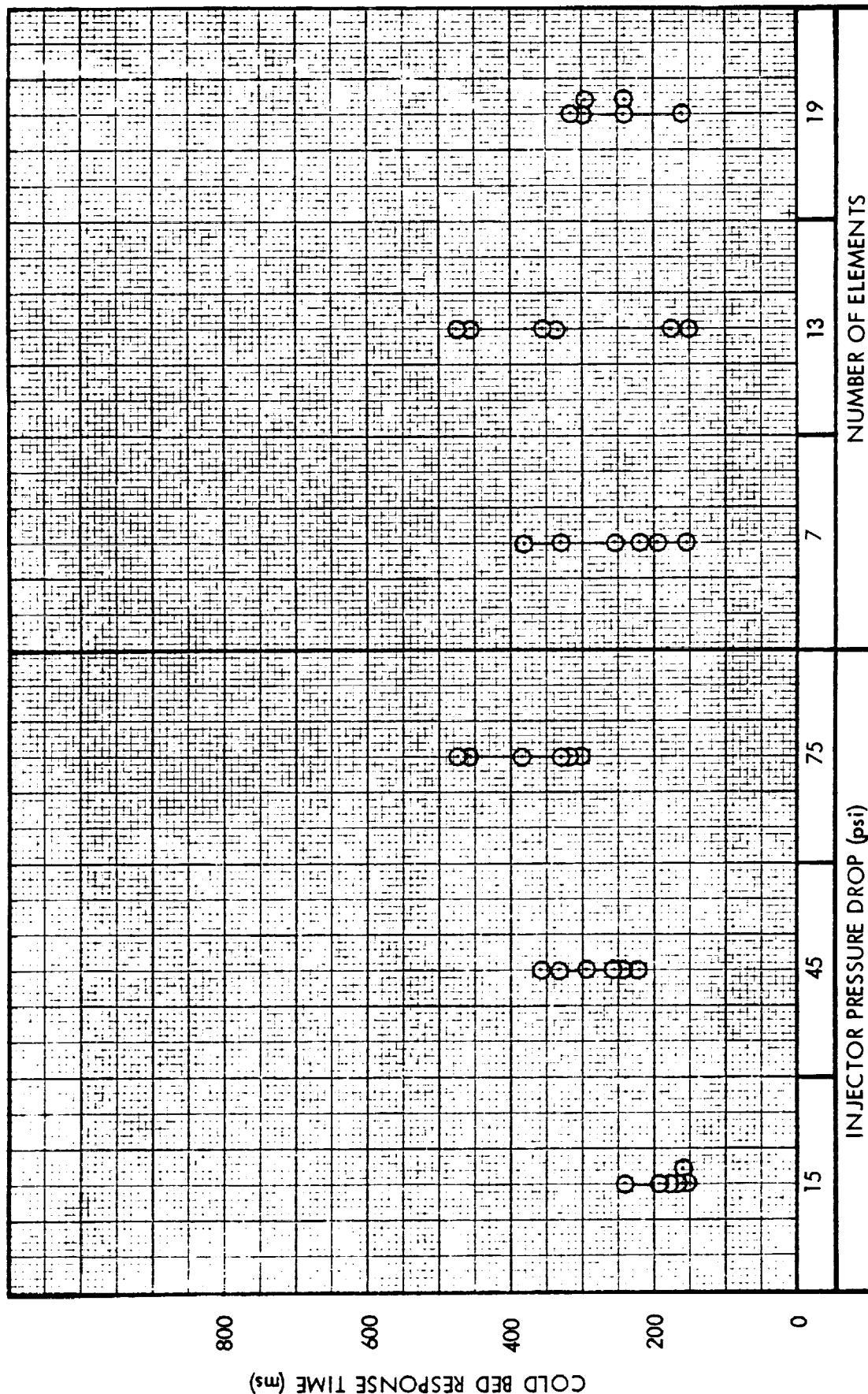
6.2.6 50 lbf Engine - Rigimesh Injector

Testing of the rigimesh injector was conducted with injectors having 7, 13, and 19 elements at 15, 45, and 75 psid nominal pressure drop with each injector. Tests of each injector configuration were made with the injector flush with the catalyst bed. The 13 element injector was also tested at 0.25 inches from the catalyst bed at pressure drops of 15 and 75 psid. The test data obtained is summarized in Table X. Scatter diagrams of the data for cold bed response time, ignition delay, chamber pressure decay time, and chamber pressure roughness are plotted in Figures 43 through 46.

Figure 47 presents a plot of average cold bed response time versus injector pressure drop. An increase in response time with injector pressure drop is noted. The response times with the rigimesh injector are similar to or slightly better than those with the showerhead injector. The response times with the rigimesh injector do not appear to be as dependent on the pressure drop as those for the showerhead injector or the rigimesh injector at the 0.5 and 5 lbf thrust levels. The response times for all three hole patterns are similar at the low pressure drops with the 19 element injector being superior as the pressure drop is increased.

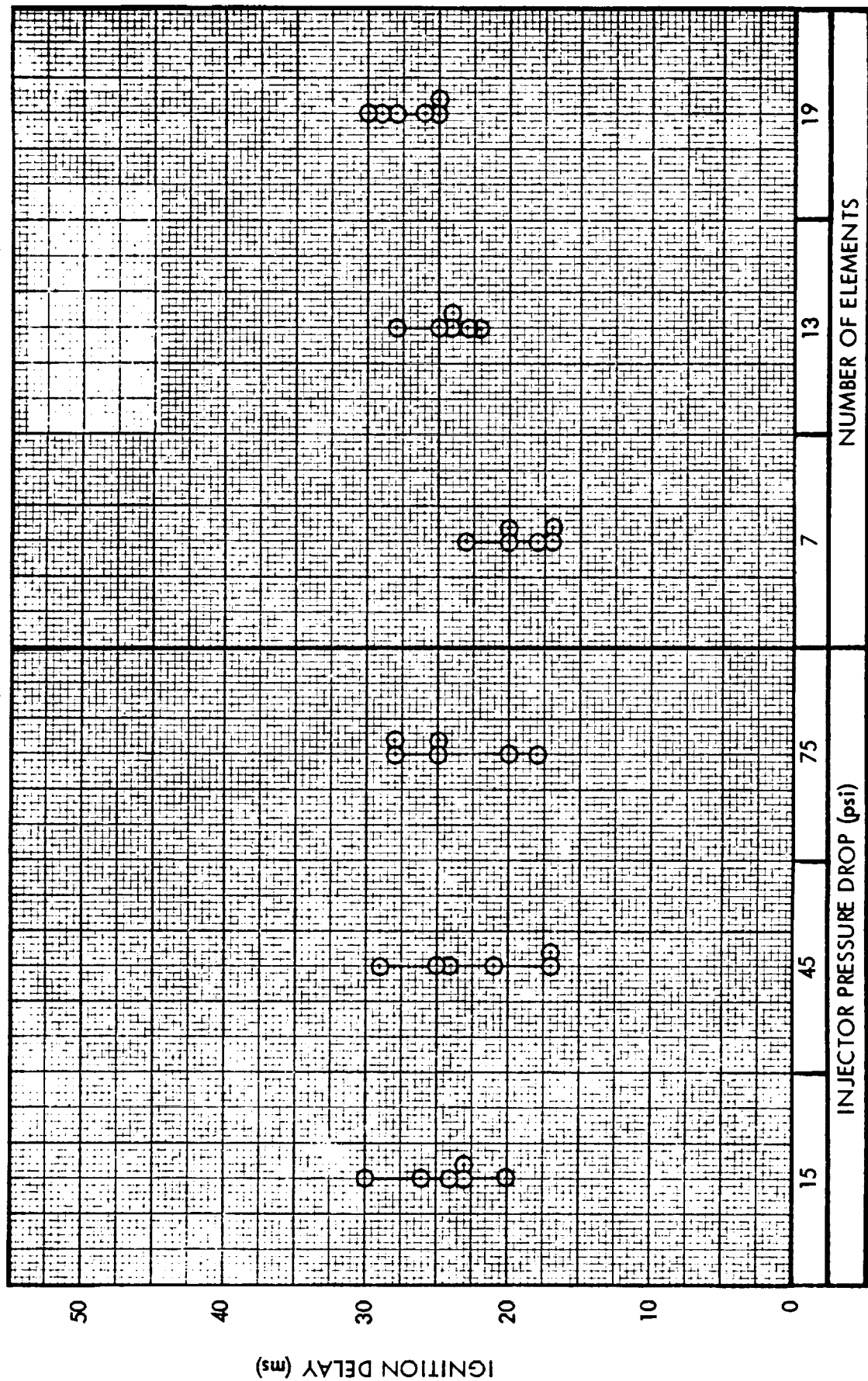
The scatter diagram in Figure 44 indicates no change in ignition delay with pressure drop. An increase in ignition delay does occur, however, as the number of injector elements is increased. Average values are 19.2, 24.3, and 27.2 milliseconds with injector elements of 7, 13, and 19 respectively.

50 1bF ENGINE RIGIMESH INJECTOR SCATTER DIAGRAM COLD BED RESPONSE TIME

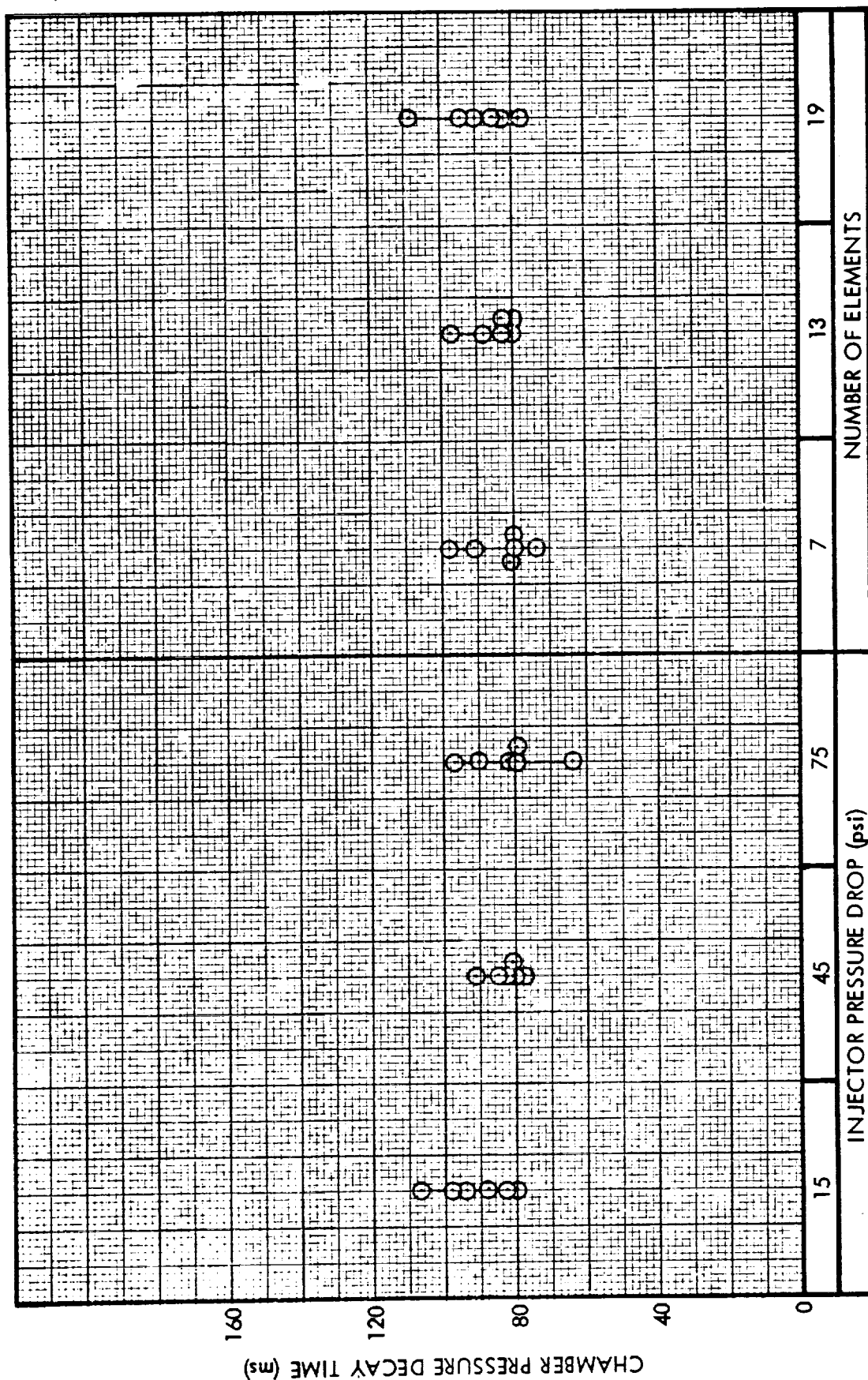


INJECTOR VARIABLE

50 hp ENGINE RIGIMESH INJECTOR SCATTER DIAGRAM IGNITION DELAY

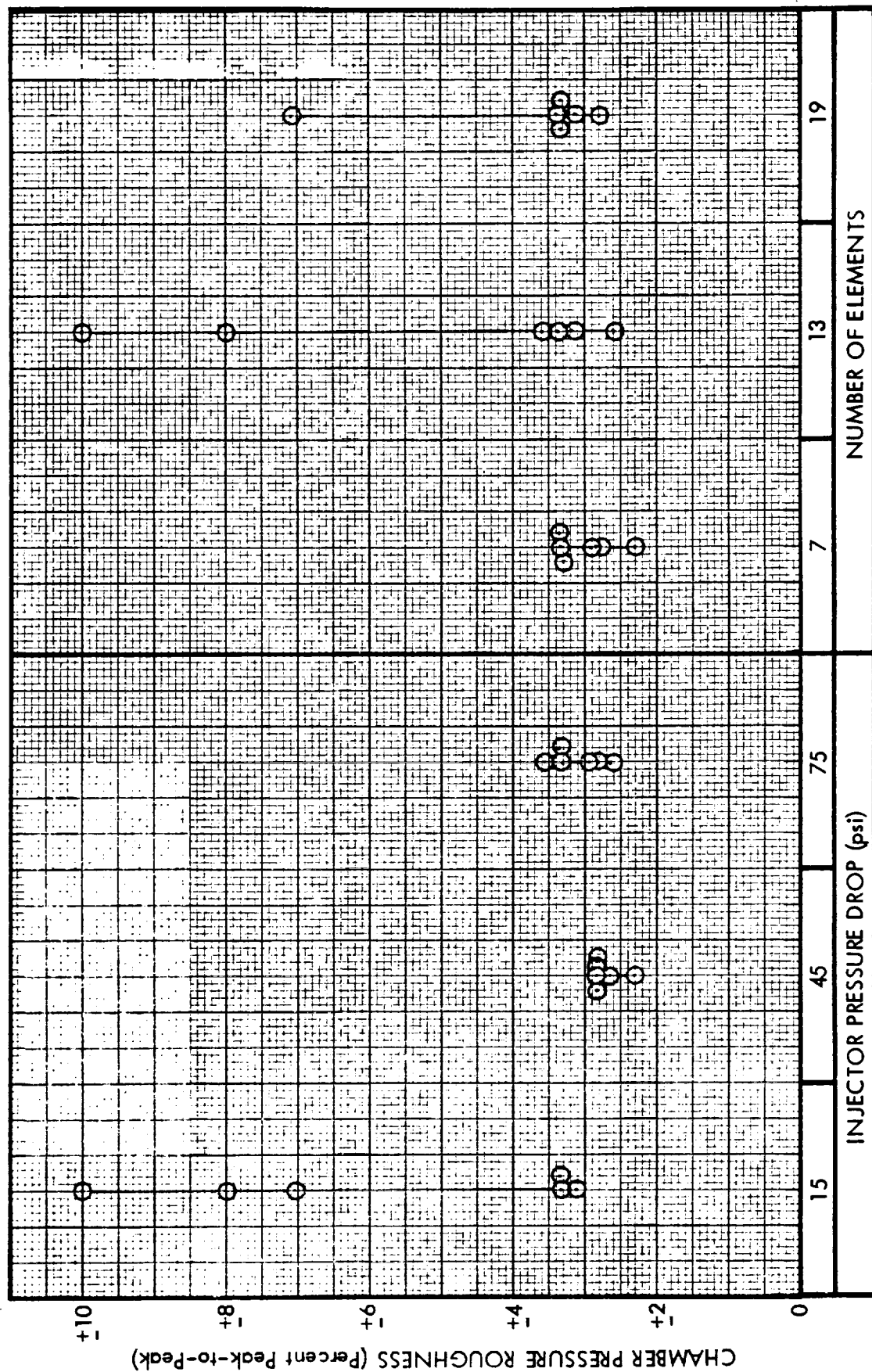


INJECTOR VARIABLE



INJECTOR VARIABLE

50 lbf ENGINE RIGIMESH INJECTOR SCATTER DIAGRAM CHAMBER PRESSURE ROUGHNESS



INJECTOR VARIABLE

50 lbf ENGINE RIGIMESH INJECTOR AVERAGE COLD BED RESPONSE TIME
VS INJECTOR PRESSURE DROP

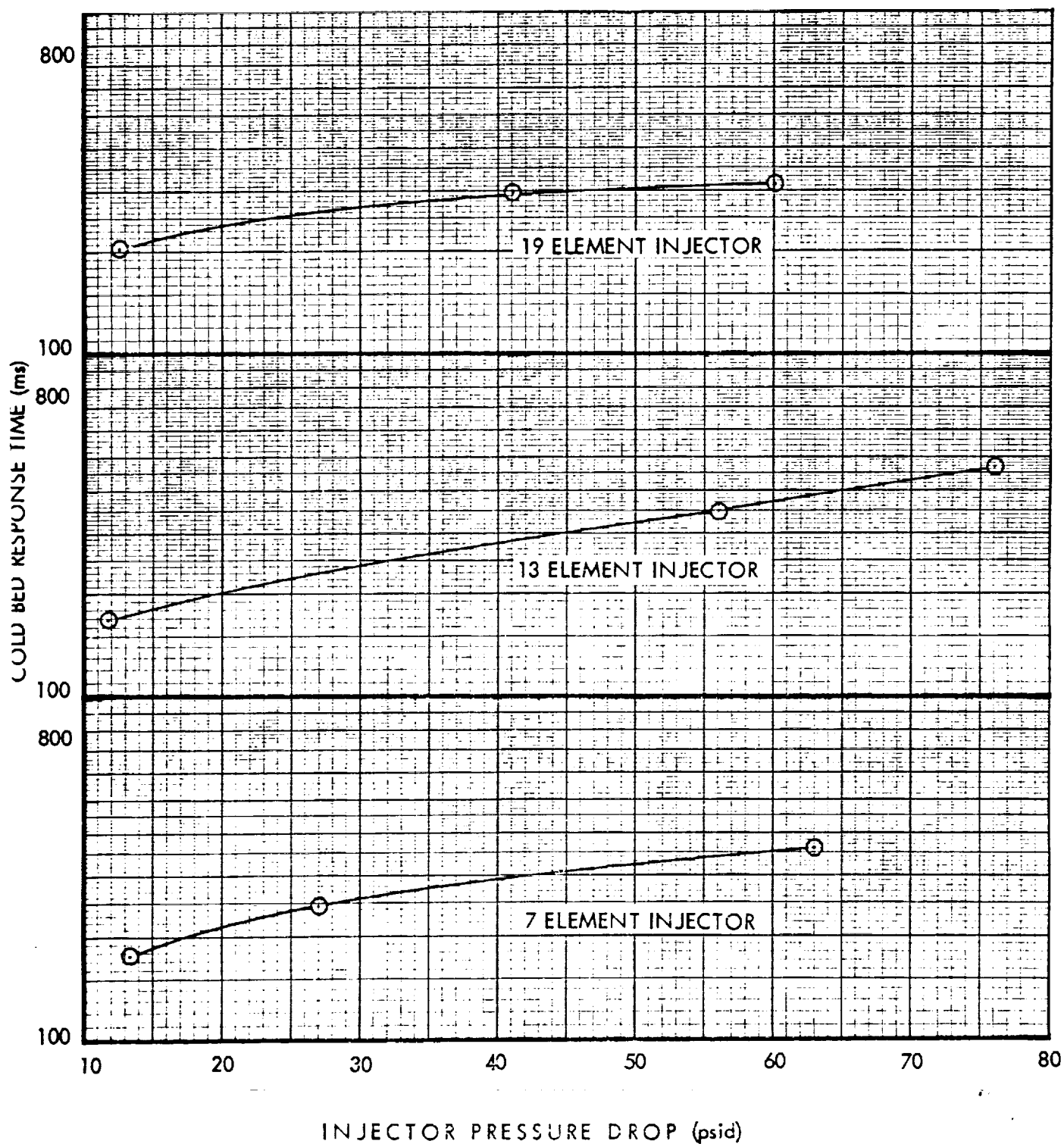


TABLE X
50 LBF ENGINE - TEST DATA SUMMARY - RIGMESH INJECTOR

Test No.	Test Code (1)	Fuel Temperature °F	Initial Catalyst Bed Temperature °F	Ignition Delay ms.	Response Time ms.	Decay Time ms.	Upstream Chamber Pressure psia	Downstream Chamber Pressure psia	Injection Pressure psia	Thrust lbf	Flow Rate lbm/sec	Characteristic Velocity ft/sec	Specific Impulse (2)	Thrust Coefficient (2)	Chamber Pressure % Peak-to-peak
171-31-221	15-0-7	53	61	23	160	80	176.2	150.4	203.4	34.726	0.2201	4228	157.75	1.200	+3.32
171-31-227	15-0-7	48	62	20	195	98	173.3	149.4	201.6	34.532	0.2192	4217	157.53	1.202	+3.35
171-31-223	45-0-7	46	71	17	255	91	177.8	152.1	221.1	35.124	0.2234	4213	157.25	1.202	+2.30
171-31-224	45-0-7	53	67	17	230	81	174.7	149.6	219.0	34.433	0.2197	4213	156.73	1.197	+2.84
171-31-225	45-0-7	46	73	20	382	74	174.8	150.1	248.4	34.872	0.2203	4215	157.95	1.205	+2.95
171-31-226	75-0-7	50	61	18	330	80	176.4	151.5	253.2	34.950	0.2218	4227	157.61	1.200	+3.30
171-31-220	15-0-13	50	60	24	153	83	176.7	150.1	204.0	35.074	0.2209	4205	158.79	1.215	+8.00
171-31-231	15-0-13	47	59	23	184	88	178.7	150.9	204.6	34.975	0.2213	4219	158.02	1.205	+9.94
171-31-234	45-0-13	42	68	22	331	81	177.8	150.0	247.2	34.706	0.2209	4201	157.09	1.203	+3.17
171-31-235	45-0-13	40	55	24	356	83	---	148.5	251.7	34.250	0.2197	4183	155.92	1.199	+3.37
171-31-233	75-0-13	42	48	25	473	80	177.6	151.3	291.6	35.172	0.2242	4176	156.89	1.209	+2.64
171-31-232	75-0-13	49	56	28	456	97	163.2	139.7	272.4	31.980	0.2036	4246	157.07	1.190	+3.58
171-31-242	15-0-19	53	59	30	160	94	176.2	143.6	203.1	32.970	0.2118	4196	155.69	1.194	+3.13
171-31-243	15-0-19	45	60	26	240	107	179.5	141.9	204.6	32.400	0.2079	4224	155.84	1.187	+7.04
171-31-238	45-0-19	43	59	29	240	85	173.4	148.0	228.9	33.960	0.2168	4224	156.63	1.193	+3.38
171-31-239	45-0-19	49	68	25	294	78	178.0	150.2	233.7	34.925	0.2216	4195	157.64	1.209	+3.33
171-31-240	75-0-19	49	55	28	292	82	190.5	158.8	264.6	37.050	0.2333	4216	158.79	1.213	+2.83
171-31-241	75-0-19	47	67	25	315	90	189.7	158.0	264.3	36.850	0.2325	4205	158.50	1.213	+3.32
171-31-236	15-25-13	46	62	32	180	165	176.7	149.9	205.2	35.074	0.2232	4178	157.16	1.210	+7.34
171-31-237	75-25-13	47	39	44	470	88	183.7	158.9	294.6	37.206	0.2318	4242	160.51	1.217	+6.29

(1) First number refers to nominal injector pressure drop. Second number refers to distance of injector from catalyst bed. Third number refers to the number of elements.

(2) Nozzle Expansion Ratio is 4.03:1

Chamber pressure decay time does not appear affected by either the number of orifices or the injector pressure drop.

At all conditions the engine does not run as smoothly with the rigi-mesh injector as with the showerhead injector. This appears to be the major difference between the injectors.

When the injector was moved 0.25 inches from the catalyst bed erratic start transients were obtained and the chamber pressure oscillations were higher than with the injector flush with the catalyst bed.

Characteristic velocity averaged 4,211 feet per second for the tests reported in Table X. Specific impulse averaged 157.5 lbf-sec/lbm and the thrust coefficient averaged 1.203.

6.3 Summary of Injector Optimization Testing

The injector testing reveals certain consistencies in the data obtained at all three thrust levels. These trends and recommendations for injector design criteria are described in the ensuing paragraphs.

It was found that cold bed response time increased as the injector pressure drop was increased at all three thrust levels. This result appears to be caused by the higher surge flow rates which exist at engine start for the low pressure drop injectors. Since chamber pressure was held constant for all of the tests, as the injector pressure drop is lowered, the flow resistance decreases resulting in higher transient flow rates. It appears that in all cases the catalyst is capable of decomposing the propellant faster than it is being supplied. The data obtained suggests that faster response times can be obtained by increasing bed loading. It is noteworthy that the trend in cold bed response was obtained at each thrust level although the nominal design bed loading increased with thrust level. The effects of bed loading on response time will be more fully investigated during later phases of the program.

The data obtained with the 5 and 50 lbf engines with the showerhead injector suggests that an optimum number of orifices exists which minimizes cold bed response time. It is noted that minimum response times were obtained with the 5 and 50 lbf engines with 6 and 40 orifice injectors respectively. These numbers of orifices correspond to 5.3 and 5.6 orifices per square inch of catalyst bed cross sectional area

respectively. It would thus appear that the true minimum occurs with approximately 6 orifices per square inch of catalyst bed area.

It was found that with the injector flush with the catalyst bed, smooth start-transient and steady state operation could be obtained with low pressure drop injectors. These results indicate that atomization of the propellant is not a necessary design criteria as was the case for the nonspontaneous catalyst (Reference 3).

At the 5 and 50 lbf thrust levels it was found that large chamber pressure oscillations existed when large size catalyst pellets were used throughout the catalyst bed. These oscillations could be virtually eliminated through the use of a layer of finer mesh catalyst at the top of the catalyst bed. The size and depth of catalyst required appears to be related to the bed loading and is not yet fully defined. These effects will be studied in more detail in later phases of the program. A penalty is incurred, however, through the use of the fine mesh catalyst and the resultant increase in catalyst bed pressure drop; however, at no time in the testing did the pressure drop become large enough to cause damage to the catalyst. It is noteworthy that during testing on the 50 lbf engine, pressure drops across the catalyst bed as high as 35 psid were realized with no evidence of catalyst breakup or damage. It thus appears that the spontaneous catalyst has a strength which is significantly higher than the nonspontaneous catalyst, designated by JPL as H-A-3, which was limited to pressure drops of 20 psid.

It was found that smooth operation could be obtained with the injector away from the catalyst bed. There appears to be no advantage, however, to having the injector away from the catalyst bed. Ignition delay and chamber pressure response times were higher and the engines tended to run rougher at the 0.5 and 5 lbf thrust levels when the injector was away from the catalyst bed. At the 50 lbf thrust level very similar results were obtained with the injector located either flush or 0.25 inches from the catalyst bed.

The rigimesh injector is a workable injector concept and gives results similar to the showerhead injector with the following exceptions:

- a. Chamber pressure oscillations are higher
- b. Chamber pressure decay times are higher

- c. The rigimesh injector gives poor operation when it is not flush with the catalyst bed. This is probably caused by nonaxial flow from the injector and the impingement of this flow on the chamber walls.

One of the main advantages of the rigimesh injector is that it offers better resistance to being plugged by catalyst fines which might be generated from a vibration environment than does the showerhead injector (Reference 4). This is especially true if small orifices must be employed in the showerhead injector design. One of the disadvantages of the rigimesh injector is the inability to reproducibly size the injector for a given pressure drop. Prior to detail design of the rigimesh injector, flow tests were conducted with a number of sizes of rigimesh to obtain flow rate per unit cross sectional area. It was found that this data was not consistent with that obtained when the injectors were manufactured. There are probably two problems which lend to this lack of consistency. Rigimesh is made of sintered woven wire sheet. Various pore openings are obtained by utilizing either various numbers of layers of the sheet, of using different wire diameters, or by pressing the layers to varying thicknesses. Variation in wire diameter for the same thickness of rigimesh can produce marked changes in the flow rate per unit cross sectional area. Up to 50% variations have been quoted by the vendor. The rigimesh was machined by clamping the material between two flat plates. Application of excessive pressure from the clamping can result in decreasing the thickness of the rigimesh and thus reductions in the pore size. If this material is to be used it must be ordered to produce a given flow rate per unit cross sectional area and then pressed until the desired value is obtained.

It is felt that the showerhead injector represents a superior injector concept over the rigimesh injector for most applications. In most cases orifice diameters can be kept relatively large through the use of low pressure drop injectors. Additionally, reactor operation is not critically dependent on the number of orifices so that the number of orifices can be reduced over the indicated optimum without significant degradation in reactor operation. Orifice sizes as small as 0.010 inches have been used on the program with no problems of orifice plugging during engine tests. It should be noted, however, no vibration tests were conducted to determine whether or not orifice plugging would occur from catalyst fines generated by launch vehicle type vibration levels.

The following design criteria is recommended for the showerhead injector:

- a. Use approximately six orifices per square inch of catalyst bed cross sectional area. If required, this can be reduced by a factor of at least two without serious degradation in engine operation.
- b. Utilize low pressure drop injectors. The pressure drop can be held to 10 to 15% of the steady state chamber pressure.
- c. Mount the injector flush with the top of the catalyst bed.
- d. Propellant can be fed into the injector manifold through a single supply tube. Propellant velocities in the supply tube as high as 50 to 75% of the injector stream velocities were utilized in the study with no adverse effect on propellant distribution and/or reactor operation.
- e. Velocities in the propellant distribution manifold as high as 20 to 30% of the injector stream velocities were utilized in the study without having maldistribution of flow to the injector orifices.
- f. No evidence was found to indicate high L/D orifices and turbulent stream characteristics are necessary design criteria. It appears that orifice lengths are dictated by the required injector plate thickness needed to meet structural requirements.

7.0 CATALYST BED DESIGN PARAMETER STUDIES

Parametric tests were conducted to determine the effects of chamber pressure bed loading, catalyst particle size and bed length on reactor operation. Data to be obtained during these tests included:

- a. Ignition Delay Time
- b. Cold Bed Response Time
- c. Ammonia Dissociation
- d. Catalyst Bed Pressure Drop
- e. Characteristic Velocity and Sea Level Specific Impulse
- f. Chamber Pressure Roughness.

Identical tests were conducted at nominal thrust levels of 0.5, 5, and 50 lbf. The test data accumulated served as a basis for development of design and scaling criteria defining reactor performance and operation.

7.1 Test Conditions Studied

The range of study was to cover chamber pressure from 50 to 1,000 psia, bed loading over at least a 3:1 range, and catalyst bed lengths over at least a 3:1 range. The test matrixes in Figures 48, 49, and 50 list the conditions tested with the 0.5, 5, and 50 lbf engines. Chamber pressure was varied from 50 to 1,000 psia with intermediate values of 105, 225, and 475 psia. Bed loading was varied in increments of 0.01, 0.021, and 0.045 lbf/in²-sec. Catalyst bed lengths for the 5 lbf engine were 0.5, 1.0, 1.5, and 2.0 inches; for the 50 lbf engine were 1.0, 2.0, and 3.0 inches; and for the 0.5 lbf engine were 0.5, 1.25, and 2.0 inches.

Tests were conducted at each point in the matrixes shown except where the estimated catalyst bed pressure drop exceeded 70 psid or where previous tests at a longer bed length had resulted in unsatisfactory operation. Instrumentation utilized for the tests is tabulated in Table XI.

7.2 Test Results

7.2.1 5 lbf Engine

Prior to initiating the bed loading chamber pressure, and bed length tests, a series of tests was conducted to determine the required fine mesh

0.5 lbf ENGINE
TEST MATRIX FOR BED LOADING, CHAMBER PRESSURE, AND BED LENGTH STUDIES

Bed Loading lbm/in ² -sec Chamber Pressure (psia)	0.01						0.02115						0.0447					
	50	105.7	223.5	472.6	1000		50	105.7	223.5	472.6	1000		50	105.7	223.5	472.6	1000	
0.5 Catalyst Bed Length (in)	A3-1	A3-2	A3-3	A3-4	A3-5			A3-6	A3-7	A3-8	A3-9				A3-10	A3-11	A3-12	
1.25	A3-13	A3-14	A3-15	A3-16	A3-17		A3-18	A3-19	A3-20	A3-21	A3-22			A3-23	A3-24	A3-25	A3-26	
2.0	A3-27	A3-28	A3-29	A3-30	A3-31			A3-32	A3-33	A3-34	A3-35					A3-36	A3-37	

5 lbf ENGINE
TEST MATRIX FOR BED LOADING, CHAMBER PRESSURE, AND BED LENGTH STUDIES

	Bed Loading (lbm/in ² -sec)	0.01						0.02115						0.1447					
		50	105.7	223.5	472.6	1000		50	105.7	223.5	472.6	1000		50	105.7	223.5	472.6	1000	
	Chamber Pressure (psia)																		
	0.5	83-1	83-2	83-3	83-4					83-5	83-6	83-7					83-8	83-9	
	1.0	83-10	83-11	83-12	83-13	83-14		83-15	83-16	83-17	83-18	83-19				83-20	83-21	83-22	
	1.5	83-23	83-24	83-25	83-26	83-27		83-28	83-29	83-30	83-31	83-32				83-33	83-34	83-35	
	2.0	83-36	83-37	83-38	83-39	83-40		83-41	83-42	83-43	83-44	83-45				83-46	83-47	83-48	
	BED LENGTH (INCHES)																		

50 lbf ENGINE
TEST MATRIX FOR BED LOADING, CHAMBER PRESSURE, AND BED LENGTH STUDIES

Bed Loading (lb/in ² -sec)	.01					.02115					.0447				
	50	105	224	473	1000	50	106	224	473	1000	50	106	224	473	1000
Chamber Pressure (psia)															
1.0		C3-1	C3-2	C3-3	C3-4*			C3-5	C3-6	C3-7			C3-8	C3-9	C3-10
2.0	C3-11	C3-12	C3-13	C3-14*	C3-15*	C3-16	C3-17	C3-18	C3-19	C3-20		C3-21	C3-22	C3-23	C3-24
3.0	C3-25	C3-26	C3-27	C3-28*	C3-29*	C3-30	C3-31	C3-32	C3-33	C3-34		C3-35	C3-36	C3-37	C3-38
BED LENGTH (INCHES)															

*These tests were not conducted because of damage to test hardware.

TABLE XI

INSTRUMENTATION LIST FOR REACTOR DESIGN PARAMETER STUDIES

PARAMETER	SYMBOL	TYPE RECORDER		
		Strip Chart	Oscillograph	Digital
Injection Pressure	P_i	X	X	X
Upstream Chamber Pressure	P_{cu}	X	X	X
Downstream Chamber Pressure	P_{cd}	X	X	X
Gas Sample Bottle Pressure	P_g			X
Thrust	F	X	X	
Propellant Flowrate	\dot{w}_1		X	
Propellant Flowrate	\dot{w}_2		X	
Fuel Temperature	T_f			X
Injector Head Temperature	T_{i1}	X		
Injector Head Temperature	T_{i2}	X		
Catalyst Bed Temperature	T_{b1}	X		
Catalyst Bed Temperature	T_{b2}	X		
Gas Outlet Temperature	T_g	X		
Valve Position	Y_v		X	

catalyst on the top of the catalyst bed. Earlier tests (See Paragraph 6.2.3) had indicated this was required to assure smooth steady state operation. These tests were conducted with the 1.5 inch chamber at a bed loading of $0.045 \text{ lb/in}^2\text{-sec}$ and a chamber pressure of 225 psia. The results of this testing are summarized in Table XII. The catalyst bed configuration arrived at was 0.3 inches of 25-30 mesh catalyst on the top of the bed, with the remainder of the bed 14-16 mesh granular catalyst.

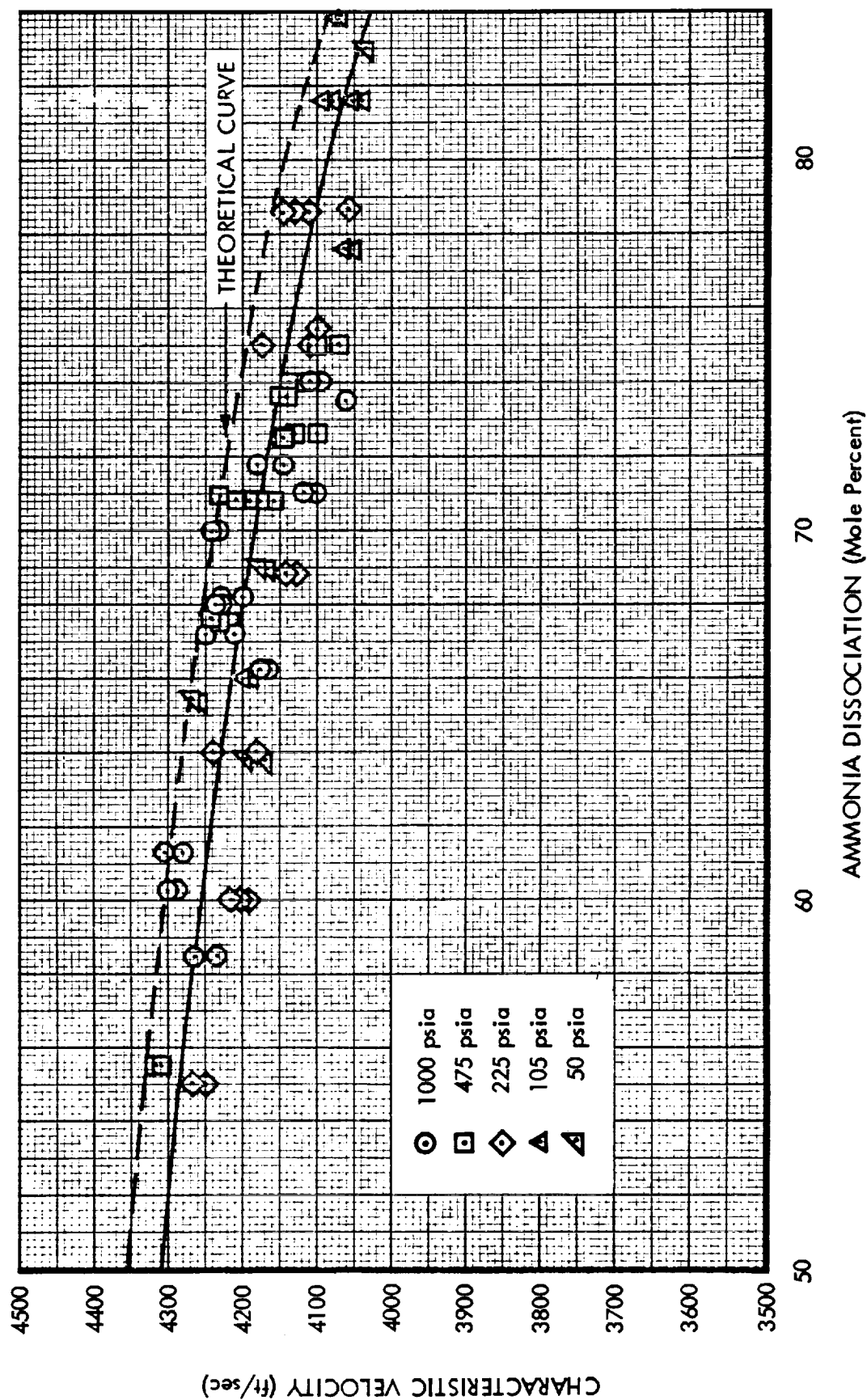
Data obtained from testing on the 5 lbf engine is summarized in Table XIII. The characteristic velocity data has been corrected for chamber radiation heat losses and propellant temperature effects and is plotted against fractional ammonia dissociation in Figure 51. Radiation heat loss corrections were made assuming radiation to free space with a chamber emissivity of 0.9. All test data was normalized to a propellant temperature of 70°F (Reference 5). When these corrections are made to the data, the mean curve falls within approximately 98.5% of the theoretical curve.

Sea level thrust coefficient data for expansion ratios of 1.0 and 2.2 is plotted versus chamber pressure in Figure 52. The theoretical curve has been corrected for divergence losses assuming a 15° conical nozzle. From the curve it is noted that the data at an expansion ratio of 1.0 falls on the theoretical curve while the data at an expansion ratio of 2.2 averages approximately 99% of the theoretical value.

7.2.2 50 lbf Engine

Prior to initiation of the bed loading, chamber pressure, and bed length studies, tests were conducted with 20-25 and 25-30 mesh granules on the top of the catalyst bed to determine the required fine mesh catalyst size for smooth decomposition. Previous testing (see Paragraph 6.2.5) had shown that larger size granules resulted in unsatisfactory operation. These tests were conducted with the 3.0 inch length chamber at a bed loading of $0.045 \text{ lb/in}^2\text{-sec}$ and a chamber pressure of 225 psia. Chamber pressure oscillations of ± 3 to 9% occurred during testing with 20-25 mesh granules on the top of the catalyst bed. Testing with 25-30 mesh granules resulted in maximum chamber pressure oscillations of $\pm 2\%$. A catalyst bed configuration was finalized which consisted of

CORRECTED CHARACTERISTIC VELOCITY
VS
AMMONIA DISSOCIATION FOR 5 lbf ENGINE



SEA LEVEL THRUST COEFFICIENT VS CHAMBER PRESSURE FOR 5 lbf ENGINE

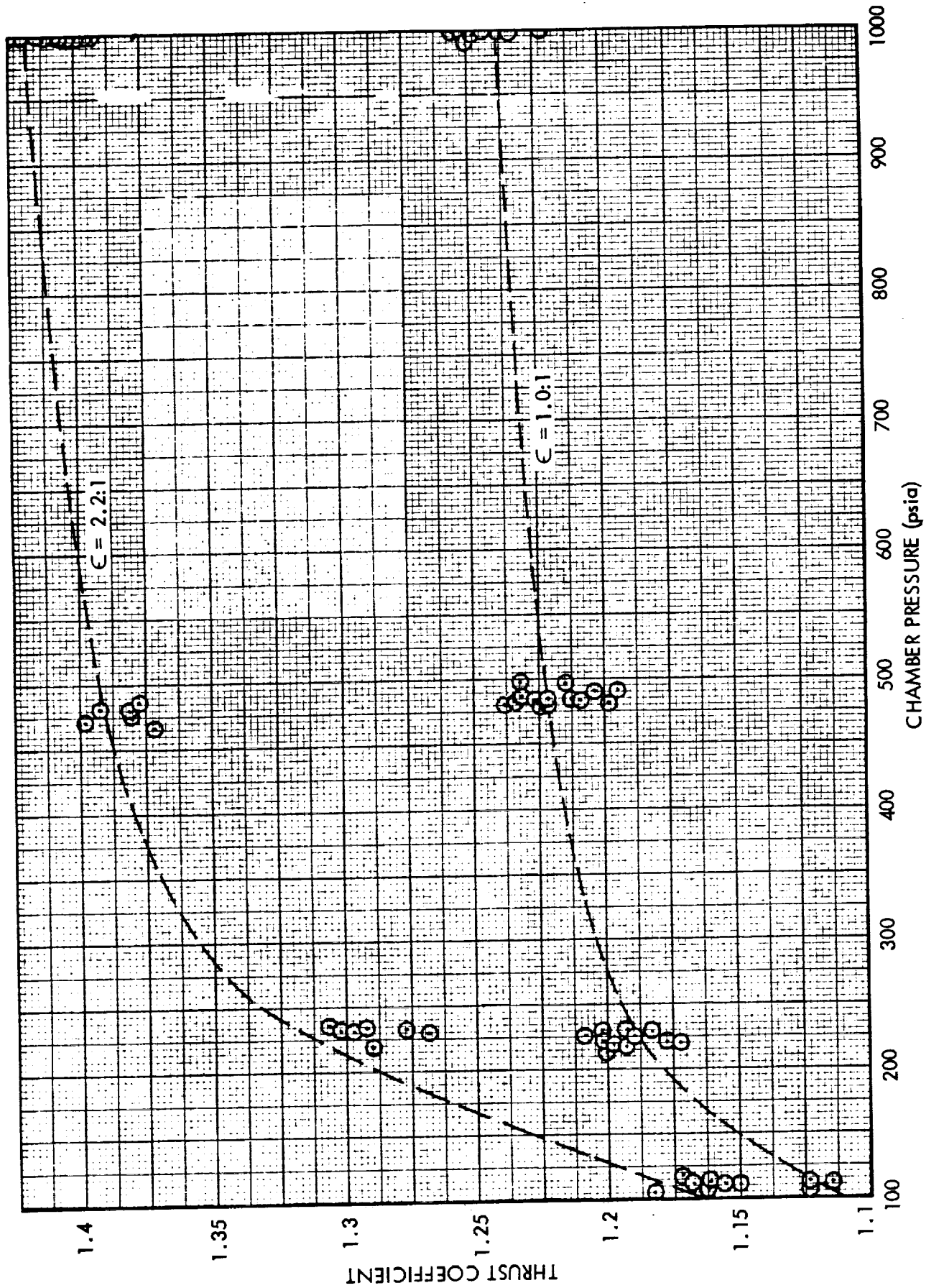


TABLE XII
SUMMARY OF 5 lbf ENGINE CATALYST PARTICLE SIZE STUDIES

TEST NO.	CATALYST BED CONFIGURATION	TEST RESULTS
244	Entire bed composed of $1/8 \times 1/16$ " pellets. Bed length 1.5 inches.	Chamber pressure oscillations of ± 36 psia occurred throughout test of 5 seconds duration. Frequency of oscillations was 8.3 cps. Ignition delay was 20 ms.
245	0.3 inches of 16-20 mesh catalyst on top of catalyst bed. Remaining 1.2 inches of bed $1/8 \times 1/16$ " pellets.	Test was very smooth ($\pm 1.5\%$ chamber pressure oscillations) up to 9 seconds. Random oscillations of $\pm 16\%$ chamber pressure variation for remainder of 30 second test. Ignition delay was 4 ms. Chamber pressure decay time was 340 ms.
246	0.3 inches of 20-25 mesh catalyst on top of catalyst bed. Remaining 1.2 inches of bed $1/8 \times 1/16$ " pellets.	Test was smooth in operation up to 20.6 seconds and then very rough for remainder of test of 30 seconds duration. Chamber pressure decay time was 460 ms.
247	0.3 inches of 20-25 mesh catalyst on top of catalyst bed. Remaining 1.2 inches of bed $1/8 \times 1/16$ " pellets.	Test was smooth in operation up to 22 seconds and then very rough for remainder of test of 30 seconds duration. Chamber pressure decay time was 390 ms.
248	0.5 inches of 20-25 mesh catalyst on top of catalyst bed. Remaining 1.2 inches of bed $1/8 \times 1/16$ " pellets.	Test was smooth in operation up to 17.8 seconds. Random oscillations which tend to damp out and return occur throughout remainder of 30 second test. Chamber pressure decay time was 425 ms.
249	0.5 inches of 25-30 mesh catalyst on top of catalyst bed. Remaining 1.2 inches of bed $1/8 \times 1/16$ " pellets.	Smooth operation up to 11 seconds. Pressure spikes and random roughness occur periodically up to 27.6 seconds at which time engine starts to run smooth again. Chamber pressure decay time was 105 ms.
250	0.3 inches of 20-30 mesh catalyst on top of catalyst bed. Remaining 1.2 inches of bed $1/8 \times 1/16$ " pellets.	Smooth operation to 12 seconds at which time chamber pressure spikes and random oscillations occur until end of test. Chamber pressure decay time was 217 ms.
251	0.3 inches of 25-30 mesh catalyst on top of catalyst bed. Remaining 1.2 inches of bed 14-16 mesh catalyst.	Test was smooth except for 5 pressure spikes of approximately 50 psid overshoot which occur between 13 and 25 seconds into 30 second test. Chamber pressure decay time was 90 ms.
252	Same as 251.	Test was smooth except for two small pressure spikes at 25 and 27 seconds. Chamber pressure decay time was 81 ms.

TABLE XIII
SUMMARY OF 1.205 DIAMETER REACTOR BED LOADING, CHAMBER PRESSURE, AND BED LENGTH TESTS

Test No.	Bed Length in.	Initial Catalyst Temperature °F	Downstream Chamber Pressure psia	Thrust lbf	(1) Flow Rate lbm/sec	Exit Gas Temperature °F	(2) Ignition Delay ms.	(3) Response Time ms.	(4) Decay Time ms.	Characteristic Velocity ft/sec	(5) Specific Impulse lbf-sec/lbm	Chamber Pressure Roughness % peak to peak	Catalyst Bed Pressure Drop psia	(6) Ammonia Dissociation mole %	(5) Thrust Coefficient
338	0.5	43	1014	2.040	0.01158	1429	40	164	221	4052	176.1	+0.6	0	---	1.398
340	0.5	52	1016	2.067	0.01161	1494	11	146	220	4050	178.0	+0.5	0	71.6	1.414
279	0.5	40	995	3.712	0.02280	1525	14	92	113	4222	162.8	+3.6	0	---	1.243
281	0.5	51	1003	3.752	0.02304	1529	9	100	135	4207	162.8	+1.8	0	58.5	1.243
306	0.5	44	1015	9.07	0.04870	---	11	46	84	4264	186.2	+5.9	8	---	1.408
309	0.5	44	1009	8.03	0.04883	1641	12	48	76	4246	164.4	+4.8	9	60.3	1.247
314	1.0	50	1000	2.01	0.01167	1398	18	267	228	3964	172.2	+0.6	2	---	1.396
316	1.0	46	1011	2.07	0.01183	1420	12	206	237	3956	175.0	+0.3	0	71.0	1.424
273	1.0	44	1011	3.748	0.02346	1472	10	108	102	4173	159.8	+1.8	0	---	1.233
278	1.0	54	1012	3.716	0.02356	1472	12	108	80	4160	157.7	+0.8	1	68.3	1.222
300	1.0	47	1011	9.040	0.04856	1542	11	66	95	4259	186.2	+3.2	5	---	1.407
302	1.0	62	997	7.950	0.04819	1543	9	79	92	4252	165.0	+3.2	7	61.3	1.247
325	1.5	51	1014	2.000	0.01206	1269	12	200	258	3892	169.2	+0.6	2	73.7	1.401
266	1.5	54	1013	3.796	0.02385	1398	10	133	133	4114	159.5	+0.8	4	---	1.250
268	1.5	46	1000	3.756	0.02351	1415	10	120	136	4119	159.8	+0.5	2	66.2	1.250
287	1.5	56	966	7.728	0.04730	1468	11	90	62	4197	163.4	+1.1	23	---	1.255
285	1.5	49	975	7.784	0.04784	1481	11	76	87	4188	162.7	+1.2	12	68.0	1.251
319	2.0	52	1011	2.040	0.01192	1329	16	253	302	3926	171.2	+0.5	3	---	1.403
321	2.0	51	1006	2.010	0.01183	1329	17	325	393	3935	170.0	+0.8	2	74.0	1.393
283	2.0	46	1006	3.744	0.02348	1428	11	168	165	4141	159.5	+0.9	2	---	1.239
284	2.0	49	1009	3.772	0.02360	1424	11	164	173	4149	159.8	+0.6	3	68.6	1.241
296	2.0	62	986	7.860	0.04814	1485	10	103	84	4209	163.3	+0.9	16	---	1.250
298	2.0	53	1003	8.900	0.04880	1472	9	141	117	4198	182.1	+2.4	18	70.0	1.397
332	0.5	52	485	1.780	0.01140	1437	10	193	160	4084	156.2	+1.7	0	---	1.222
334	0.5	47	476	1.760	0.01111	1437	13	216	179	4142	157.5	+1.5	0	70.8	1.223
272	0.5	48	482	3.750	0.02488	1536	10	145	275	3978	150.7	+10.5	36.2	---	1.221
342	0.2	54	484	4.245	0.02414	1513	9	128	112	4105	175.8	+5.4	3.2	62.8	1.378
311	0.5	49	481	8.260	0.05064	1614	9	70	72	4280	163.1	+6.0	51	---	1.226
313	0.5	45	475	9.220	0.04993	1587	13	61	80	4273	184.7	+3.1	27	55.3	1.393
307	1.0	46	496	1.815	0.01179	1338	12	292	175	4076	153.9	+0.6	0	---	1.215
308	1.0	44	494	1.831	0.01174	1329	22	297	175	4070	156.0	+1.1	0	74.0	1.233

TABLE XIII (Cont'd)

Test No.	Bed Length in.	Initial Catalyst Temperature °F	Downstream Chamber Pressure psia	Thrust lbf	(1) Flow Rate lbm/sec	Exit Gas Temperature °F	(2) Ignition Delay ms.	(3) Response Time ms.	(4) Decay Time ms.	Characteristic Velocity ft/sec	(5) Specific Impulse lbf-sec/lbm	Chamber Pressure Roughness % peak to peak	Catalyst Bed Pressure Drop psid	(6) Ammonia mole %	(5) Thrust Coefficient
265	1.0	46	489	3.732	0.02388	1424	9	143	110	4212	156.3	+2.5	5.0	---	1.195
267	1.0	51	488	3.740	0.02387	1442	--	161	108	4199	156.7	+1.2	7.0	67.6	1.203
304	1.0	49	478	9.190	0.05050	1494	9	163	85	4240	182.0	+3.8	23.6	---	1.381
305	1.0	55	476	9.220	0.05046	1492	12	185	86	4257	182.7	+2.5	21.8	67.4	1.381
318	1.5	45	481	1.770	0.01170	1278	14	303	200	3992	151.3	+0.8	1.6	---	1.221
320	1.5	47	479	1.750	0.01160	1261	19	375	215	4005	151.8	+1.2	1.0	75.0	1.222
261	1.5	46	482	3.739	0.02453	1372	10	250	---	4042	152.4	+2.3	6.6	---	1.214
262	1.5	56	484	3.731	0.02341	1372	12	260	120	4090	153.5	+2.1	7.2	62.4	1.210
315	1.5	41	486	3.830	0.02454	1385	15	179	112	4075	156.1	+2.2	6.4	72.6	1.233
289	1.5	43	439	---	0.04774	1424	9	370	108	4132	---	+6.8	46.6	---	---
291	1.5	63	469	9.060	0.05048	1494	10	246	78	4180	179.5	+2.3	22.0	---	1.398
293	1.5	62	473	7.970	0.04905	1450	8	262	70	4218	162.5	+6.3	23.6	70.8	1.241
328	2.0	51	477	1.750	0.01166	1286	16	329	217	3953	150.1	+0.6	3.6	---	1.223
329	2.0	55	476	1.710	0.01147	1295	18	566	233	4009	149.2	+1.3	3.0	71.8	1.198
292	2.0	58	494	3.890	0.02482	1407	10	197	131	4094	156.7	+1.7	6.0	---	1.233
294	2.0	64	481	3.805	0.02421	1394	11	398	213	4085	157.2	+2.3	7.0	73.5	1.238
299	2.0	46	466	8.920	0.05005	1442	13	338	81	4185	178.2	+2.1	43.4	---	1.372
301	2.0	56	474	7.950	0.04899	1441	10	440	77	4235	162.3	+1.8	39.6	70.0	1.234
352	0.5	56	232.7	1.780	0.01164	1398	5	440	110	4130	153.0	+2.8	1.0	---	1.193
354	0.5	53	234.1	1.910	0.01140	1415	8	476	121	4125	167.6	+2.0	1.0	64.0	1.305
310	1.0	44	233.1	1.914	0.01181	1308	15	787	133	4038	162.0	+1.7	3.8	---	1.292
312	1.0	49	225.5	1.716	0.01148	1312	14	888	119	4039	149.5	+1.7	3.8	75.0	1.193
254	1.0	59	226.5	3.600	0.02369	1421	4	318	88	4129	152.0	+1.3	36.4	---	1.183
256	1.0	59	224.9	3.636	0.02384	1407	5	548	82	4132	152.6	+2.3	10.2	59.8	1.190
263	1.0	49	228.3	3.779	0.02415	1442	7	622	92	4139	154.4	+1.8	11.0	---	1.203
345	1.0	57	232.2	8.860	0.05166	1512	10	257	53	4230	171.6	+4.5	31.0	---	1.305
347	1.0	46	231.5	8.770	0.05162	1503	9	275	72	4216	169.9	+10.5	28.8	55.0	1.297
322	1.5	54	216.7	1.650	0.01152	1244	18	1469	139	3888	143.3	+2.9	5.2	---	1.193
323	1.5	46	219.7	1.680	0.01159	1252	19	319	122	3897	145.0	+1.7	5.2	73.0	1.198
251	1.5	64	220.7	3.528	0.02388	1351	6	173	90	4047	147.7	+2.4	16.1	---	1.177
252	1.5	51	221.3	3.528	0.02389	1351	5	319	81	4056	147.7	+2.2	17.0	68.9	1.173
295	1.5	65	215.7	7.290	0.04640	1424	6	257	140	4211	157.1	+2.2	47.4	---	1.201

TABLE XIII (Cont'd)

Test No.	Bed Length in.	Initial Catalyst Temperature °F	Downstream Chamber Pressure psia	Thrust lbf	(1)		Exit Gas Temperature °F	(2)	(3)	(4)	Characteristic Velocity ft/sec	(5)		Chamber Pressure Roughness % peak to peak	Catalyst Bed Pressure Drop psid	(6)	(5)
					Flow Rate lbm/sec	Ignition Delay ms.						Specific Impulse lbf-sec/lbm	Ammonia Dissociation mole %				
330	2.0	49	226.7	1.840	0.01178	14	1261	14	335	160	3939	156.2	---	+ 1.8	8.4	---	1.277
331	2.0	55	229.1	1.860	0.01184	13	1273	13	956	147	3988	157.1	---	+ 1.9	6.8	78.8	1.268
286	2.0	55	217.9	3.972	0.02446	10	1359	10	214	120	4054	162.4	---	+ 2.3	28.4	---	1.290
288	2.0	58	227.1	3.732	0.02432	12	1420	12	242	96	4090	153.5	---	+ 2.2	28.0	---	1.209
290	2.0	58	223.7	3.667	0.02406	16	1359	16	346	83	4072	152.4	---	+ 2.3	53.4	78.5	1.205
324	2.0	59	193.9	6.470	0.04197	13	1407	13	424	87	4185	154.2	---	+ 2.0	57.8	---	1.188
326	2.0	53	216.5	7.273	0.04637	10	1407	10	482	80	4230	156.8	---	+ 2.2	73.8	77.0	1.194
356	0.5	49	108.4	1.723	0.01166	5	---	5	650	91	4095	147.8	---	+ 4.4	1.8	---	1.163
336	1.0	49	109.5	1.747	0.01213	12	1342	12	986	91	4005	144.1	---	+ 3.2	5.7	---	1.160
337	1.0	53	111.3	1.780	0.01230	12	1321	12	874	151	4013	144.7	---	+ 2.4	2.9	---	1.161
341	1.0	54	105.5	1.720	0.01215	6	1355	6	813	80	3852	141.6	---	+ 3.7	3.3	77.6	1.183
269	1.0	51	111.8	3.516	0.02446	5	1394	5	545	57	4163	144.5	---	+ 4.6	16.9	---	1.118
270	1.0	50	109.7	3.448	0.02393	10	1398	10	640	59	4152	144.1	---	+ 4.1	17.2	66.0	1.116
366	1.5	55	117.3	1.890	0.01293	12	1261	12	1450	85	4024	146.2	---	+ 3.6	5.6	81.5	1.170
253	1.5	49	107.3	3.391	0.02407	8	1321	8	1363	83	4038	140.9	---	+ 3.5	22.3	---	1.123
255	1.5	58	106.5	3.364	0.02399	6	1321	6	1586	90	4022	140.2	---	+ 4.7	21.4	56.7	1.123
317	1.5	51	104.6	3.360	0.02422	9	1329	9	985	---	3913	138.7	---	+ 5.1	24.6	78.2	1.141
351	2.0	56	107.4	1.700	0.01199	9	1261	9	3000	80	3971	141.8	---	+ 3.6	10.5	---	1.150
353	2.0	53	106.7	1.700	0.01190	7	1270	7	3000	86	3978	142.9	---	+ 4.9	11.6	81.6	1.156
343	1.0	57	59.4	1.770	0.01387	1	1364	1	1132	58	4028	127.7	---	+ 5.5	8.5	---	1.022
344	1.0	56	54.1	1.550	0.01266	5	1329	5	1224	60	4017	125.6	---	+ 4.6	7.9	63.7	1.005
280	1.0	43	54.8	3.312	0.02604	3	1411	3	816	39	4236	127.2	---	+ 5.0	30.0	---	0.968
282	1.0	55	53.7	3.200	0.02529	5	1377	5	851	53	4275	126.5	---	+ 4.2	30.1	69.0	0.953
365	1.5	61	53.4	1.510	0.01256	4	1314	4	1810	59	3990	120.2	---	+ 0.8	11.8	83.0	0.971
257	1.5	49	51.5	3.016	0.02504	6	1312	6	3180	58	4265	120.4	---	+ 3.8	38.7	---	0.912
259	1.5	56	49.5	2.910	0.02440	9	1321	9	500	40	4207	119.2	---	+ 14.0	41.8	65.3	0.912
355	2.0	53	50.3	1.380	0.01164	0	1235	0	2900	62	4062	118.6	---	+ 5.3	18.0	---	0.940
357	2.0	50	51.3	1.440	0.01184	0	1244	0	4200	128	4074	121.6	---	+ 4.3	18.3	---	0.961
359	2.0	45	50.8	1.380	0.01169	5	1252	5	3090	135	4087	118.1	---	+ 7.7	17.9	85.2	0.907

- (1) Average of two flowmeters in series.
 (2) Time from propellant entry into chamber to 1% of steady state chamber pressure.
 (3) Time from propellant entry into chamber to 90% of steady state chamber pressure.
 (4) Time from chamber pressure start decay to 10% of steady state chamber pressure.
 (5) Sea level conditions at expansion ratio of 1.0:1 or 2.2:1.
 (6) Average value obtained from ammonia to hydrogen and ammonia to nitrogen mole ratios.

0.2 inches of 25-30 mesh catalyst on the top of the bed with the remainder of the bed $1/8" \times 1/8"$ cylindrical pellets.

Data obtained from testing on the 50 lbf engine is summarized in Table XIV. Corrected characteristic velocity (see Paragraph 7.2.1) is plotted against ammonia dissociation in Figure 53. The mean curve falls within approximately 99% of the theoretical curve.

Sea level thrust coefficient data is plotted versus chamber pressure in Figure 54. The theoretical curve has been corrected for divergence losses assuming a 15° conical nozzle. The test data averages approximately 98.5% of the theoretical curve.

7.2.3 0.5 lbf Engine

Because of the small size of the 0.5 lbf engine, a layered bed technique was not utilized. Rather, the chamber was filled with a single size catalyst throughout. Testing was conducted with both 16-20 mesh and 20-25 mesh size catalyst in the engine. The 16-20 mesh catalyst resulted in excessive chamber pressure excursions while smooth operation was obtained with the 20-25 mesh catalyst. This size catalyst was subsequently used for all of the reactor design parameter studies.

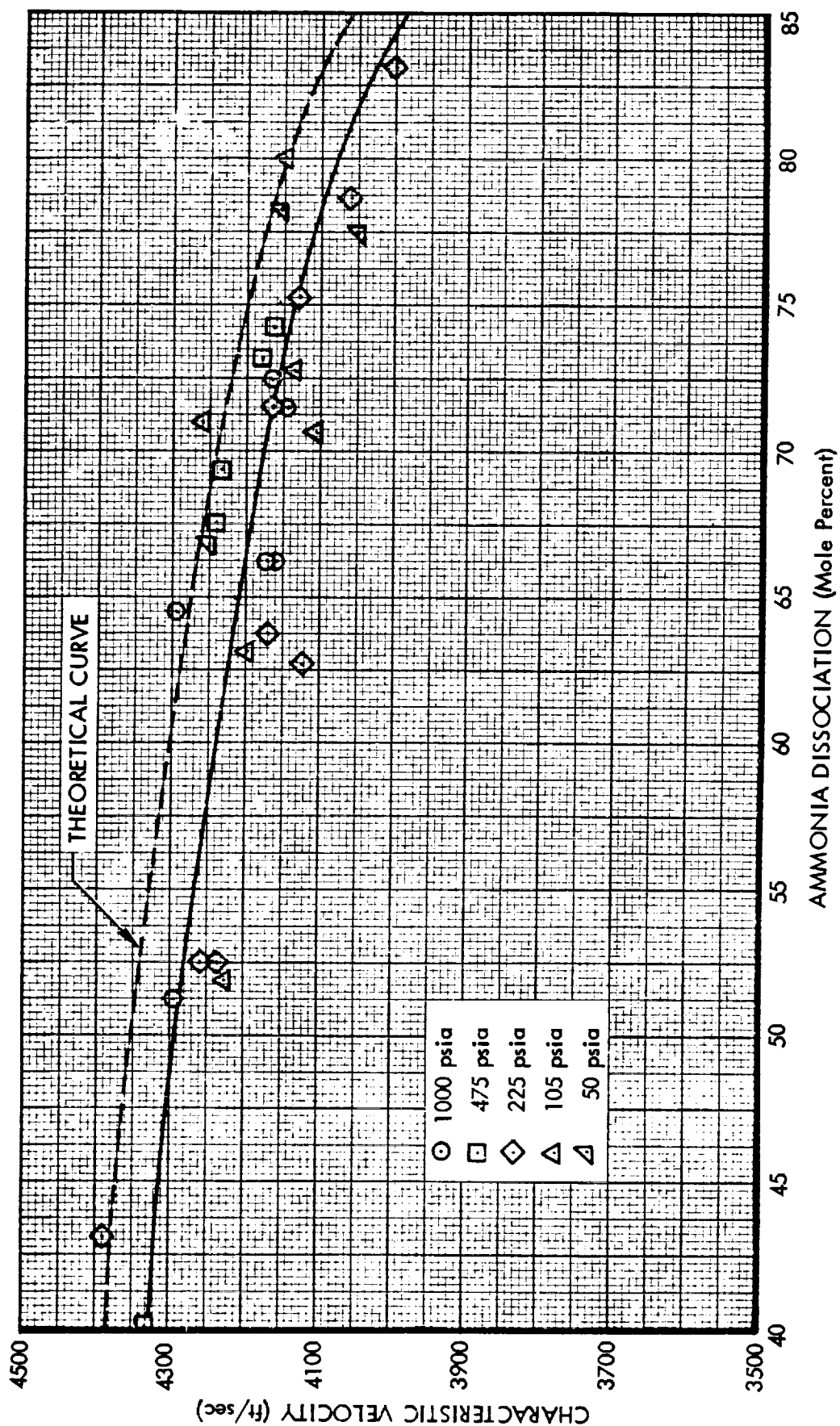
Data obtained from testing on the 0.5 lbf engine is summarized in Table XV. Corrected characteristic velocity is plotted against measured ammonia dissociation in Figure 55. The mean curve falls within approximately 99% of the theoretical curve.

Sea level thrust coefficient data is plotted versus chamber pressure in Figure 56. The theoretical curve (for $\gamma = 1.28$) has been corrected for divergence losses assuming a 15° half angle conical nozzle. The test data averages approximately 99% of the theoretical value.

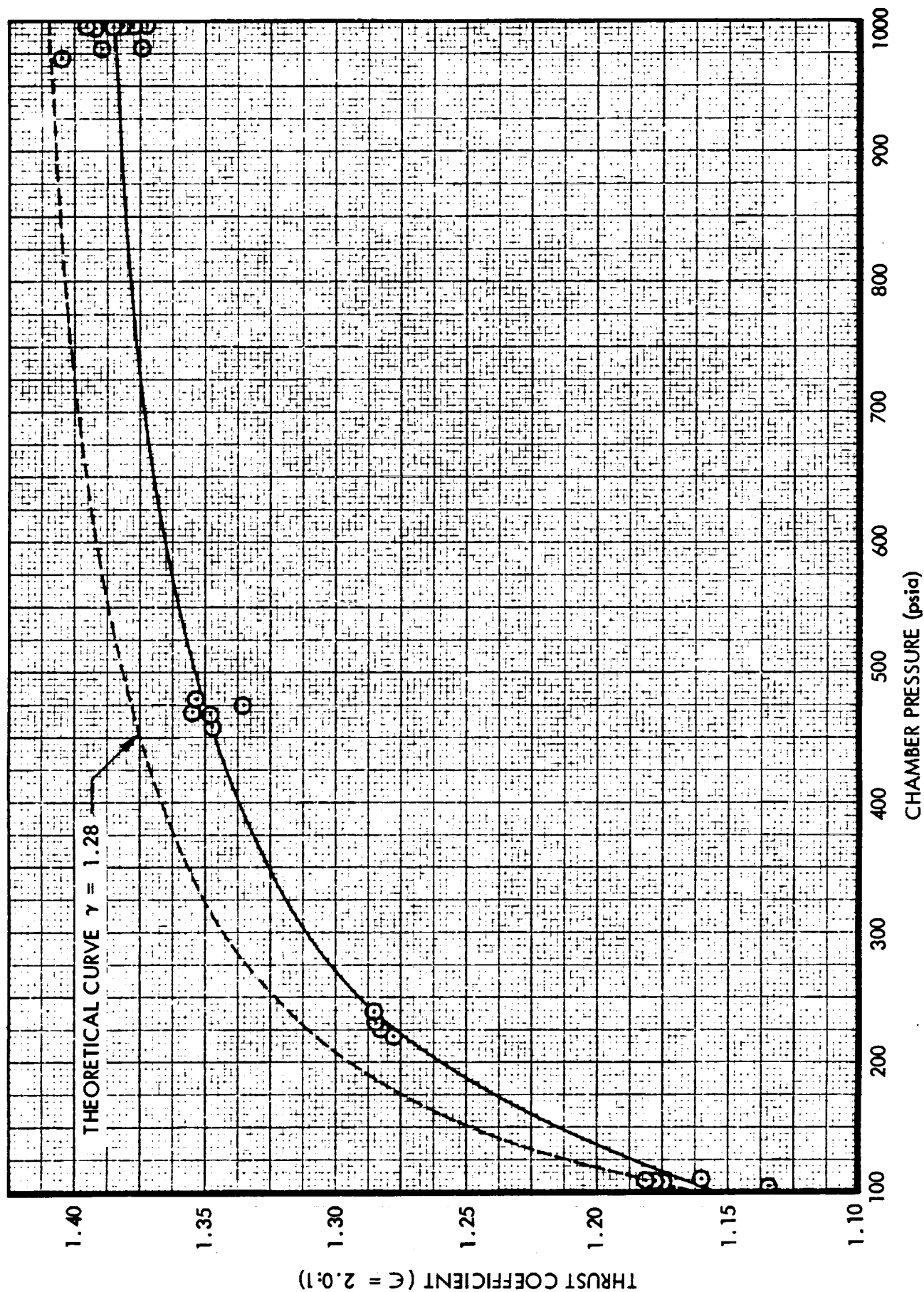
7.3 Summary of Test Data

Detailed, analysis, correlation, and development of design and scaling criteria from the test data obtained is presented in Volume II of the final report. The following sections summarize the design and scaling criteria developed as a result of the test data obtained.

CORRECTED CHARACTERISTIC VELOCITY
VS AMMONIA DISSOCIATION
FOR 50 lbf ENGINE



SEA LEVEL THRUST COEFFICIENT VERSUS
CHAMBER PRESSURE FOR $\epsilon = 2.0:1$ 50 lbf ENGINE



CORRECTED CHARACTERISTIC VELOCITY VS
AMMONIA DISSOCIATION FOR 0.5 lbf ENGINE

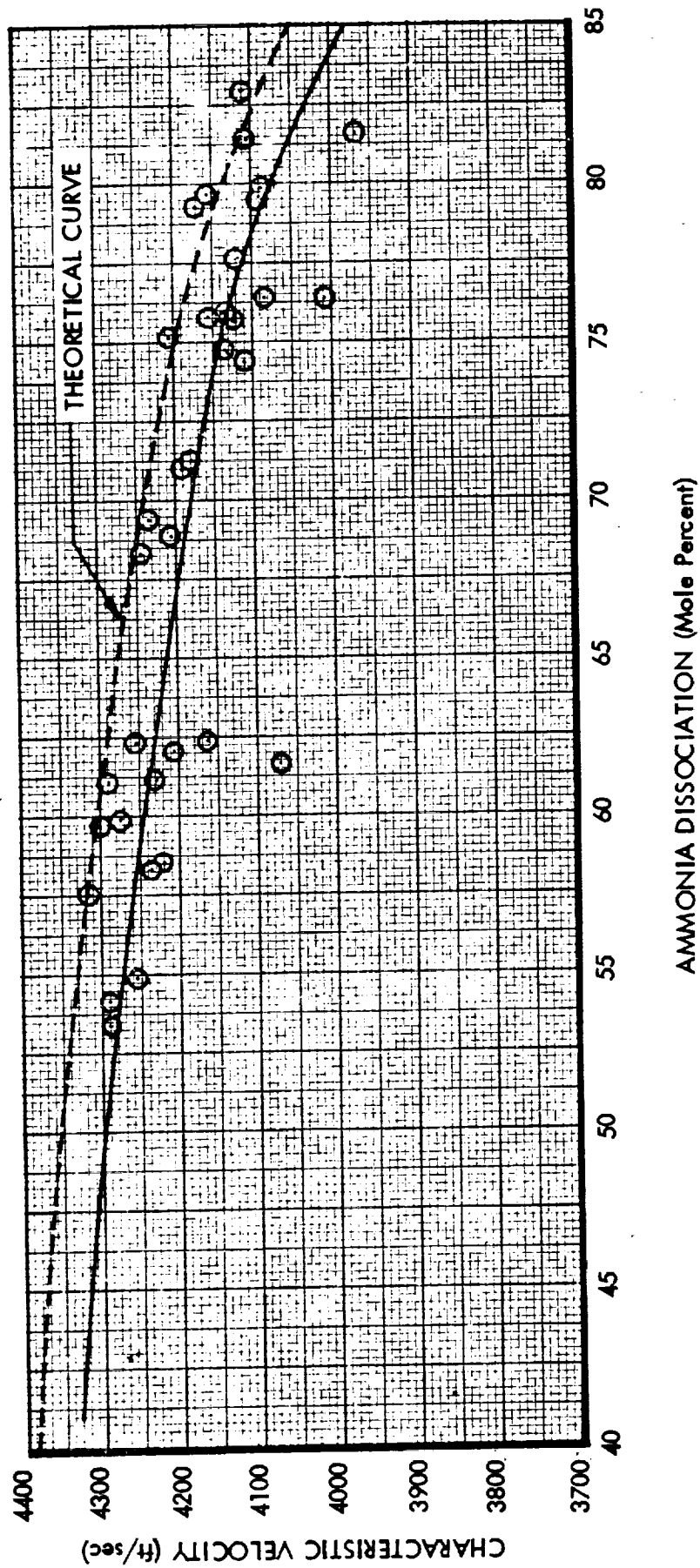


FIGURE 55

SEA LEVEL THRUST COEFFICIENT VS CHAMBER PRESSURE FOR $C=20:1$ 0.5 lbf ENGINE

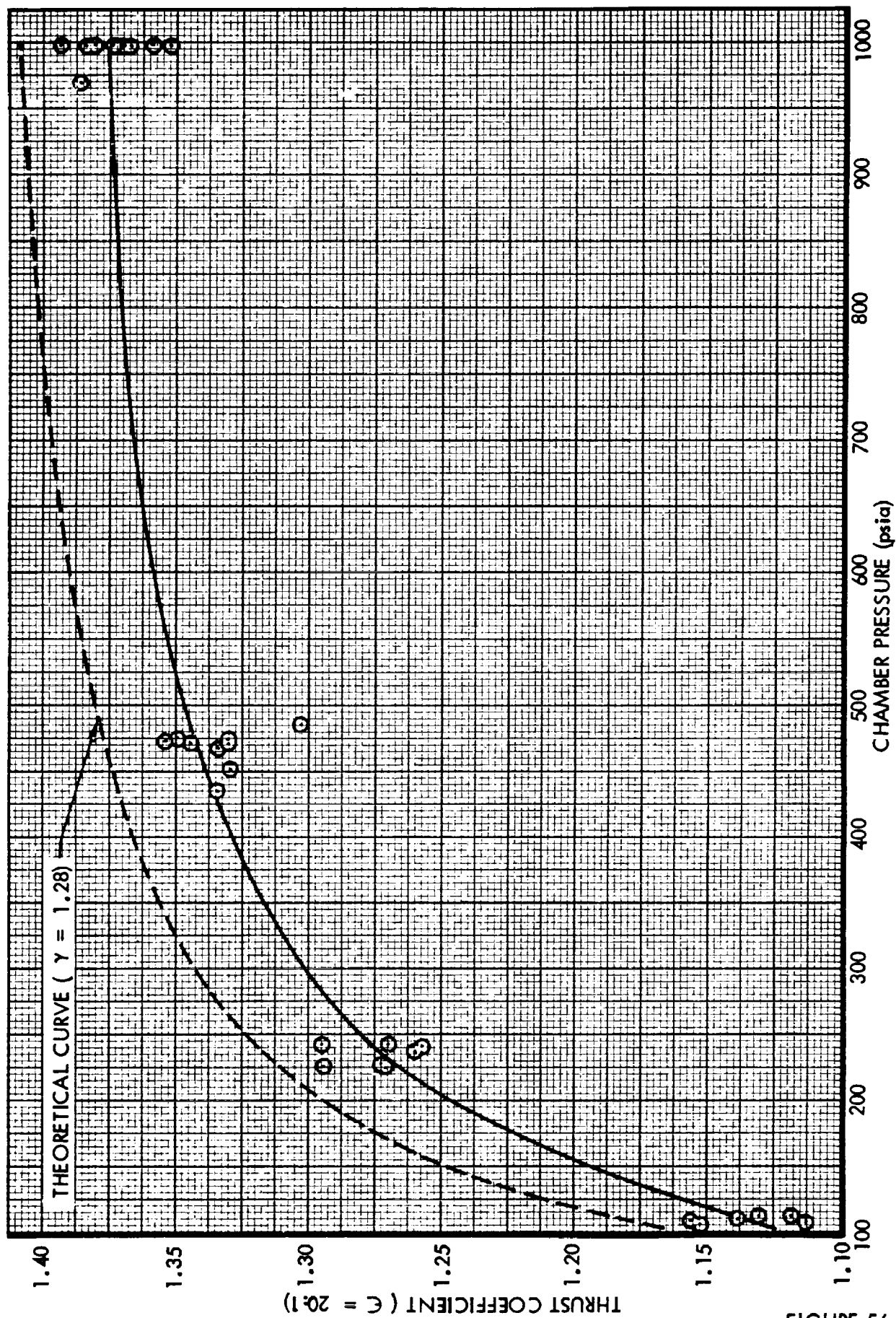


TABLE XIV
SUMMARY OF 3.010 DIAMETER REACTOR BED LOADING, CHAMBER PRESSURE, AND BED LENGTH TESTS

Test No.	Bed Length in.	Initial Catalyst Temperature °F	Downstream Chamber Pressure psia	Thrust lbf	(1) Flow Rate lbm/sec	Exit Gas Temperature °F	(2) Ignition Delay ms	(3) Response Time ms.	(4) Decay Time ms.	Characteristic Velocity ft/sec	(5) Specific Impulse lbf-sec/lbm	Chamber Pressure Roughness % peak to peak	Catalyst Bed Pressure Drop Dissociation psid	(6) Ammonia mole %	(5) Thrust Coefficient
390	1.0	69	1030	21.13	0.11762	1555	11	84	170	4143	179.6	± 3.5	10	66.4	1.395
400	2.0	62	1038	21.03	0.11918	1460	14	203	209	4121	176.5	± 0.3	2	73.5	1.378
386	3.0	61	1040	21.32	0.12000	1455	11	176	296	4101	177.7	± 0.5	2	71.5	1.394
387	1.0	53	977	56.25	0.30512	1713	9	88	58	4268	184.4	± 2.0	5	51.3	1.390
395	2.0	56	978	55.65	0.30734	1605	16	102	64	4241	181.1	± 0.9	7	64.5	1.374
376	3.0	54	968	55.90	0.31066	1565	16	128	59	4123	179.9	± 0.8	18	66.3	1.404
412	1.0	63	500.7	9.93	0.07375	1424	19	187	51	4175	175.3	± 0.2	0.6	75.3	1.350
399	2.0	67	468.5	26.30	0.15084	1472	19	229	111	4137	174.4	± 1.9	4.2	73.1	1.356
382	3.0	55	477.1	26.75	0.15426	1481	20	311	105	4119	173.4	± 1.9	4.8	74.0	1.354
383	1.0	56	472.8	55.30	0.30981	1770	17	182	86	4301	178.5	± 4.7	1.1	39.6	1.335
393	2.0	63	455.9	53.90	0.30440	1636	16	185	73	4221	177.1	± 2.2	14.8	67.6	1.350
373	3.0	60	457.5	54.10	0.30651	1584	18	272	71	4207	176.5	± 2.4	19.0	69.5	1.350
410	1.0	60	226.9	12.33	0.07311	1477	19	769	110	4134	168.7	± 17.5	1.0	63.9	1.312
403	2.0	58	227.3	12.16	0.07550	1402	24	907	128	4010	161.1	± 1.1	3.0	78.7	1.292
407	3.0	71	221.7	12.10	0.07464	1353	18	935	142	3956	162.1	± 3.5	2.8	83.0	1.318
392	1.0	70	247.3	24.58	0.15440	1600	13	420	90	4246	159.2	± 11.7	2.4	---	1.208
398	2.0	55	223.7	25.15	0.15242	1457	21	618	84	4137	165.1	± 2.2	7.4	64.8	1.283
381	3.0	53	225.8	25.40	0.15574	1481	22	760	80	4086	163.1	± 2.2	11.2	75.1	1.284
378	1.0	53	219.7	51.00	0.30103	1726	15	336	64	4368	169.4	± 10.5	12.4	43.0	1.248
391	2.0	57	211.3	50.25	0.30095	1578	24	547	61	4202	167.0	± 1.7	23.4	52.3	1.278
372	3.0	79	220.7	52.80	0.31819	1570	20	789	55	4151	165.9	± 2.7	38.4	71.5	1.286
411	1.0	59	110.7	11.20	0.07401	1538	19	2800	102	4193	151.3	± 4.5	2.0	51.8	1.161
405	2.0	63	107.1	11.02	0.07154	1422	27	2400	122	4219	154.0	± 2.9	3.0	70.8	1.175
408	3.0	67	107.4	11.08	0.07393	1338	19	3300	97	4095	149.9	± 1.9	6.2	79.8	1.177
401	2.0	60	105.2	22.20	0.15085	1485	16	1735	64	4174	147.2	± 2.1	13.9	64.2	1.134
380	3.0	54	120.0	26.15	0.17560	1492	24	2300	63	4090	148.9	± 2.4	22.4	72.6	1.171
397	2.0	70	110.4	51.35	0.33545	1627	19	1414	43	4167	153.1	± 3.5	46.5	39.7	1.182
375	3.0	74	89.0	39.50	0.27569	1560	20	2780	38	4087	143.3	± 1.9	60.7	70.7	1.128
406	2.0	69	52.1	9.42	0.07390	1407	40	3000	57	4220	127.48	± 4.8	7.2	66.7	0.9718
409	3.0	79	50.8	9.17	0.07371	1362	15	5100	68	4125	124.4	± 2.7	11.0	78.7	0.9702
402	2.0	69	52.1	19.55	0.16138	1509	22	3000	55	4088	121.1	± 5.0	22.8	52.0	0.9533
374	3.0	64	46.6	17.10	0.14728	1472	23	2200	48	4006	116.1	± 3.0	34.9	77.4	0.9324

(1) Average of two flowmeters in series.
 (2) Time from propellant entry into chamber to 1% of steady state chamber pressure.
 (3) Time from propellant entry into chamber to 90% of steady state chamber pressure.
 (4) Time from chamber pressure start decay to 10% of steady state chamber pressure
 (5) Sea level conditions at expansion ratio of 2.0:1.
 (6) Average value determined from ammonia to hydrogen and ammonia to nitrogen mole ratios.

TABLE XV
SUMMARY OF 0.5 lbf ENGINE BED LOADING, CHAMBER PRESSURE, AND BED LENGTH STUDIES

Test No.	Bed Length in	Initial Catalyst Temperature °F	Downstream Chamber Pressure psia	Thrust lbf	Flowrate lbm/sec	Ignition Delay ms	Response Time ms	Decay Time ms	Characteristic Velocity ft/sec	Specific Impulse lbf-sec/lbm	Chamber Pressure Roughness % peak-to-peak	Catalyst Bed Pressure Drop psid	Ammonia Disassociation mole %	Thrust Coefficient
431	0.5	61	53.6	0.305	0.002562	0	880	148	4009	118.9	+7.3	10.1	63.0	0.9572
449	0.5	70	107.5	0.335	0.002341	2	461	190	4164	143.0	+5.6	5.1	57.8	1.1127
444	0.5	54	238.3	0.410	0.002504	5	646	620	4182	163.7	+4.9	3.5	62.2	1.2593
446	0.5	56	485.5	0.426	0.002474	18	630	470	4246	172.5	+1.2	1.0	57.5	1.3043
447	0.5	64	1000	0.409	0.002341	10	317	510	4101	174.7	+1.5	0	62.5	1.3705
438	0.5	65	107.7	0.740	0.004858	5	300	490	4256	152.4	+5.9	18.3	53.4	1.1558
436	0.5	59	225.5	0.811	0.004913	5	317	640	4212	165.2	+6.7	13.6	55.0	1.2722
440	0.5	50	473.7	0.880	0.004920	15	359	370	4250	179.2	+2.4	4.5	--	1.3540
453	0.5	65	469.9	0.858	0.004939	13	294	285	4200	174.1	+2.8	4.2	58.0	1.3308
442	0.5	58	1000	0.922	0.005120	9	283	400	4237	180.3	+2.5	0	59.8	1.3677
422	0.5	68	205.1	1.580	0.009312	7	357	147	4212	169.5	+2.2	25.0	57.1	1.2958
434	0.5	61	969	1.844	0.010151	5	174	185	4220	181.7	+5.6	19.4	54.2	1.3870
445	1.25	54	51.9	0.292	0.002522	1	2030	130	3959	115.8	+3.7	11.3	81.5	0.9464
443	1.25	54	112.6	0.360	0.002511	2	1143	183	4085	143.4	+2.2	3.8	61.1	1.1309
437	1.25	63	240.1	0.414	0.002605	9	810	295	4069	159.0	+3.1	3.2	75.2	1.2568
439	1.25	61	472.3	0.424	0.002578	7	1260	440	3973	164.8	+0.7	2.0	72.4	1.3318
441	1.25	51	1005	0.418	0.002364	14	323	510	4093	177.5	+1.2	56.0	67.1	1.395
435	1.25	61	52.9	0.643	0.005494	8	1400	90	3939	117.5	+2.6	30.1	--	0.961
433	1.25	54	109.6	0.742	0.005252	5	575	138	4006	141.5	+3.2	16.6	76.3	1.1388
424	1.25	65	221.5	0.796	--	9	630	--	--	--	+3.6	10.0	79.2	1.2712
423	1.25	71	460.7	0.818	--	15	918	490	--	--	+2.4	7.6	72.8	--
431	1.25	60	475.7	0.841	0.004946	15	546	328	4218	170.5	+2.1	3.0	--	1.3500
426	1.25	79	1000	0.925	0.005198	11	358	--	4155	178.2	+1.1	17.5	68.8	1.375
414	1.25	67	245.2	--	0.011063	10	617	137	4239	--	+2.0	54.2	--	--
417	1.25	55	212.5	1.670	0.009938	8	495	440	4090	168.1	+1.9	33.0	76.0	1.3219
420	1.25	65	449.5	1.692	0.009699	10	330	615	4215	174.5	+2.0	--	76.5	1.3315

TABLE XV (Cont'd)
SUMMARY OF 0.5 lbf ENGINE BED LOADING, CHAMBER PRESSURE, AND BED LENGTH STUDIES

Test No.	Bed Length in	Initial Catalyst Temperature °F	Downstream Chamber Pressure psia	Thrust lbf	Flowrate lbm/sec	Ignition Delay ms	Response Time ms	Decay Time ms	Characteristic Velocity ft/sec	Specific Impulse lbf-sec/lbm	Chamber Pressure Roughness % peak-to-peak	Catalyst Bed Pressure Drop psid	Ammonia Dissociation mole %	Thrust Coefficient
421	1.25	59	957	1.820	0.01011	11	311	380	4194	179.8	+2.5	17.0	69.5	1.385
455	2.0	59	52.8	0.307	0.002580	27	3800	130	3927	119.2	+3.4	29.6	81.8	0.9780
454	2.0	57	113.3	0.358	0.002629	3	1770	255	3895	136.3	+1.4	15.0	83.2	1.1177
448	2.0	73	241.7	0.430	0.002693	8	1202	300	3961	160.0	+3.3	7.0	79.6	1.2967
450	2.0	57	471.9	0.427	0.002575	10	2020	320	3975	166.1	+0.7	3.0	71.2	.345
452	2.0	65	1005	0.464	0.002428	13	323	590	3973	180.5	+0.6	1.0	71.3	1.382
430	2.0	55	104.0	0.713	0.005008	9	3500	664	3972	142.5	+1.0	56.5	85.6	1.1532
427	2.0	60	226.9	0.817	0.005088	11	1010	600	4055	160.8	+1.8	28.6	82.5	1.2737
425	2.0	73	466.3	0.854	0.005277	17	2350	1137	3900	162.0	+2.2	13.6	79.5	1.3353
428	2.0	61	1018	0.930	0.005184	11	378	540	3905	179.5	+0.7	3.4	75.5	1.3552
418	2.0	58	434.5	1.640	0.009730	14	782	322	4061	168.4	+2.1	43.4	77.7	1.3351
419	2.0	64	925	1.722	0.009958	11	838	265	4100	173.3	+3.0	26.0	75.7	1.3569

7.3.1 Ammonia Dissociation

Analysis and correlation of the ammonia dissociation data indicated that diffusion of the reactants and products to and from the catalyst surface may be important in the amount of ammonia dissociation which occurs in the reactor. In view of the apparent importance of diffusion controlling dissociation of ammonia, a relation was developed relating fractional ammonia dissociation to temperature, bed loading, chamber pressure, residence time, and catalyst particle size for the limiting case of zero ammonia concentration at the catalyst surface. That is, it is assumed that chemical equilibrium is obtained if the ammonia reaches the catalyst surface. This relation developed is given as:

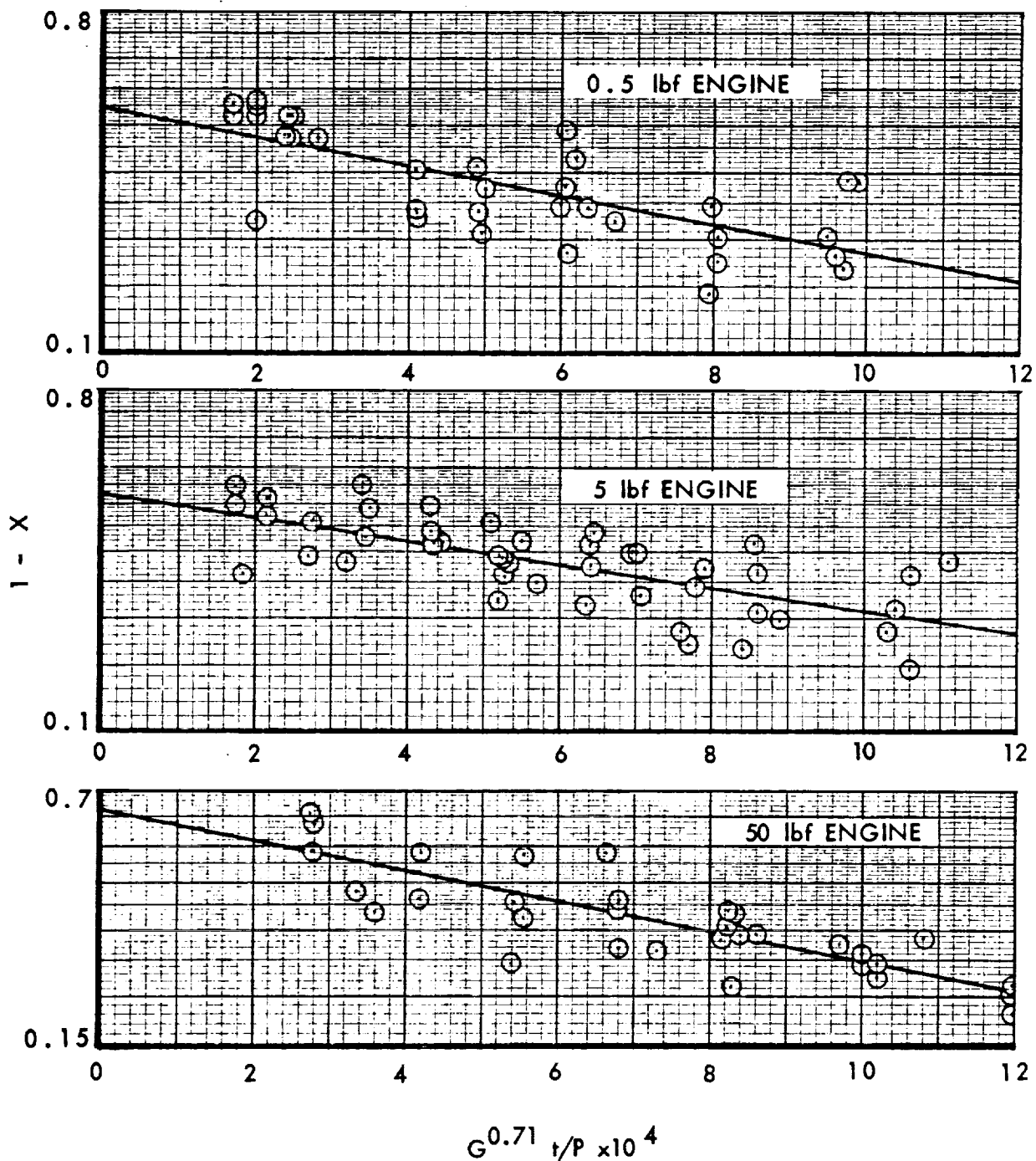
$$\int_X^{X_1} \frac{dX}{(1-X)(3+X)(5-4X)(1650-780X^2)} = K_d d_p^m \frac{G^{0.71} t}{P}$$

Where

X	=	Fractional ammonia dissociation
K _d	=	Experimental constant
d _p	=	Catalyst particle diameter, ft.
m	=	Experimental constant
G	=	Superficial bed loading lbm/in ² -sec
t	=	Residence time, ms
P	=	Average chamber pressure, psia

Examination of the above equation indicates that for a given particle size, the ammonia dissociation should be proportional to the parameters $G^{0.71} t/P$. Ammonia dissociation data obtained from the 0.5, 5, and 50 lbf engines is plotted against this group in Figure 57 to test its usefulness as a correlation parameter. As can be seen a quite consistent correlation is obtained at all three thrust levels.

CORRELATION OF AMMONIA DISSOCIATION DATA FOR A DIFFUSION CONTROLLED REACTION



Additional correlation of the data was accomplished to develop an expression which includes the effect of particle size on an ammonia dissociation. The semi-empirical equation developed is given by:

$$\ln \left(\frac{1 - X_0}{1 - X} \right) = -153.2 d_p^{-0.32} \frac{G^{0.71} t}{P}$$

Where previously undefined parameters are:

X_0 = Zero time intercept on plot of experimental data.

Ammonia dissociation data from all three thrust levels is plotted and compared to the above equation in Figure 58. Although there is some scatter in the data it does appear very useful for initial design purposes. The 3σ deviation of the data from that given by the above equation is 6%.

7.3.2 Catalyst Bed Length Requirements

During the program, tests were conducted to define the minimum catalyst bed length requirements required for smooth and stable operation. This data was correlated and an empirical expression developed to relate catalyst bed length requirements to bed loading, chamber pressure, and catalyst specific surface area. This relation is given as:

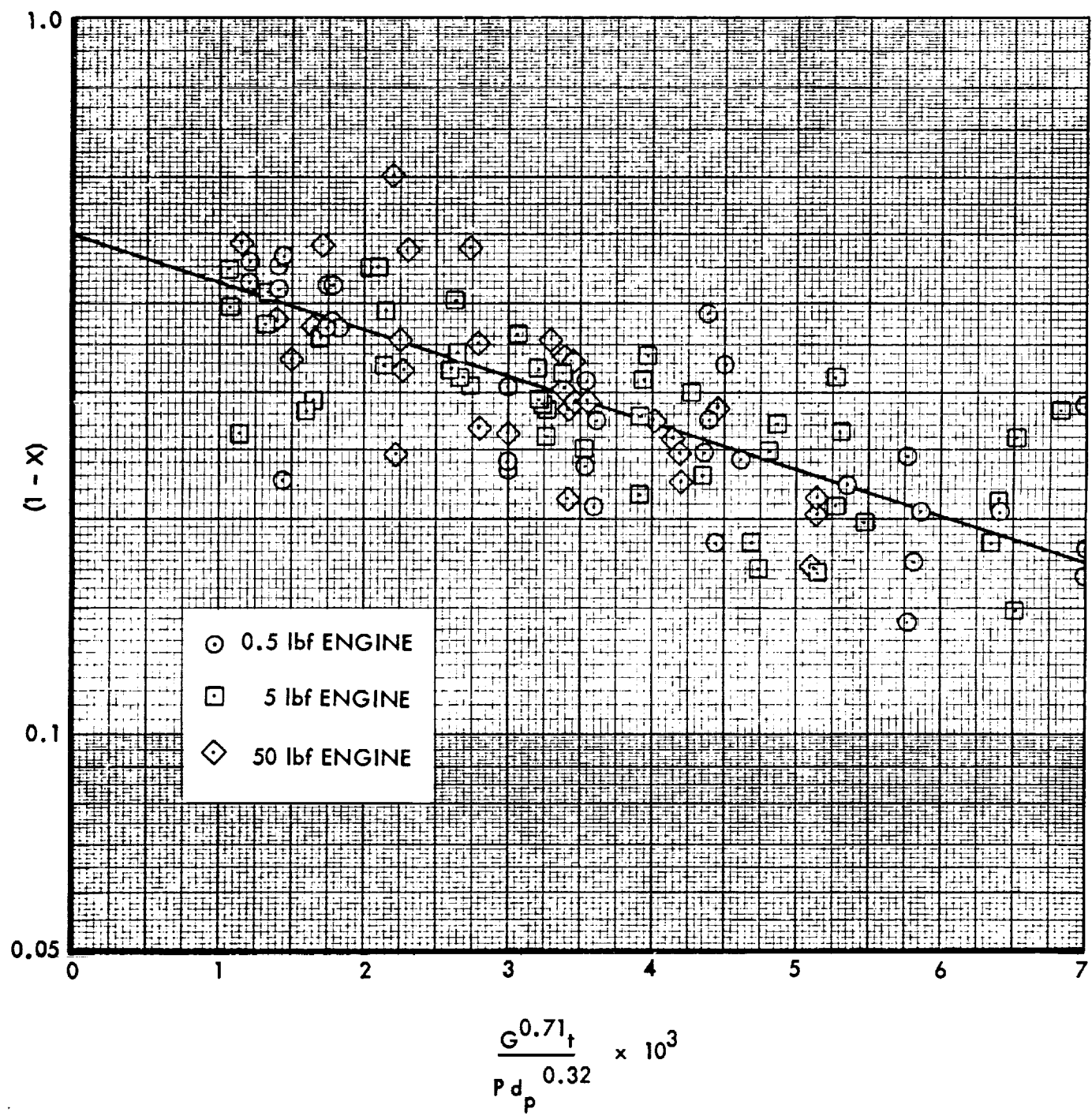
$$L_B = 0.2 + 145 \frac{G^{0.554}}{P_c^{0.306} A_s^{0.3}}$$

The bed length predicted by the above equation is compared with that found experimentally in Figure 59. It should be noted that the use of the above equation will result in an ammonia dissociation of 55 to 60%.

7.3.3 Catalyst Bed Pressure Drop

Experimental catalyst bed pressure drop data was compared to a relation developed by Grant (Reference 3) in his work with the nonspontaneous catalyst and with the Ergun equation (Reference 13) to see if those equations adequately predicted the measured catalyst bed pressure drop. Data obtained is compared with that predicted by Grants equation in

GENERAL CORRELATION OF AMMONIA DISSOCIATION DATA



CORRELATION OF CATALYST BED LENGTH REQUIREMENTS

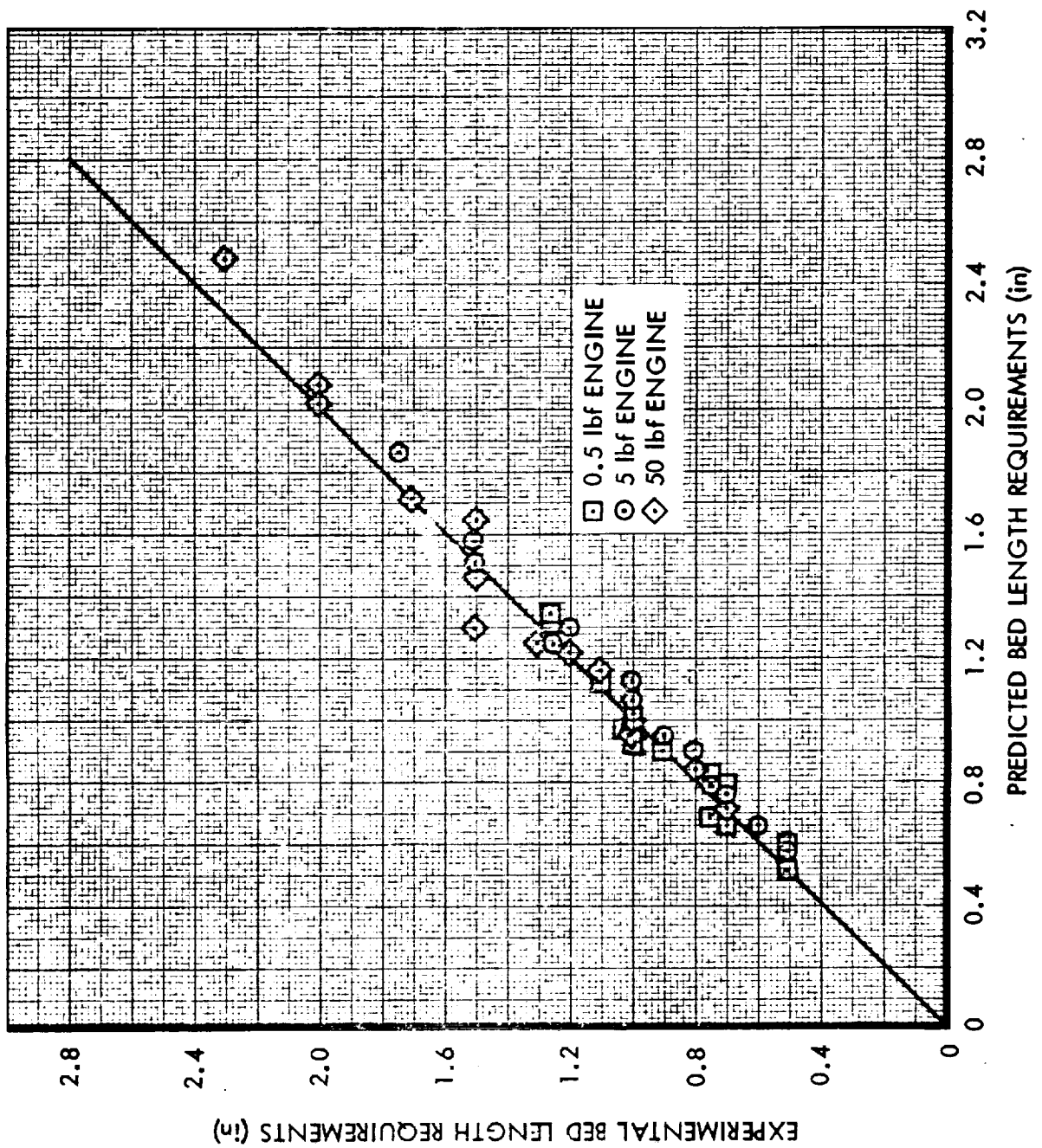


Figure 60. As can be seen quite good correlation is obtained with all test data. The Ergun equation was found not to fit the experimental data throughout the full range of Reynolds number covered and is not recommended for use.

7.3.4 Chamber Pressure Response Time

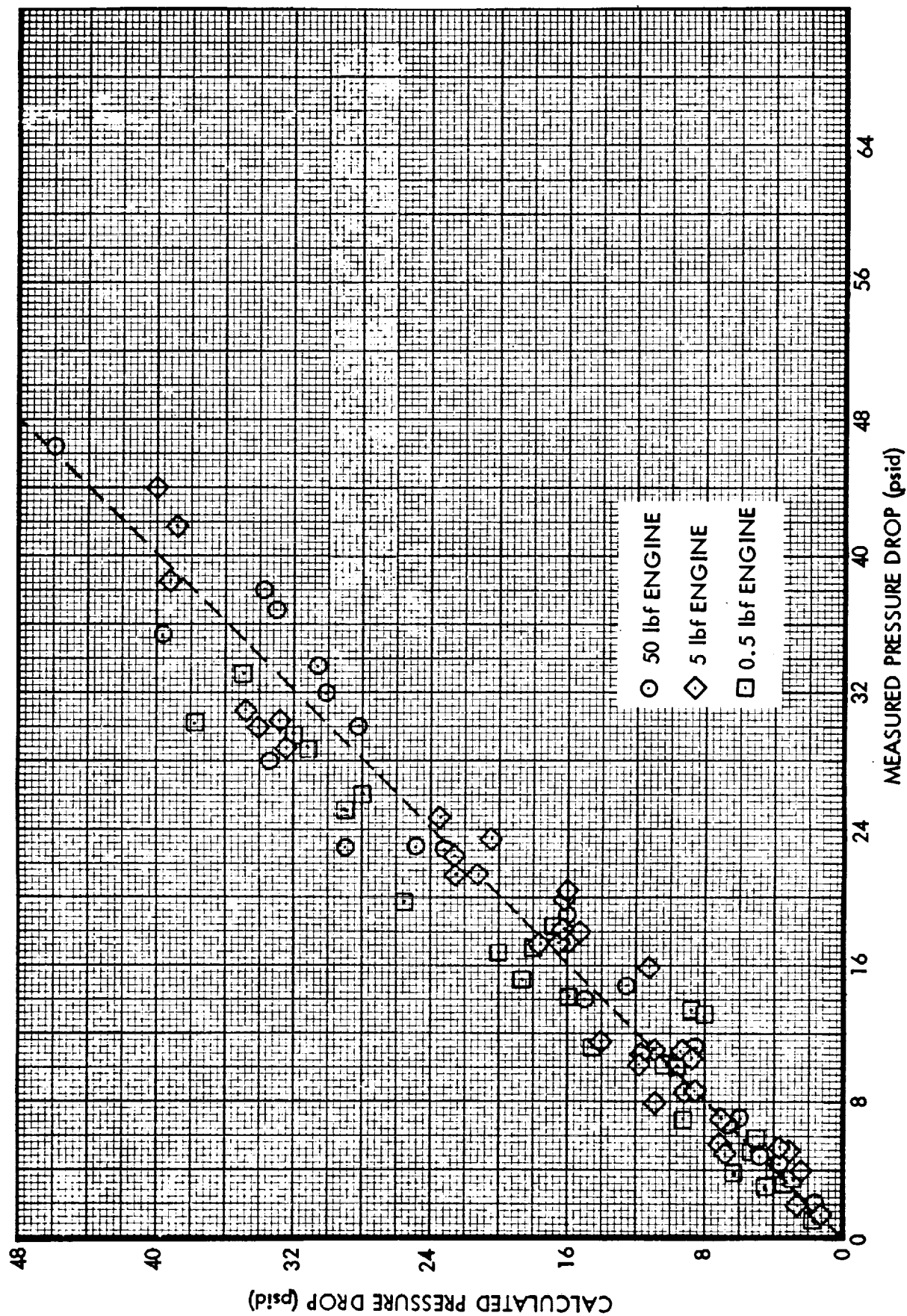
Chamber pressure rise time is defined herein as the time for chamber pressure measured downstream of the catalyst bed to change from 1% of the steady state value to some specified higher percentage of the steady state pressure. An analytical model of the pressure rise time was developed by assuming complete decomposition during the start transient and then empirically modifying the model generated to account for kinetic effects (i.e., rate limitations imposed by propellant atomization process and/or decomposition reaction kinetics). The model was developed treating the pressure rise transient as a two stage process.

Stage 1 is treated as an isothermal pressurization process in which the accumulation of gas in the reactor void space is the predominant factor. The system temperature is assumed to be constant at the initial catalyst temperature during this relatively short portion of the pressure rise period. During Stage 2, the catalyst bed heat up as it affects the temperature of the gas entering the nozzle is considered to be the predominant factor. The result of this analysis is:

$$t_1 = \frac{K_{c1} \bar{M}_1 V_c P_{cd\infty}}{\dot{w}_\infty RT_{co}} \int_{\eta_0}^{\eta_1} \frac{d\eta}{\sqrt{\frac{(F-\eta)\eta}{(F-D)\eta + (D-1)Z}} - \eta \sqrt{\frac{1}{Z}}}$$

$$t_2 = K_{c2} \frac{C_c (F-D)^{3/2}}{C_{pg} \dot{w}_\infty} \int_{\eta_1}^{\eta} \frac{(2F-D\eta)\eta d\eta}{(F-D\eta)^{3/2} [F-D\eta - (F-D)\eta^2]}$$

CORRELATION OF CATALYST BED PRESSURE DROP DATA WITH GRANT'S EQUATION



Where:

- t_1 = Time for completion of Stage 1, sec
- t_2 = Time for completion of Stage 2, sec
- K_{c1} = Stage 1 empirical constant
- \bar{M}_1 = Average molecular weight, lbm/lb mole
- V_c = Volume to be pressurized, in³
- $P_{cd\infty}$ = Steady state chamber pressure, psia
- W = Steady state propellant flow rate, lbm/sec
- R = Universal gas constant, in-lbf/lb mole °R
- T_{co} = Initial catalyst temperature, °R
- F = $P_f/P_{cd\infty}$ (feed ratio)
- D = P_{cu}/P_{cd} (catalyst bed pressure drop ratio)
- η = $P_{cd}/P_{cd\infty}$ (fractional approach of downstream chamber pressure to steady state)
- η_o = Value of $P_{cd}/P_{cd\infty}$ at end of ignition delay
- K_{c2} = Stage 2 empirical constant
- C_c = Catalyst heat capacity Btu/°F
- \bar{C}_{pg} = Gas specific heat, Btu/16°F

The value of η_1 is given by:

$$\eta_1 = -\frac{DT_{co}}{2(F-D)T_{co}} + 1/2 \sqrt{\left(\frac{DT_{co}}{(F-D)T_{co}}\right)^2 + \frac{4FT_{co}}{(F-D)T_{co}}}$$

From experimental test data the empirical constants in the above equations were developed as:

$$K_{c1} \bar{M}_1 = \frac{3.69 \times 10^4}{P_{d\infty}}$$

$$\frac{K_{c2}}{C_{pg}} = \frac{570}{P_f}$$

8.0 CATALYST DEGRADATION MEASUREMENTS

Catalyst changes as a function of accumulated engine burn time were correlated by three means. Periodic weight measurements were made of the catalyst from which catalyst loss rates could be calculated. Additionally, samples of catalyst were periodically removed from the engine and measurements were made of the total catalyst surface area and of the active metal surface area. Total catalyst surface area was measured using nitrogen adsorption techniques while the active metal surface area was measured by hydrogen chemisorption. For all surface area measurements, the catalyst was reduced in a hydrogen atmosphere at 500°F for one hour prior to the measurement being made.

Due to the nature of the program (i.e., investigation of many variables) it was not possible to obtain quantitative measurements of catalyst loss rates. However, several qualitative trends were noted which are discussed in the ensuing paragraphs.

Optimization tests were conducted with granular or pellet size catalyst all made on a Harshaw alumina carrier. The granular catalyst was made by breaking 1/8" x 1/8" pellets into the desired mesh size. The loss rates for these granular pellets tended to be higher by a factor of at least 10 than that for the 1/8" x 1/8" pellets. It is strongly felt that this method of manufacturing results in a catalyst structurally inferior to the 1/8" x 1/8" pellets. Subsequent testing on the program employed granular catalyst made on the Reynolds RA-1 alumina carrier. This carrier is made in granular pellets and was found to have much lower loss rates (reduction by a factor of up to 10) than that of the Harshaw granular discussed above. During later phases of the program a granular catalyst which was prepared on the Reynolds alumina carrier and subsequently surface hardened (Shell Development Company Proprietary Procedure) was tested. Further reduction in loss rates were noted with this catalyst.

During the studies of the effect of bed loading upon reactor operation it was noted that loss rates increased with increasing bed loading. Although no quantitative numbers were obtained a definite correlation between loss rate and bed loading was noted.

As stated above, samples of the catalyst were periodically removed from the engine and surface area measurements made. In most cases the catalyst was removed from a point in the chamber just below the layer of fine mesh catalyst. Thermocouple measurements had indicated that the flame front was near this point, and thus, the surface area changes should be the greatest at this point of maximum temperature.

Results of the hydrogen chemisorption and nitrogen absorption measurements are summarized in Table XVI. A rather large drop-off in both carrier and metal surface area is noted with run time. This drop-off appears to occur after a short period of test time has been accumulated on the catalyst. After this drop-off the carrier and metal surface areas appear to stabilize at approximately 70% and 50% of their original values respectively. It should be noted that the engine testing with the catalyst summarized in Table XVI indicated essentially no change in reactor operation despite the rather large surface area changes.

TABLE XVI

CATALYST SURFACE AREA CHANGES

Engine Thrust lbf	Catalyst Size	Accumulated Test Time sec	Original BET Area m ² /gm	Original H ₂ Chemisorption μ mole/gm @ 0°C	Measured BET Area m ² /gm	Measured H ₂ Chemisorption μ mole/gm @ 0°C
50	1/8" x 1/8" Cylindrical pellets	296	118	480	78	226
		421	118	480	81	354
		696	118	480	74	230
		730	118	480	89	260
5	10-12 Mesh	475	139.5	480	115	280
5	20-25 Mesh	1420	122.5	480	98	302
5	12-16 Mesh	2100	118	482	89	260

9.0 100 lbf ENGINE

9.1 Design

To test the validity of the design and scaling formulae at higher thrust levels a 100 lbf engine was designed and subjected to testing. The design criteria used was as outlined in Volume II of the subject report. Detailed analyses of the catalyst bed design are outlined in Volume II, Appendix I.

The design of the 100 lbf thrust engine is shown in Figure 61. Pertinent reactor design parameters and estimated engine performance are summarized in Table XVII.

The engine chamber is made of Haynes Alloy Number 25 to which is welded a 347 stainless steel nozzle of 4:1 expansion ratio. The showerhead injector, made of 347 stainless steel, is flanged to the chamber. Propellant is supplied to a distribution manifold in the injector through a single supply tube. The upper part of the catalyst bed contains 0.2 inches of 25-30 mesh granular catalyst contained in a 60 x 60 mesh molybdenum screen basket. The remainder of the catalyst bed is 1/8" x 1/8" cylindrical pellets. A photograph of the engine assembly is shown in Figure 62.

9.2 Test Results

All tests with the 100 lbf engine were conducted at ambient temperature and pressure conditions. A total of six (6) steady state tests each of 30 seconds duration were conducted. The test data from the engine is summarized in Table XVIII. A gas sample of the decomposition products was taken during the last two tests and analyzed using a gas chromatograph. This data is also summarized in Table XVIII.


Very smooth start transient and steady state operation was achieved in all tests. Characteristic velocity average 4,240 ft/sec which is within 0.45 percent of the value predicted for the engine. Sea level specific impulse and thrust coefficient corrected to 193.5 psia chamber pressure averaged 166.80 and 1.265 respectively. Ammonia dissociation, as determined by gas sample analysis was 62.5% which is within 2.5% of the 60% predicted value.

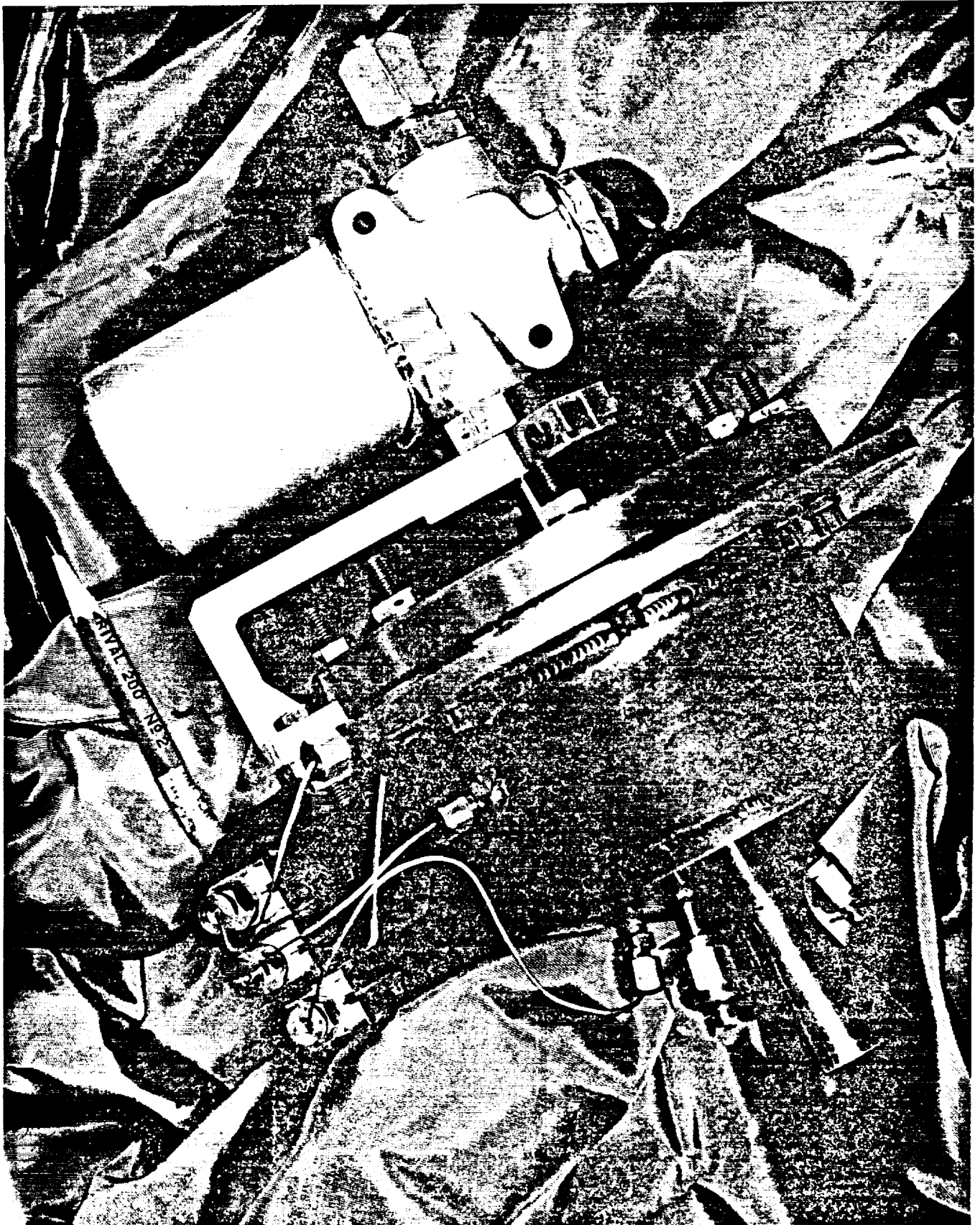
In summary, the test results obtained with the 100 lbf engine were virtually identical with that predicted using the design and scaling formula developed at the lower thrust levels. The validity of using the design and scaling formula at higher thrust levels was therefore clearly established.

1

REVISIONS				
SYM	ZONE	DESCRIPTION	DATE	APPROVED

AR		NO 405	1/8 DIARK LONG CATALYST	SHELL DEVELOPMENT CORP EMERYVILLE, CALIF.					25
AR		OC-11	LUBE	DOW CORNING CORP 3033 W. MISSION RD. ALHAMBRA, CALIF.					25
									25
									22
									21
1		2-41- ES15-B	O-RING	PARKER SEAL CO. CULVER CITY, CALIF.					20
									19
									18
									17
									16
8		NA51351 -3-20	SCREW						15
									14
1		MS35769 -B6	GASKET						13
8		MS21042 -B	LOCKNUT						12
									11
8		AN96060L	WASHER						10
									9
1		R111-03360	SCREEN						8
									7
									6
1		24670-9	CHAMBER & NOZZLE ASSY						5
1		24668-1	INJECTOR BODY						4
1		24667-1	INJECTOR PL						3
1		24661-1	BED PLATE						2
1		24597-39	CATALYST BASKET ASSY						1
-9	SYM	CODE IDENT. NO.	PART OR IDENTIFYING NO.	NOMENCLATURE OR DESCRIPTION	MATERIAL	SPECIFICATION	UNIT WT	ZONE	ITEM NO.
PT 5222									

				UNLESS OTHERWISE SPECIFIED DIMENSIONS ARE IN INCHES DECIMAL ANGULAR TOLERANCE XX ± .05 XXX ± .010 ±		DRAWN <u>JOHNSON</u> CHECKED <u>DAVE</u> REVISION <u>1/11/66</u> DATE <u>4/1/66</u> FREE WEIGHT		LIST OF MATERIALS  ROCKET RESEARCH CORPORATION SEATTLE, WASHINGTON	
				DO NOT SCALE DRAWING				TITLE ROCKET ENGINE - 100 LBF, HYDRAZINE, SHOWERHEAD INJECTOR	
TREATMENT									
FINISH						DESIGN ACTIVITY APPD <u>D. White</u> <u>4/1/66</u>		CODE IDENT. NO. DWG. NO. 21562 D 24666	
PART NEXT PART DASH CITY RECD PER ASSY				APPLICATION		WEIGHT CALC ACT		DWG. LEVEL CUSTOMER	
WORK CHARGE NO. 171-31								SCALE 1/1 RELEASE DATE 6-10-66 SHEET	



100 lbf MONOPROPELLANT HYDRAZINE ENGINE

TABLE XVII
100 lbf ENGINE DESIGN PARAMETERS

<u>Performance</u>	
Vacuum Thrust	100 lbf
Predicted Characteristic Velocity	4262 ft/sec
Propellant Flow Rate	0.4255 lbm/sec
Downstream Chamber Pressure	200 psia
Upstream Chamber Pressure	230 psia
Bed Loading	0.045 lb/in ² -sec
Injector Pressure Drop	25 psid
Nozzle Area Ratio	4:1
Predicted Ammonia Dissociation	60%
<u>Chamber Configuration</u>	
Catalyst Bed Diameter	3.470 in
Catalyst Bed Length	2.0 in
Catalyst Type	0.2 in 25-30 mesh 1.8 in 1/8" x 1/8" pellets
Chamber Material	Haynes Alloy No. 25
Nozzle Throat Diameter	0.602 in
<u>Injector Configuration</u>	
Injector Type	Showerhead
Number of Orifices	60
Orifice Diameter	0.0176 in

TABLE XVIII
SUMMARY OF 100 lbf ENGINE TEST DATA

Test No.	Initial Catalyst Temperature °F	Downstream Chamber Pressure psia	Thrust lbf	(1) Flowrate lbm/sec	Exit Gas Temperature °F	(2) Ignition Delay ms	(4) Decay Time ms	Characteristic Velocity ft/sec	(5) Specific Impulse lbf-sec/lbm	Chamber Pressure Roughness % peak-to-peak	Catalyst Bed Pressure Drop psid	(6) Ammonia Dissociation mole %	(5) Thrust Coefficient	(3) Response Time ms
470	73	158.9	55.7	0.35121	1772	20	67	4250	158.60	+1.6	29.0	--	1.2005	660
471	65	164.5	58.6	0.36507	1620	20	50	4233	160.52	+2.1	31.6	--	1.2199	666
472	69	181.3	66.0	0.40222	1595	19	53	4234	164.09	+1.6	33.0	--	1.2468	646
473	68	188.3	68.3	0.41457	1556	30	56	4244	164.75	+1.7	33.9	--	1.2488	600
474	73	191.7	70.2	0.42317	1601	18	56	4255	165.89	+1.4	34.8	62.5	1.2542	455
475	64	193.5	71.5	0.42885	1587	19	58	4239	166.72	+1.6	32.8	62.9	1.2653	495

- (1) Average of two flowmeters in series
- (2) Time from propellant entry into chamber to 1% of steady state chamber pressure
- (3) Time from propellant entry into chamber to 90% of steady state chamber pressure
- (4) Time from chamber pressure start decay to 10% of steady state chamber pressure
- (5) Sea level conditions at expansion ratio of 4:1
- (6) Average value determined from ammonia to hydrogen and ammonia to nitrogen mole ratios

10.0 FLIGHTWEIGHT 5 lbf ENGINE

10.1 Design

The design of the flightweight 5 lbf engine was based on the results of the engine design criteria developed under Task I of the study. As described in Section 2.0, this engine was to be capable of pulse mode testing, throttling tests over a 10:1 thrust ratio, and tests with low freezing point propellant mixtures of hydrazine, hydrazinium nitrate and water. The design of the flightweight 5 lbf engine is shown in Figure 63. Pertinent reactor design parameters and estimated performance are summarized in Table XIX.

Significant design features of the engine design shown in Figure 63 are:

- a. Thermal standoffs between the injector and the propellant valve to provide thermal isolation between the chamber and the propellant valve.
- b. Propellant distribution by radial flow passages to each orifice which minimizes the propellant holdup and maintains adequate coolant velocities in the injector.
- c. A 0.3 inch deep 60 x 60 mesh molybdenum wire basket holding 25-30 mesh granular catalyst, in the upper part of the catalyst bed. The remainder of the catalyst bed is composed of 14-16 mesh granular catalyst.
- d. The nozzle of 50:1 expansion ratio and chamber are machined out of 347 stainless steel barstock.
- e. The engine is designed such that the injector can be flanged to the chamber and checkout firings conducted. A final meltdown weld of the chamber to injector is then performed following reactor acceptance tests.
- f. Differential thermal expansion between the thermal standoffs and the propellant feed tube is accommodated by the double "O"-ring seal on the propellant feed tube.
- g. The engine is mounted at the propellant valve thus minimizing heat input to mounting structure for possible flight applications and providing a propellant valve heat sink for maintenance of low valve seat temperatures under pulse mode, heat soak operating conditions.

1. INTERPRET DWS PER MIL-STD-100.

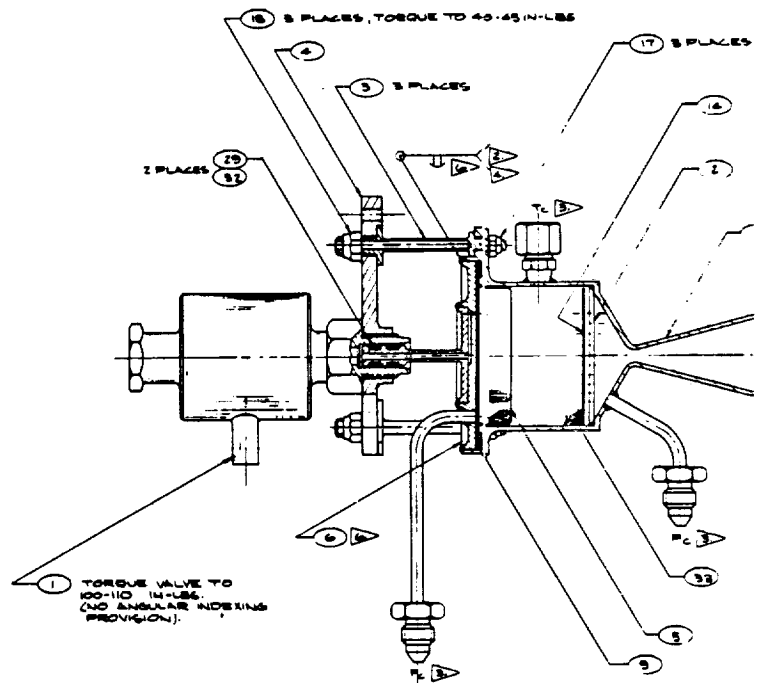
2. T.I.G. WELD PER MIL-W-8611.

3. FITTINGS ARE SHOWN ROTATED 90° FOR CLARITY.

4. DYE PENETRANT INSPECT WELD PER MIL-I-6866, TYPE 2 METHOD OPT.

5. LEAK TEST ALL WELDS WITH GN_2 AT 100 PSIG.

6. INSPECT MATING DIAMETERS TO DETERMINE RADIAL CLEARANCE; PLACE SWAY STOCK OR WIRES IN THE GAP IN AT LEAST 3 PLACES TO INSURE CONCENTRICITY IN THE WELDING OPERATION.

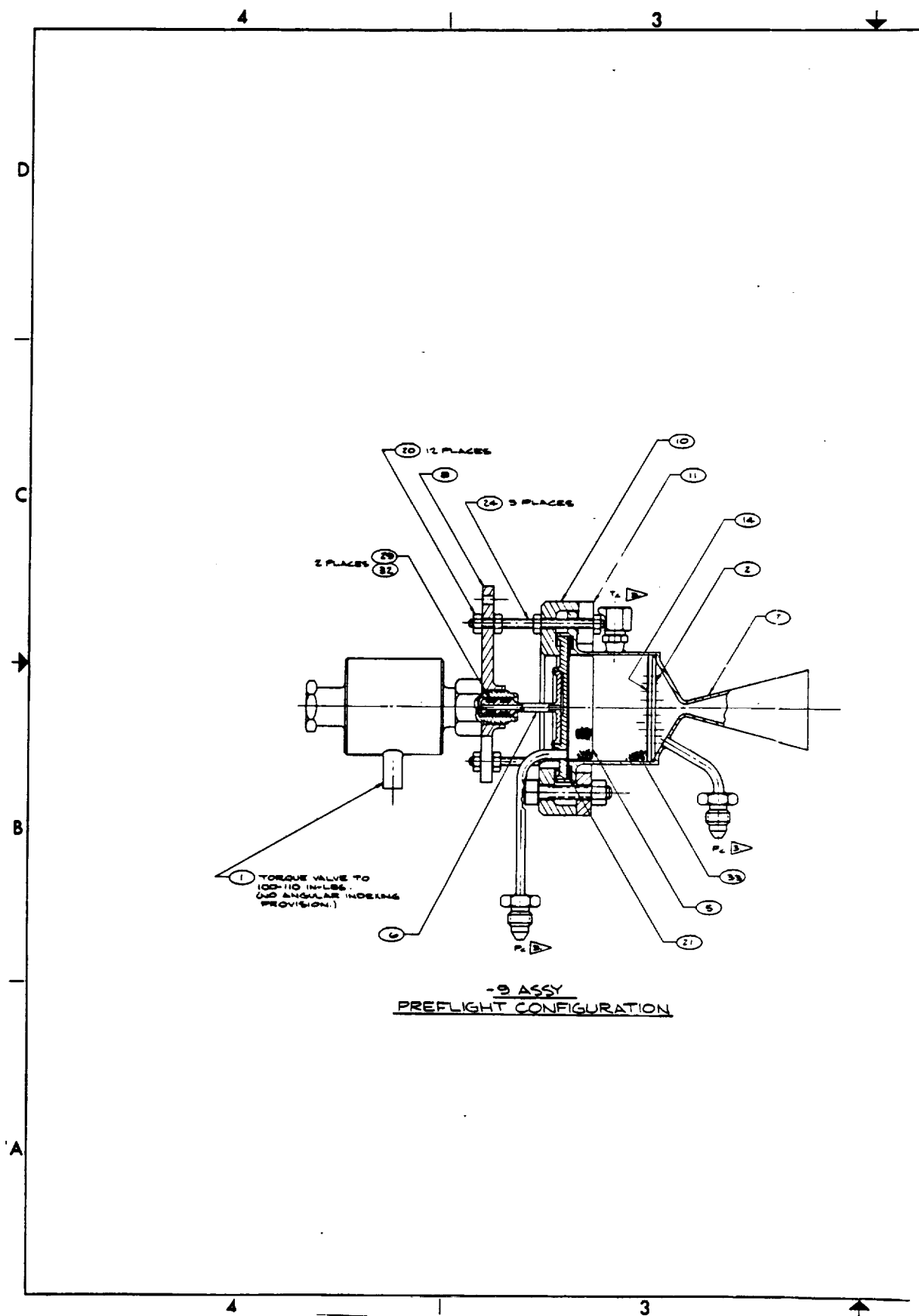


- 19 ASSY
FLIGHT CONFIGURATION

[illegible]

- 153-A

FIGURE 63



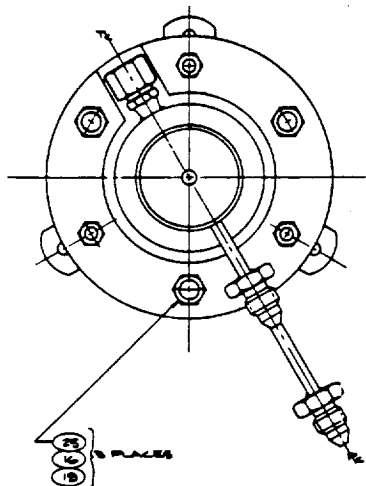
[illegible][illegible]

TABLE XIX
5 lbf FLIGHTWEIGHT ENGINE DESIGN

<u>Performance</u>	
Vacuum Thrust	5.0 lbf
Vacuum Specific Impulse	221.4 lbf-sec/lbm
Vacuum Thrust Coefficient	1.704
Characteristic Velocity	4180 ft/sec
Propellant Flow Rate	0.0227 lb/sec
Downstream Chamber Pressure	200 psia
Upstream Chamber Pressure	206 psia
Nozzle Area Ratio	50:1
Bed Loading	.015 lb/in ² -sec
Injector Pressure Drop	25 psid
Exhaust Gas Stagnation Temperature	1580°F
Chamber Operating Temperature	1600°F
<u>Chamber Configuration</u>	
Catalyst Bed Diameter	1.388 in.
Catalyst Bed Length	1.04 in.
Catalyst Type	0.3 inches 25-30 0.74 inches 14-16
Chamber Material	347 Stainless Steel
Chamber Safety Factor	1.5:1 at 300 psi
<u>Engine Weight Breakdown</u>	
Chamber and Nozzle	0.26 lbm
Injector	0.12 lbm
Thermal Standoffs	0.02 lbm
Valve Mounting Bracket	0.03 lbm
Catalyst	0.08 lbm
Total Engine Weight (less propellant valve)	0.41 lbm

- h. The propellant valve can be removed and replaced without disassembly of the engine.

A photograph of the engine assembly is shown in Figure 64.

10.2 Low Freezing Point Propellant Mixture Tests

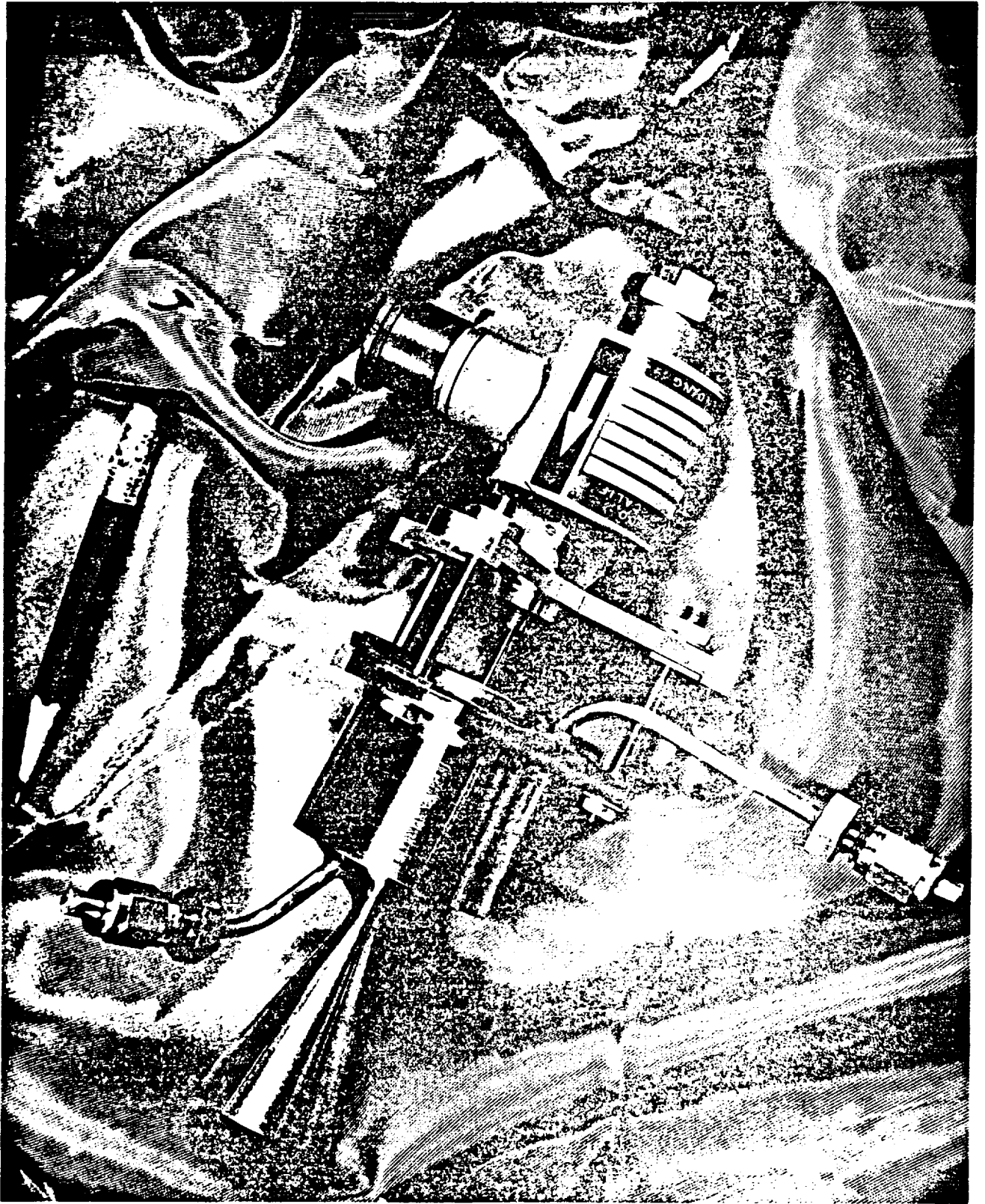
10.2.1 Propellant Selection

Three low freezing point propellant mixtures of hydrazine, hydrazine nitrate, and water which had freezing points of $+20^{\circ}\text{F}$, 0°F , and -20°F were selected for study. The criteria for selection was that the theoretical flame temperature of the propellant mixture be no greater than that of neat hydrazine. A point of comparison at 40% ammonia dissociation was selected. At 40% ammonia dissociation neat hydrazine has a theoretical flame temperature of $1,355^{\circ}\text{K}$. Figure 65 is a plot of theoretical flame temperature versus the percent hydrazine in a mixture of hydrazine, hydrazinium nitrate, and water. Figure 66 is a ternary diagram of the hydrazine, hydrazinium nitrate, water propellant system. Lines of constant freezing point and vacuum specific impulse have been plotted on the diagram. The line of a constant vacuum specific impulse of 240 lbf-sec/lbm is plotted on Figure 65 for freezing point mixtures of $+20^{\circ}\text{F}$, 0°F , and -20°F . This line falls very close to the theoretical flame temperature of neat hydrazine and mixtures falling on this line were selected for the propellant mixture tests.

The propellant mixtures were prepared by adding ammonium nitrate and water in the required quantities to hydrazine. The resulting ammonia in solution was removed by evacuating the propellant mixture, causing the ammonia to boil off. Table XX lists the desired and actual propellant mixtures as determined by chemical and analytical analysis.

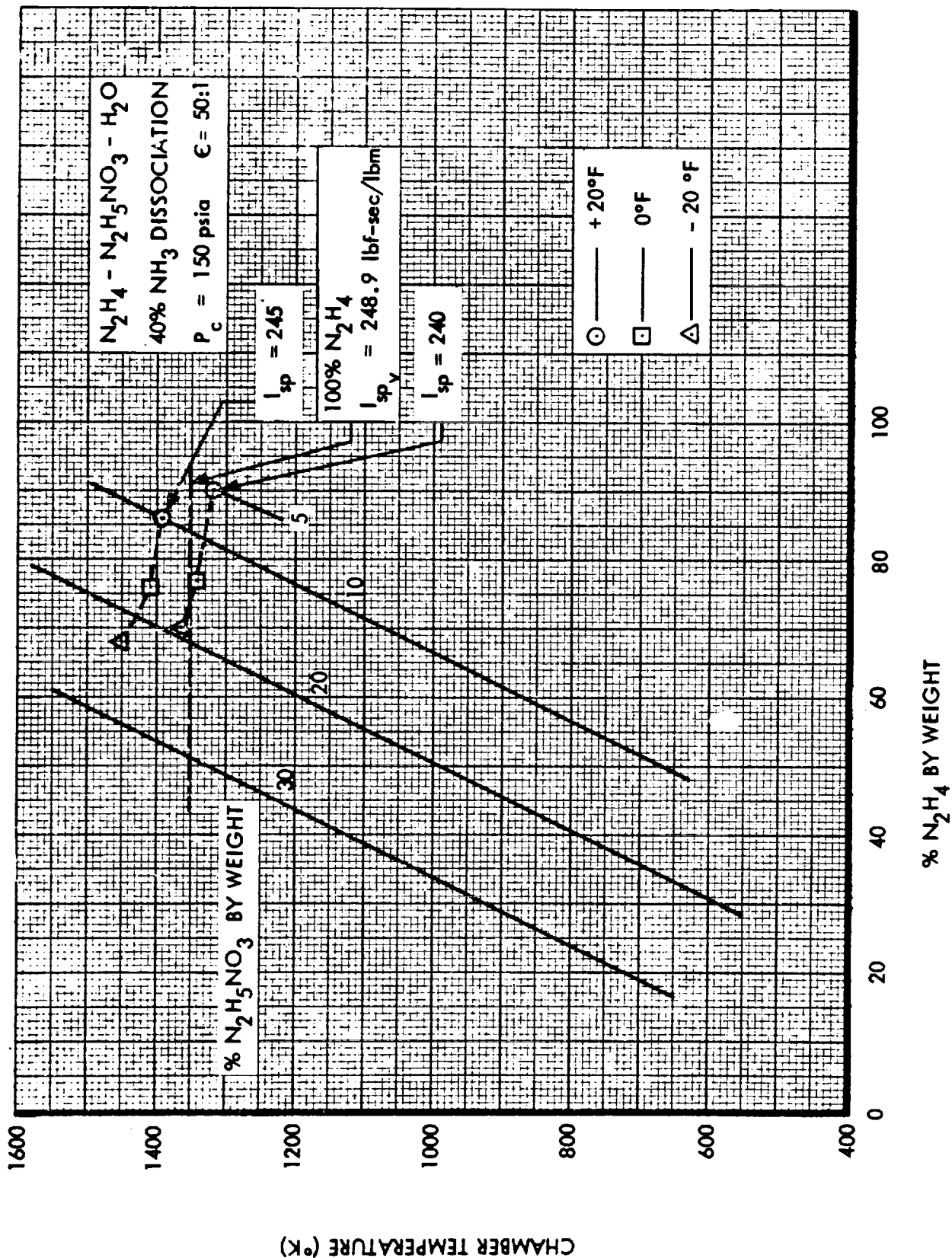
10.2.2 Test Results

All propellant mixture tests were conducted at ambient temperature and pressure conditions. A flightweight engine with a sea level nozzle of 1.5:1 expansion ratio was utilized for the tests. Steady state tests of 30 seconds duration were conducted with the engine. Five (5) tests were conducted with the $+20^{\circ}\text{F}$ and 0°F freezing point propellant mixtures and four (4) tests were conducted with the -20°F propellant mixture.



FLIGHTWEIGHT 516F ENGINE

PERFORMANCE OF TERNARY PROPELLANT MIXTURES



HYDRAZINE-HYDRAZINE NITRATE - WATER
TERNARY DIAGRAM SHOWING FREEZING
POINT AND VACUUM SPECIFIC IMPULSE

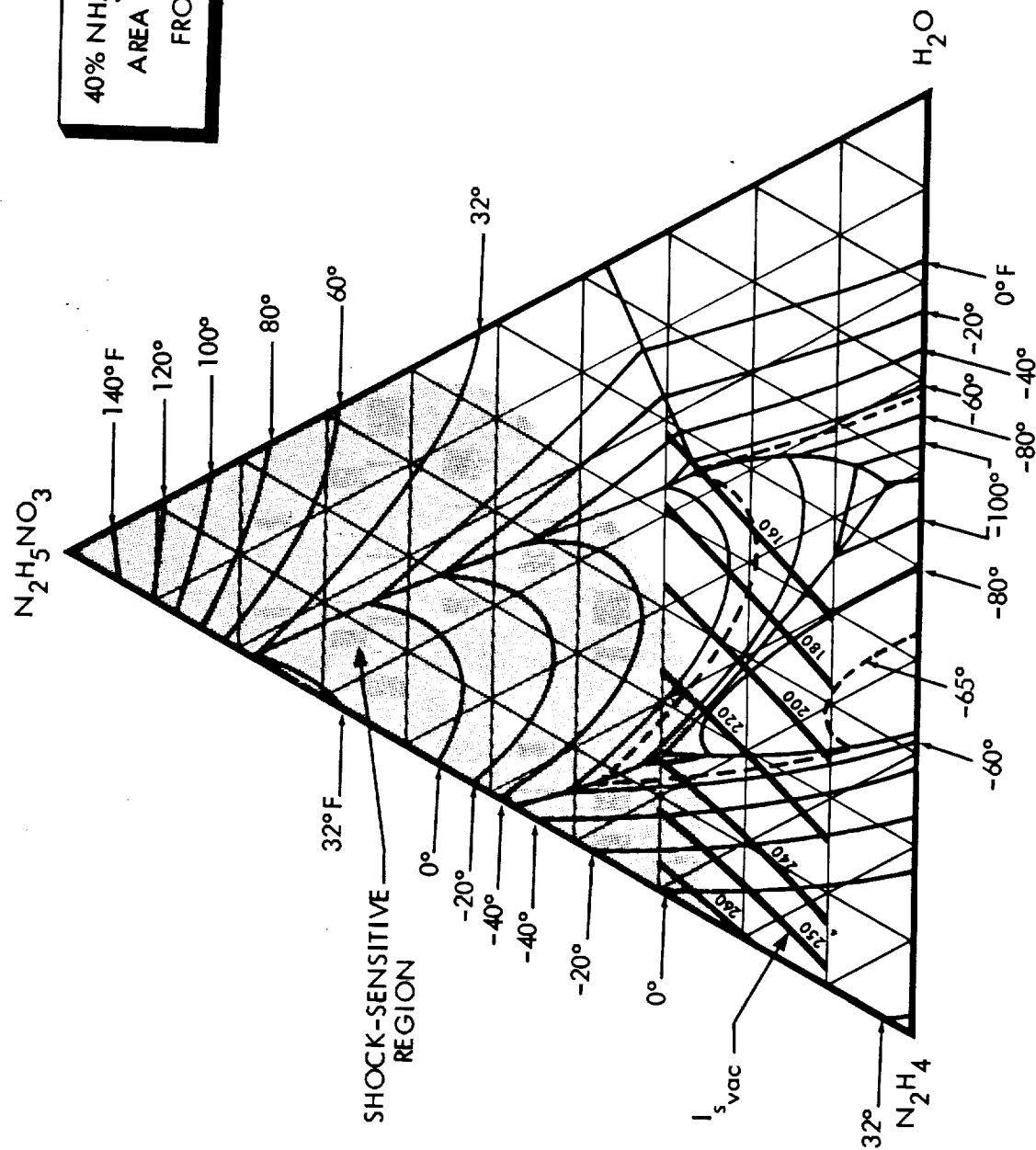


TABLE XX
LOW FREEZING POINT PROPELLANT MIXTURES

	<u>+ 20°F Mixture</u>	
	<u>Desired</u>	<u>Actual</u>
Hydrazine	89.0%	87.18%
Hydrazine Nitrate	9.0%	9.01%
Water	2.0%	3.15%
Ammonia	0%	0.66%

	<u>0°F Mixture</u>	
	<u>Desired</u>	<u>Actual</u>
Hydrazine	76.0%	75.14%
Hydrazine Nitrate	18.0%	17.87%
Water	6.0%	5.41%
Ammonia	0%	0.79%

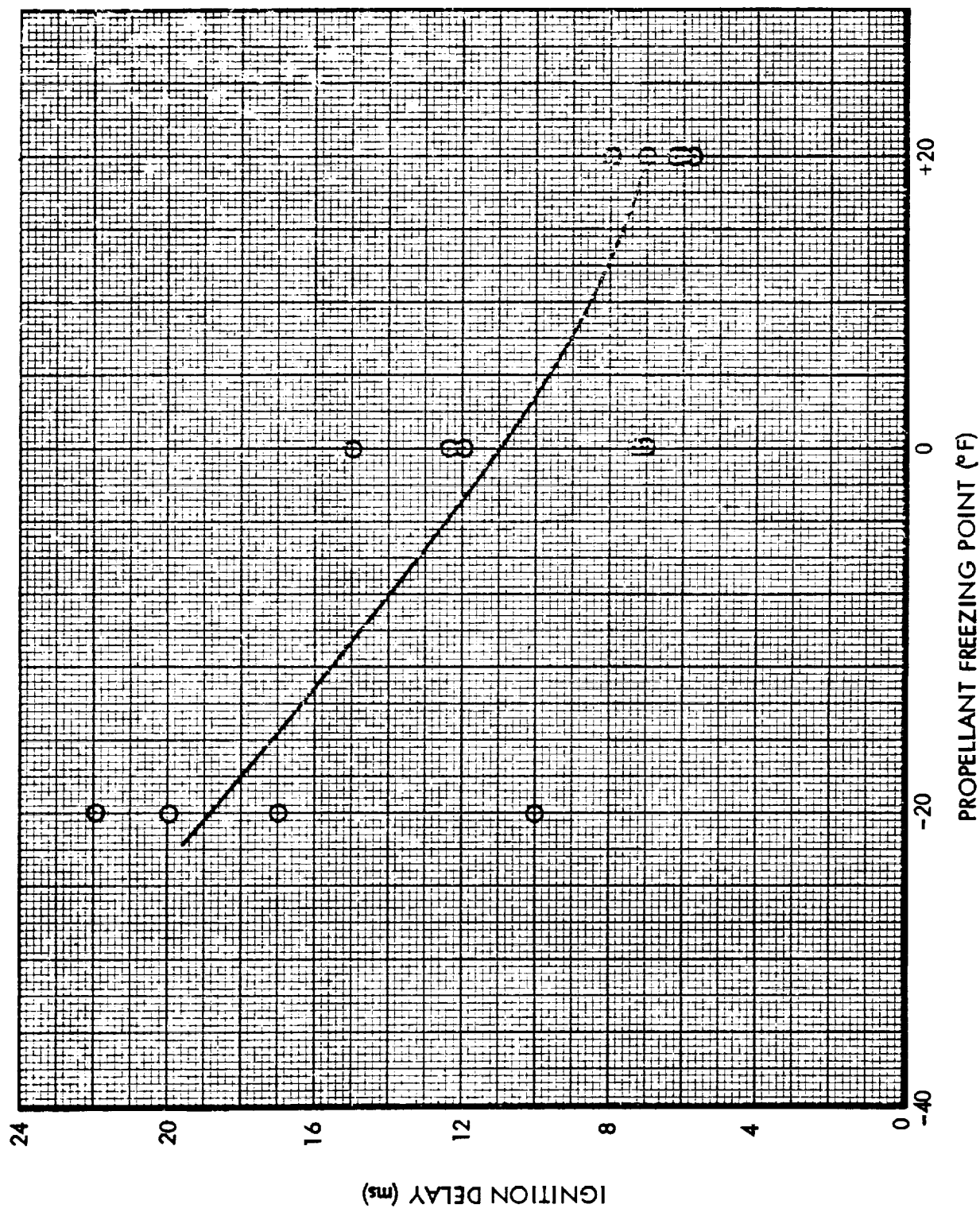
	<u>- 20°F Mixture</u>	
	<u>Desired</u>	<u>Actual</u>
Hydrazine	69.0%	67.2%
Hydrazine Nitrate	23.0%	22.9%
Water	8.0%	9.0%
Ammonia	0%	0.9%

Data obtained from the testing is summarized in Table XXI.

Smooth start transient and steady state operation were achieved during all tests. No significant engine performance difference was noted between the three propellant mixtures. Characteristic velocity averaged 4,189 ft/sec for the 14 tests conducted which is virtually identical to the predicted value of 4,180 ft/sec. Two major trends were noted in the test data. Ignition delay times and chamber pressure roughness both increased slightly as the propellant freezing point was lowered. This trend is shown in Figures 67 and 68 wherein ignition delay times and chamber pressure roughness are plotted versus the propellant freezing point.

Pre- and post test catalyst bed weights were virtually identical with no indication of any catalyst loss during the tests of 420 seconds total test duration.

IGNITION DELAY TIME VS PROPELLANT FREEZING POINT
FOR 5 lbf FLIGHTWEIGHT ENGINE



CHAMBER PRESSURE ROUGHNESS
VS
PROPELLANT FREEZING POINT
FOR
5 lbf FLIGHTWEIGHT ENGINE

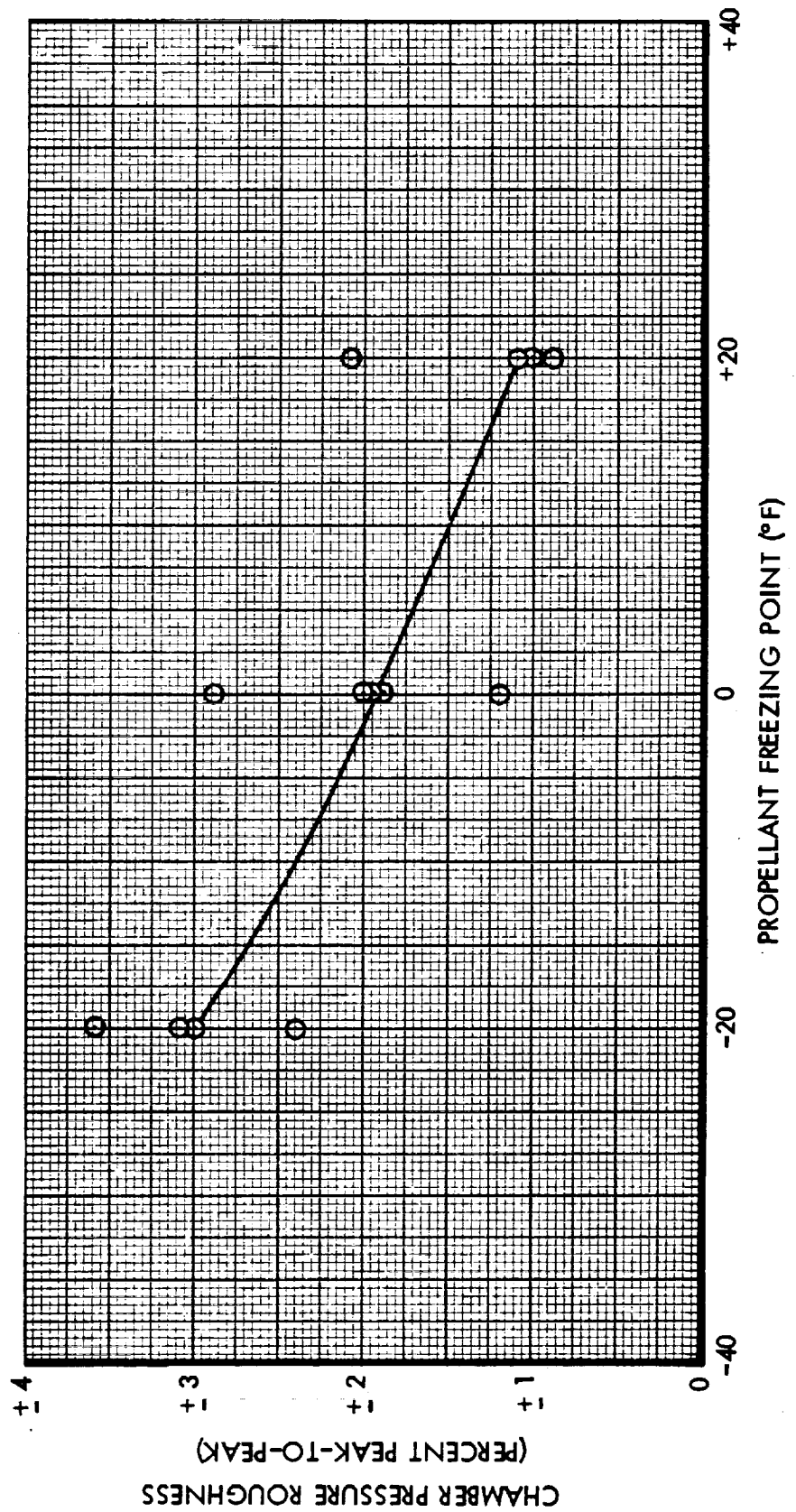


TABLE XXI
SUMMARY OF 5 lbf FLIGHTWEIGHT ENGINE PROPELLANT MIXTURE TESTS

Test No.	Propellant Freezing Point °F	Initial Catalyst Bed Temperature °F	Fuel Temperature °F	(1) Ignition Delay ms	(2) Response Time ms	(3) Response Time ms	Upstream Chamber Pressure psia	Downstream Chamber Pressure psia	Thrust lbf	(4) Flowrate lbf/sec	c* ft/sec	I _s (5) lbf-sec/lbm	C _f (5)	Chamber Pressure Roughness % peak-to-peak
456	+20		67	6	195	545	217.5	214.5	3,980	0.02414	4243	164.9	1.250	+ 2.1
457	+20		66	6	195	520	206.7	201.5	3,740	0.02321	4145	161.1	1.251	
458	+20		58	6	175	450	206.3	202.5	3,710	0.02299	4217	161.8	1.234	+ 1.0
459	+20		63	7	202	520	207.9	204.3	3,750	0.02324	4198	161.6	1.239	+ 1.0
460	+20		66	8	200	520	206.9	203.3	3,745	0.02322	4181	161.3	1.241	+ 1.0
461	0		64	7	190	490	208.1	204.1	3,760	0.02337	4170	161.1	1.243	+ 1.9
462	0		63	7	170	435	205.7	202.1	3,740	0.02319	4161	161.5	1.249	+ 1.9
463	0		65	12	157	480	205.1	201.7	3,710	0.02294	4196	161.7	1.239	+ 2.0
464	0		58	15	175	520	206.5	203.1	3,735	0.02313	4194	161.3	1.238	+ 1.2
465	0		53	12	222	567	205.8	201.9	3,730	0.02279	4230	163.7	1.245	+ 2.9
466	-20		67	10	235	570	205.3	202.3	3,725	0.02328	4162	160.5	1.241	+ 3.0
467	-20		63	20	235	660	205.5	202.3	3,710	0.02310	4182	160.6	1.236	+ 2.4
468	-20		65	17	185	515	206.1	200.1	3,685	0.02290	4172	160.9	1.241	+ 3.0
469	-20		65	22	230	710	199.1	194.7	3,540	0.02209	4208	160.3	1.225	+ 3.6

- (1) Time from propellant entry into chamber to 1% of steady state chamber pressure
- (2) Time from propellant entry into chamber to 80% of steady state chamber pressure
- (3) Time from propellant entry into chamber to 90% of steady state chamber pressure
- (4) Average of two flowmeters in series
- (5) Sea level conditions at expansion ratio of 1.5:1